

D^\pm

$$I(J^P) = \frac{1}{2}(0^-)$$

 D^\pm MASS

The fit includes D^\pm , D^0 , D_s^\pm , $D^{*\pm}$, D^{*0} , and $D_s^{*\pm}$ mass and mass difference measurements.

VALUE (MeV)	EVTS	DOCUMENT ID	TECN	COMMENT
1869.3 ± 0.4 OUR FIT		Error includes scale factor of 1.1.		
1869.4 ± 0.5 OUR AVERAGE				
1870.0 ± 0.5 ± 1.0	317	BARLAG	90C ACCM	π^- Cu 230 GeV
1863 ± 4		DERRICK	84 HRS	$e^+ e^-$ 29 GeV
1869.4 ± 0.6		¹ TRILLING	81 RVUE	$e^+ e^-$ 3.77 GeV
• • • We do not use the following data for averages, fits, limits, etc. • • •				
1875 ± 10	9	ADAMOVICH	87 EMUL	Photoproduction
1860 ± 16	6	ADAMOVICH	84 EMUL	Photoproduction
1868.4 ± 0.5		¹ SCHINDLER	81 MRK2	$e^+ e^-$ 3.77 GeV
1874 ± 5		GOLDHABER	77 MRK1	D^0 , D^+ recoil spectra
1868.3 ± 0.9		¹ PERUZZI	77 MRK1	$e^+ e^-$ 3.77 GeV
1874 ± 11		PICCOLO	77 MRK1	$e^+ e^-$ 4.03, 4.41 GeV
1876 ± 15	50	PERUZZI	76 MRK1	$K^\mp \pi^\pm \pi^\pm$

¹ PERUZZI 77 and SCHINDLER 81 errors do not include the 0.13% uncertainty in the absolute SPEAR energy calibration. TRILLING 81 uses the high precision $J/\psi(1S)$ and $\psi(2S)$ measurements of ZHOLENTZ 80 to determine this uncertainty and combines the PERUZZI 77 and SCHINDLER 81 results to obtain the value quoted.

 D^\pm MEAN LIFE

Measurements with an error $> 100 \times 10^{-15}$ s have been omitted from the Listings.

VALUE (10^{-15} s)	EVTS	DOCUMENT ID	TECN	COMMENT
1040 ± 7 OUR AVERAGE				
1039.4 ± 4.3 ± 7.0	110k	LINK	02F FOCS	γ nucleus, \approx 180 GeV
1033.6 ± 22.1 ± 9.9	3777	BONVICINI	99 CLE2	$e^+ e^-$ \approx $\Upsilon(4S)$
1048 ± 15 ± 11	9k	FRAEBETTI	94D E687	$D^+ \rightarrow K^- \pi^+ \pi^+$
• • • We do not use the following data for averages, fits, limits, etc. • • •				
1075 ± 40 ± 18	2455	FRAEBETTI	91 E687	γ Be, $D^+ \rightarrow K^- \pi^+ \pi^+$
1030 ± 80 ± 60	200	ALVAREZ	90 NA14	γ , $D^+ \rightarrow K^- \pi^+ \pi^+$
1050 ± 77 ± 72	317	² BARLAG	90C ACCM	π^- Cu 230 GeV
1050 ± 80 ± 70	363	ALBRECHT	88I ARG	$e^+ e^-$ 10 GeV
1090 ± 30 ± 25	2992	RAAB	88 E691	Photoproduction

² BARLAG 90C estimates the systematic error to be negligible.

D^+ DECAY MODES

Most decay modes (other than the semileptonic modes) that involve a neutral K meson are now given as K_S^0 modes, not as \bar{K}^0 modes. Nearly always it is a K_S^0 that is measured, and interference between Cabibbo-allowed and doubly Cabibbo-suppressed modes can invalidate the assumption that $2\Gamma(K_S^0) = \Gamma(\bar{K}^0)$.

Mode	Fraction (Γ_i/Γ)	Scale factor/ Confidence level
Inclusive modes		
$\Gamma_1 e^+ \text{anything}$	$(17.2 \pm 1.9) \%$	
$\Gamma_2 K^- \text{anything}$	$(27.5 \pm 2.4) \%$	
$\Gamma_3 \bar{K}^0 \text{anything} + K^0 \text{anything}$	$(61 \pm 8) \%$	
$\Gamma_4 K^+ \text{anything}$	$(5.5 \pm 1.6) \%$	
$\Gamma_5 \bar{K}^*(892)^0 \text{anything}$	$(23 \pm 5) \%$	
$\Gamma_6 K^*(892)^0 \text{anything}$	$< 6.6 \%$	CL=90%
$\Gamma_7 \eta \text{anything}$	$[a] < 13 \%$	CL=90%
$\Gamma_8 \phi \text{anything}$	$< 1.8 \%$	CL=90%
$\Gamma_9 \phi e^+ \text{anything}$	$< 1.6 \%$	CL=90%
$\Gamma_{10} \mu^+ \text{anything}$		
Leptonic and semileptonic modes		
$\Gamma_{11} e^+ \nu_e$	$< 2.4 \times 10^{-5}$	CL=90%
$\Gamma_{12} \mu^+ \nu_\mu$	$(4.4 \pm 0.7) \times 10^{-4}$	
$\Gamma_{13} \bar{K}^0 \ell^+ \nu_\ell$	$[b]$	
$\Gamma_{14} \bar{K}^0 e^+ \nu_e$	$(8.6 \pm 0.5) \%$	
$\Gamma_{15} \bar{K}^0 \mu^+ \nu_\mu$	$(9.5 \pm 0.8) \%$	
$\Gamma_{16} K^- \pi^+ e^+ \nu_e$	$(4.5 \pm 1.0) \%$	S=1.1
$\Gamma_{17} \bar{K}^*(892)^0 e^+ \nu_e,$ $\bar{K}^*(892)^0 \rightarrow K^- \pi^+$	$(3.74 \pm 0.21) \%$	
$\Gamma_{18} K^- \pi^+ e^+ \nu_e \text{ nonresonant}$	$< 7 \times 10^{-3}$	CL=90%
$\Gamma_{19} K^- \pi^+ \mu^+ \nu_\mu$	$(4.0 \pm 0.5) \%$	
$\Gamma_{20} \bar{K}^*(892)^0 \mu^+ \nu_\mu,$ $\bar{K}^*(892)^0 \rightarrow K^- \pi^+$	$(3.7 \pm 0.3) \%$	
$\Gamma_{21} K^- \pi^+ \mu^+ \nu_\mu \text{ nonresonant}$	$(2.1 \pm 0.6) \times 10^{-3}$	
$\Gamma_{22} (\bar{K}^*(892)\pi)^0 e^+ \nu_e$	$< 1.2 \%$	CL=90%
$\Gamma_{23} (\bar{K}\pi\pi)^0 e^+ \nu_e \text{ non-} \bar{K}^*(892)$	$< 9 \times 10^{-3}$	CL=90%
$\Gamma_{24} K^- \pi^+ \pi^0 \mu^+ \nu_\mu$	$< 1.7 \times 10^{-3}$	CL=90%
$\Gamma_{25} \pi^0 e^+ \nu_e$	$(4.4 \pm 0.7) \times 10^{-3}$	
$\Gamma_{26} \pi^0 \ell^+ \nu_\ell$	$[b]$	

Fractions of some of the following modes with resonances have already appeared above as submodes of particular charged-particle modes.

Γ_{27}	$\bar{K}^*(892)^0 e^+ \nu_e$	(5.61 \pm 0.31) %	S=1.1
Γ_{28}	$\bar{K}^*(892)^0 \mu^+ \nu_\mu$	(5.5 \pm 0.5) %	S=1.1
Γ_{29}	$\bar{K}_1(1270)^0 \mu^+ \nu_\mu$	< 4 %	CL=95%
Γ_{30}	$\bar{K}^*(1410)^0 \mu^+ \nu_\mu$		
Γ_{31}	$\bar{K}_0^*(1430)^0 \mu^+ \nu_\mu$	< 2.5 $\times 10^{-4}$	
Γ_{32}	$\bar{K}_2^*(1430)^0 \mu^+ \nu_\mu$	< 1.1 %	CL=95%
Γ_{33}	$\bar{K}^*(1680)^0 \mu^+ \nu_\mu$	< 1.6 $\times 10^{-3}$	
Γ_{34}	$\rho^0 e^+ \nu_e$	(2.2 \pm 0.4) $\times 10^{-3}$	
Γ_{35}	$\rho^0 \mu^+ \nu_\mu$	(3.4 \pm 0.8) $\times 10^{-3}$	
Γ_{36}	$\omega e^+ \nu_e$	(1.6 $^{+0.7}_{-0.6}$) $\times 10^{-3}$	
Γ_{37}	$\phi e^+ \nu_e$	< 2.09 %	CL=90%
Γ_{38}	$\phi \mu^+ \nu_\mu$	< 3.72 %	CL=90%
Γ_{39}	$\eta \ell^+ \nu_\ell$	< 7 $\times 10^{-3}$	CL=90%
Γ_{40}	$\eta'(958) \mu^+ \nu_\mu$	< 1.1 %	CL=90%

Hadronic modes with a \bar{K} or $\bar{K} K \bar{K}$

Γ_{41}	$K_S^0 \pi^+$	(1.47 \pm 0.06) %	S=1.1
Γ_{42}	$K^- \pi^+ \pi^+$	[c] (9.51 \pm 0.34) %	S=1.1
Γ_{43}	$\bar{K}_0^*(800)^0 \pi^+, \bar{K}_0^*(800) \rightarrow$	[d]	
Γ_{44}	$\bar{K}^*(892)^0 \pi^+,$ $\bar{K}^*(892)^0 \rightarrow K^- \pi^+$	[d] (1.33 \pm 0.11) %	
Γ_{45}	$\bar{K}_0^*(1430)^0 \pi^+,$ $\bar{K}_0^*(1430)^0 \rightarrow K^- \pi^+$	[d] (2.41 \pm 0.24) %	
Γ_{46}	$\bar{K}_2^*(1430)^0 \pi^+,$ $\bar{K}_2^*(1430)^0 \rightarrow K^- \pi^+$	[d]	
Γ_{47}	$\bar{K}^*(1680)^0 \pi^+,$ $\bar{K}^*(1680)^0 \rightarrow K^- \pi^+$	[d] (4.0 \pm 0.8) $\times 10^{-3}$	
Γ_{48}	$K^- \pi^+ \pi^+$ nonresonant	[d] (9.0 \pm 0.7) %	
Γ_{49}	$K_S^0 \pi^+ \pi^0$	[c] (7.0 \pm 0.5) %	S=1.2
Γ_{50}	$K_S^0 \rho^+$	(4.8 \pm 1.1) %	
Γ_{51}	$\bar{K}^*(892)^0 \pi^+,$ $\bar{K}^*(892)^0 \rightarrow K_S^0 \pi^0$	(1.3 \pm 0.6) %	
Γ_{52}	$K_S^0 \pi^+ \pi^0$ nonresonant	(9 \pm 7) $\times 10^{-3}$	
Γ_{53}	$K^- \pi^+ \pi^+ \pi^0$	[c] (6.00 \pm 0.28) %	S=1.1
Γ_{54}	$\bar{K}^*(892)^0 \rho^+$ total, $\bar{K}^*(892)^0 \rightarrow K^- \pi^+$	(1.3 \pm 0.8) %	
Γ_{55}	$\bar{K}_1(1400)^0 \pi^+,$ $\bar{K}_1(1400)^0 \rightarrow K^- \pi^+ \pi^0$	(1.8 \pm 0.7) %	
Γ_{56}	$K^- \rho^+ \pi^+$ total	(2.6 \pm 1.6) %	

Γ_{57}	$K^- \rho^+ \pi^+ 3\text{-body}$	$(9 \pm 6) \times 10^{-3}$	
Γ_{58}	$\overline{K}^*(892)^0 \pi^+ \pi^0 \text{total},$ $\overline{K}^*(892)^0 \rightarrow K^- \pi^+$	$(4.2 \pm 0.6) \%$	
Γ_{59}	$\overline{K}^*(892)^0 \pi^+ \pi^0 3\text{-body},$ $\overline{K}^*(892)^0 \rightarrow K^- \pi^+$	$(2.7 \pm 0.8) \%$	
Γ_{60}	$K^*(892)^- \pi^+ \pi^+ 3\text{-body},$ $K^*(892)^- \rightarrow K^- \pi^0$	$(6 \pm 3) \times 10^{-3}$	
Γ_{61}	$K^- \pi^+ \pi^+ \pi^0 \text{nonresonant}$	$[e] (1.0 \pm 0.7) \%$	
Γ_{62}	$K_S^0 \pi^+ \pi^+ \pi^-$	$[c] (3.11 \pm 0.21) \%$	S=1.1
Γ_{63}	$K_S^0 a_1(1260)^+,$ $a_1(1260)^+ \rightarrow \pi^+ \pi^+ \pi^-$	$(1.8 \pm 0.3) \%$	
Γ_{64}	$\overline{K}_1(1400)^0 \pi^+,$ $\overline{K}_1(1400)^0 \rightarrow K_S^0 \pi^+ \pi^-$	$(1.8 \pm 0.7) \%$	
Γ_{65}	$K^*(892)^- \pi^+ \pi^+ 3\text{-body},$ $K^*(892)^- \rightarrow K_S^0 \pi^-$	$(1.3 \pm 0.6) \%$	
Γ_{66}	$K_S^0 \rho^0 \pi^+ \text{total}$	$(1.86 \pm 0.34) \%$	CL=90%
Γ_{67}	$K_S^0 \rho^0 \pi^+ 3\text{-body}$	$(2.2 \pm 2.2) \times 10^{-3}$	
Γ_{68}	$K_S^0 \pi^+ \pi^+ \pi^- \text{nonresonant}$	$(3.7 \pm 1.9) \times 10^{-3}$	
Γ_{69}	$K^- 3\pi^+ \pi^-$	$[c] (5.8 \pm 0.6) \times 10^{-3}$	S=1.1
Γ_{70}	$\overline{K}^*(892)^0 \pi^+ \pi^+ \pi^-,$ $\overline{K}^*(892)^0 \rightarrow K^- \pi^+$	$(1.2 \pm 0.4) \times 10^{-3}$	
Γ_{71}	$\overline{K}^*(892)^0 \rho^0 \pi^+,$ $\overline{K}^*(892)^0 \rightarrow K^- \pi^+$	$(2.3 \pm 0.4) \times 10^{-3}$	
Γ_{72}	$\overline{K}^*(892)^0 \pi^+ \pi^+ \pi^- \text{no-}\rho,$ $\overline{K}^*(892)^0 \rightarrow K^- \pi^+$		
Γ_{73}	$K^- \rho^0 \pi^+ \pi^+$	$(1.75 \pm 0.29) \times 10^{-3}$	
Γ_{74}	$K^- 3\pi^+ \pi^- \text{nonresonant}$	$(4.1 \pm 3.0) \times 10^{-4}$	
Γ_{75}	$K^+ 2K_S^0$	$(4.7 \pm 2.1) \times 10^{-3}$	
Γ_{76}	$K^+ K^- K_S^0 \pi^+$	$(2.4 \pm 0.6) \times 10^{-4}$	

Fractions of some of the following modes with resonances have already appeared above as submodes of particular charged-particle modes.

Γ_{77}	$K_S^0 a_1(1260)^+$	$(3.6 \pm 0.6) \%$	
Γ_{78}	$K_S^0 a_2(1320)^+$	$< 1.5 \times 10^{-3}$	CL=90%
Γ_{79}	$\overline{K}^*(892)^0 \rho^+ \text{total}$	$[e] (1.8 \pm 1.4) \%$	
Γ_{80}	$\overline{K}^*(892)^0 \rho^+ S\text{-wave}$	$[e] (1.4 \pm 1.5) \%$	
Γ_{81}	$\overline{K}^*(892)^0 \rho^+ P\text{-wave}$	$< 1 \times 10^{-3}$	CL=90%
Γ_{82}	$\overline{K}^*(892)^0 \rho^+ D\text{-wave}$	$(8 \pm 7) \times 10^{-3}$	
Γ_{83}	$\overline{K}^*(892)^0 \rho^+ D\text{-wave longitudinal}$	$< 7 \times 10^{-3}$	CL=90%
Γ_{84}	$\overline{K}_1(1270)^0 \pi^+$	$< 7 \times 10^{-3}$	CL=90%
Γ_{85}	$\overline{K}_1(1400)^0 \pi^+$	$(4.3 \pm 1.5) \%$	S=1.2

Γ_{86}	$\bar{K}^*(1410)^0 \pi^+$		
Γ_{87}	$\bar{K}^*(892)^0 \pi^+ \pi^0$ total	(5.8 \pm 2.9) %	
Γ_{88}	$\bar{K}^*(892)^0 \pi^+ \pi^0$ 3-body	[e] (3.6 \pm 2.1) %	
Γ_{89}	$K^*(892)^- \pi^+ \pi^+$ total	—	
Γ_{90}	$K^*(892)^- \pi^+ \pi^+$ 3-body	(1.8 \pm 1.1) %	S=1.2
Γ_{91}	$K_S^0 f_0(980) \pi^+$		
Γ_{92}	$\bar{K}^*(892)^0 a_1(1260)^+$	(9.4 \pm 1.9) $\times 10^{-3}$	

Pionic modes

Γ_{93}	$\pi^+ \pi^0$	(1.28 \pm 0.09) $\times 10^{-3}$	
Γ_{94}	$\pi^+ \pi^+ \pi^-$	(3.31 \pm 0.21) $\times 10^{-3}$	
Γ_{95}	$\rho^0 \pi^+$	(1.07 \pm 0.11) $\times 10^{-3}$	
Γ_{96}	$\pi^+ (\pi^+ \pi^-)$ S-wave	(1.86 \pm 0.18) $\times 10^{-3}$	
Γ_{97}	$\sigma \pi^+, \sigma \rightarrow \pi^+ \pi^-$	(1.53 \pm 0.32) $\times 10^{-3}$	
Γ_{98}	$f_0(980) \pi^+,$ $f_0(980) \rightarrow \pi^+ \pi^-$	(2.1 \pm 0.5) $\times 10^{-4}$	
Γ_{99}	$f_0(1370) \pi^+,$ $f_0(1370) \rightarrow \pi^+ \pi^-$	(8 \pm 6) $\times 10^{-5}$	
Γ_{100}	$f_2(1270) \pi^+,$ $f_2(1270) \rightarrow \pi^+ \pi^-$	(4.8 \pm 1.3) $\times 10^{-4}$	
Γ_{101}	$\rho(1450)^0 \pi^+,$ $\rho(1450)^0 \rightarrow \pi^+ \pi^-$		
Γ_{102}	$\pi^+ \pi^+ \pi^-$ nonresonant		
Γ_{103}	$\pi^+ 2\pi^0$	(4.8 \pm 0.4) $\times 10^{-3}$	
Γ_{104}	$\pi^+ \pi^+ \pi^- \pi^0$	(1.18 \pm 0.09) %	
Γ_{105}	$\eta \pi^+, \eta \rightarrow \pi^+ \pi^- \pi^0$	(7.9 \pm 0.7) $\times 10^{-4}$	
Γ_{106}	$\omega \pi^+, \omega \rightarrow \pi^+ \pi^- \pi^0$	< 3 $\times 10^{-4}$	CL=90%
Γ_{107}	$3\pi^+ 2\pi^-$	(1.68 \pm 0.17) $\times 10^{-3}$	S=1.1
Γ_{108}	$3\pi^+ 2\pi^- \pi^0$		

Fractions of some of the following modes with resonances have already appeared above as submodes of particular charged-particle modes.

Γ_{109}	$\eta \pi^+$	(3.50 \pm 0.32) $\times 10^{-3}$	
Γ_{110}	$\omega \pi^+$	< 3.4 $\times 10^{-4}$	CL=90%
Γ_{111}	$\eta \rho^+$	< 7 $\times 10^{-3}$	CL=90%
Γ_{112}	$\eta'(958) \pi^+$	(5.3 \pm 1.1) $\times 10^{-3}$	
Γ_{113}	$\eta'(958) \rho^+$	< 6 $\times 10^{-3}$	CL=90%

Hadronic modes with a $K\bar{K}$ pair

Γ_{114}	$K^+ K_S^0$	(2.96 \pm 0.19) $\times 10^{-3}$	
Γ_{115}	$K^+ K^- \pi^+$	[c] (1.00 \pm 0.04) %	S=1.2
Γ_{116}	$\phi \pi^+, \phi \rightarrow K^+ K^-$	(3.2 \pm 0.4) $\times 10^{-3}$	
Γ_{117}	$K^+ \bar{K}^*(892)^0,$ $\bar{K}^*(892)^0 \rightarrow K^- \pi^+$	(3.02 \pm 0.35) $\times 10^{-3}$	

Γ_{118}	$K^+ \bar{K}_0^*(1430)^0, \bar{K}_0^*(1430)^0 \rightarrow$	$(3.7 \pm 0.4) \times 10^{-3}$	
Γ_{119}	$K^- \pi^+$ $K^+ K^- \pi^+$ nonresonant		
Γ_{120}	$K_S^0 K_S^0 \pi^+$	—	
Γ_{121}	$K^*(892)^+ K_S^0,$ $K^*(892)^+ \rightarrow K_S^0 \pi^+$	$(5.3 \pm 2.3) \times 10^{-3}$	
Γ_{122}	$K^+ K^- \pi^+ \pi^0$	—	
Γ_{123}	$\phi \pi^+ \pi^0, \phi \rightarrow K^+ K^-$	$(1.1 \pm 0.5) \%$	
Γ_{124}	$\phi \rho^+, \phi \rightarrow K^+ K^-$	$< 7 \times 10^{-3}$	CL=90%
Γ_{125}	$K^+ K^- \pi^+ \pi^0$ non- ϕ	$(1.5 \pm 0.7) \%$	
Γ_{126}	$K^+ K_S^0 \pi^+ \pi^-$	$(1.75 \pm 0.21) \times 10^{-3}$	
Γ_{127}	$K_S^0 K^- \pi^+ \pi^+$	$(2.39 \pm 0.23) \times 10^{-3}$	
Γ_{128}	$K^*(892)^+ \bar{K}^*(892)^0,$ $K^{*+} \rightarrow K_S^0 \pi^+, \bar{K}^{*0} \rightarrow K^- \pi^+$	$(5.8 \pm 2.4) \times 10^{-3}$	
Γ_{129}	$K_S^0 K^- \pi^+ \pi^+ (\text{non-}K^{*+} \bar{K}^{*0})$	$< 4 \times 10^{-3}$	CL=90%
Γ_{130}	$K^+ K^- \pi^+ \pi^+ \pi^-$	$(2.3 \pm 1.2) \times 10^{-4}$	

Fractions of the following modes with resonances have already appeared above as submodes of particular charged-particle modes.

Γ_{131}	$\phi \pi^+$	$(6.5 \pm 0.7) \times 10^{-3}$	
Γ_{132}	$\phi \pi^+ \pi^0$	$(2.3 \pm 1.0) \%$	
Γ_{133}	$\phi \rho^+$	$< 1.5 \%$	CL=90%
Γ_{134}	$K^+ \bar{K}^*(892)^0$		
Γ_{135}	$K^*(892)^+ K_S^0$	$(1.6 \pm 0.7) \%$	
Γ_{136}	$K^*(892)^+ \bar{K}^*(892)^0$	$(2.6 \pm 1.1) \%$	

Doubly Cabibbo-suppressed modes

Γ_{137}	$K^+ \pi^0$	$< 4.2 \times 10^{-4}$	CL=90%
Γ_{138}	$K^+ \pi^+ \pi^-$	$(6.4 \pm 0.8) \times 10^{-4}$	
Γ_{139}	$K^+ \rho^0$	$(2.5 \pm 0.7) \times 10^{-4}$	
Γ_{140}	$K^*(892)^0 \pi^+, K^*(892)^0 \rightarrow$ $K^+ \pi^-$	$(3.0 \pm 0.6) \times 10^{-4}$	
Γ_{141}	$K^+ f_0(980), f_0(980) \rightarrow$ $\pi^+ \pi^-$	$(5.7 \pm 3.5) \times 10^{-5}$	
Γ_{142}	$K_2^*(1430)^0 \pi^+, K_2^*(1430)^0 \rightarrow$ $K^+ \pi^-$	$(5.2 \pm 3.5) \times 10^{-5}$	
Γ_{143}	$K^+ \pi^+ \pi^-$ nonresonant		
Γ_{144}	$K^+ K^+ K^-$	$(9.0 \pm 2.1) \times 10^{-5}$	
Γ_{145}	ϕK^+		

**$\Delta C = 1$ weak neutral current (*C1*) modes, or
Lepton Family number (*LF*) or Lepton number (*L*) violating modes**

Γ_{146}	$\pi^+ e^+ e^-$	<i>C1</i>	$< 7.4 \times 10^{-6}$	CL=90%
Γ_{147}	$\pi^+ \phi, \phi \rightarrow e^+ e^-$	[f]	$(2.7^{+3.6}_{-1.8}) \times 10^{-6}$	
Γ_{148}	$\pi^+ \mu^+ \mu^-$	<i>C1</i>	$< 8.8 \times 10^{-6}$	CL=90%
Γ_{149}	$\rho^+ \mu^+ \mu^-$	<i>C1</i>	$< 5.6 \times 10^{-4}$	CL=90%
Γ_{150}	$K^+ e^+ e^-$	[g]	$< 6.2 \times 10^{-6}$	CL=90%
Γ_{151}	$K^+ \mu^+ \mu^-$	[g]	$< 9.2 \times 10^{-6}$	CL=90%
Γ_{152}	$\pi^+ e^\pm \mu^\mp$	<i>LF</i>	$[h] < 3.4 \times 10^{-5}$	CL=90%
Γ_{153}	$\pi^+ e^+ \mu^-$			
Γ_{154}	$\pi^+ e^- \mu^+$			
Γ_{155}	$K^+ e^\pm \mu^\mp$	<i>LF</i>	$[h] < 6.8 \times 10^{-5}$	CL=90%
Γ_{156}	$K^+ e^+ \mu^-$			
Γ_{157}	$K^+ e^- \mu^+$			
Γ_{158}	$\pi^- e^+ e^+$	<i>L</i>	$< 3.6 \times 10^{-6}$	CL=90%
Γ_{159}	$\pi^- \mu^+ \mu^+$	<i>L</i>	$< 4.8 \times 10^{-6}$	CL=90%
Γ_{160}	$\pi^- e^+ \mu^+$	<i>L</i>	$< 5.0 \times 10^{-5}$	CL=90%
Γ_{161}	$\rho^- \mu^+ \mu^+$	<i>L</i>	$< 5.6 \times 10^{-4}$	CL=90%
Γ_{162}	$K^- e^+ e^+$	<i>L</i>	$< 4.5 \times 10^{-6}$	CL=90%
Γ_{163}	$K^- \mu^+ \mu^+$	<i>L</i>	$< 1.3 \times 10^{-5}$	CL=90%
Γ_{164}	$K^- e^+ \mu^+$	<i>L</i>	$< 1.3 \times 10^{-4}$	CL=90%
Γ_{165}	$K^*(892)^- \mu^+ \mu^+$	<i>L</i>	$< 8.5 \times 10^{-4}$	CL=90%
Γ_{166}	A dummy mode used by the fit.		$(30 \pm 5) \%$	S=1.2

- [a] This is a weighted average of D^\pm (44%) and D^0 (56%) branching fractions. See “ D^+ and $D^0 \rightarrow (\eta \text{ anything}) / (\text{total } D^+ \text{ and } D^0)$ ” under “ D^+ Branching Ratios” in these Particle Listings.
- [b] An ℓ indicates an e or a μ mode, not a sum over these modes.
- [c] The branching fraction for this mode may differ from the sum of the submodes that contribute to it, due to interference effects. See the relevant papers.
- [d] These subfractions of the $K^- \pi^+ \pi^+$ mode are uncertain: see the Particle Listings.
- [e] The two experiments measuring this fraction are in serious disagreement. See the Particle Listings.
- [f] This is *not* a test for the $\Delta C=1$ weak neutral current, but leads to the $\pi^+ e^+ e^-$ final state.
- [g] This mode is not a useful test for a $\Delta C=1$ weak neutral current because both quarks must change flavor in this decay.
- [h] The value is for the sum of the charge states or particle/antiparticle states indicated.

CONSTRAINED FIT INFORMATION

An overall fit to 32 branching ratios uses 51 measurements and one constraint to determine 21 parameters. The overall fit has a $\chi^2 = 30.9$ for 31 degrees of freedom.

The following *off-diagonal* array elements are the correlation coefficients $\langle \delta x_i \delta x_j \rangle / (\delta x_i \cdot \delta x_j)$, in percent, from the fit to the branching fractions, $x_i \equiv \Gamma_i / \Gamma_{\text{total}}$. The fit constrains the x_i whose labels appear in this array to sum to one.

x_{15}	3										
x_{16}	0	1									
x_{27}	1	6	14								
x_{28}	3	61	1	6							
x_{34}	0	0	1	5	0						
x_{41}	9	33	2	12	34	1					
x_{42}	8	40	2	15	40	1	84				
x_{49}	4	14	1	5	14	0	45	35			
x_{53}	1	3	0	1	3	0	9	8	8		
x_{62}	6	24	1	9	24	0	66	60	58	14	
x_{69}	3	15	1	5	15	0	31	37	13	3	
x_{85}	1	5	0	2	5	0	13	12	11	61	
x_{90}	1	3	0	1	3	0	7	7	6	62	
x_{107}	3	14	1	5	14	0	29	34	12	3	
x_{109}	3	16	1	6	16	0	33	39	13	3	
x_{114}	5	21	1	8	21	0	53	52	23	5	
x_{115}	6	33	2	12	33	1	68	83	21	6	
x_{116}	2	12	1	4	12	0	25	31	9	2	
x_{131}	2	12	1	4	12	0	25	31	9	2	
x_{166}	-12	-32	-19	-13	-29	-1	-35	-36	-28	-86	
	x_{14}	x_{15}	x_{16}	x_{27}	x_{28}	x_{34}	x_{41}	x_{42}	x_{49}	x_{53}	

x ₆₉	22									
x ₈₅	19	4								
x ₉₀	11	2	38							
x ₁₀₇	21	78	4	2						
x ₁₀₉	23	14	4	3	13					
x ₁₁₄	36	19	7	4	18	20				
x ₁₁₅	45	31	9	5	29	35	43			
x ₁₁₆	17	11	3	2	11	43	16	33		
x ₁₃₁	17	11	3	2	11	43	16	33	99	
x ₁₆₆	-37	-14	-73	-66	-13	-15	-21	-28	-13	-13
	x ₆₂	x ₆₉	x ₈₅	x ₉₀	x ₁₀₇	x ₁₀₉	x ₁₁₄	x ₁₁₅	x ₁₁₆	x ₁₃₁

D⁺ BRANCHING RATIOS

Some now-obsolete measurements have been omitted from these Listings.

c-quark decays

$\Gamma(c \rightarrow e^+ \text{ anything})/\Gamma(c \rightarrow \text{ anything})$

For the Summary Table, we only use the average of e^+ and μ^+ measurements from $Z^0 \rightarrow c\bar{c}$ decays; see the second data block below.

VALUE	EVTS	DOCUMENT ID	TECN	COMMENT
0.103±0.009^{+0.009}_{-0.008}	378	³ ABBIENDI	99K OPAL	$Z^0 \rightarrow c\bar{c}$

³ ABBIENDI 99K uses the excess of right-sign over wrong-sign leptons opposite reconstructed $D^*(2010)^+ \rightarrow D^0\pi^+$ decays in $Z^0 \rightarrow c\bar{c}$.

$\Gamma(c \rightarrow \mu^+ \text{ anything})/\Gamma(c \rightarrow \text{ anything})$

For the Summary Table, we only use the average of e^+ and μ^+ measurements from $Z^0 \rightarrow c\bar{c}$ decays; see the next data block.

VALUE	EVTS	DOCUMENT ID	TECN	COMMENT
0.082±0.005 OUR AVERAGE				
0.073±0.008±0.002	73	KAYIS-TOPAK.05	CHRS	ν_μ emulsion
0.095±0.007 ^{+0.014} _{-0.013}	2829	ASTIER	00D NOMD	$\nu_\mu Fe \rightarrow \mu^- \mu^+ X$
0.090±0.007 ^{+0.007} _{-0.006}	476	⁴ ABBIENDI	99K OPAL	$Z^0 \rightarrow c\bar{c}$
0.086±0.017 ^{+0.008} _{-0.007}	69	⁵ ALBRECHT	92F ARG	$e^+ e^- \approx 10 \text{ GeV}$
0.078±0.009±0.012		ONG	88 MRK2	$e^+ e^- 29 \text{ GeV}$
0.078±0.015±0.02		BARTEL	87 JADE	$e^+ e^- 34.6 \text{ GeV}$
0.082±0.012 ^{+0.02} _{-0.01}		ALTHOFF	84G TASS	$e^+ e^- 34.5 \text{ GeV}$
• • • We do not use the following data for averages, fits, limits, etc. • • •				
0.093±0.009±0.009	88	KAYIS-TOPAK.02	CHRS	See KAYIS-TOPAKSU 05
0.089±0.018±0.025		BARTEL	85J JADE	See BARTEL 87

⁴ ALBRECHT 92F uses the excess of right-sign over wrong-sign leptons opposite reconstructed $D^*(2010)^+ \rightarrow D^0\pi^+$ decays in $Z^0 \rightarrow c\bar{c}$.

⁵ ALBRECHT 92F uses the excess of right-sign over wrong-sign leptons in a sample of events tagged by fully reconstructed $D^*(2010)^+ \rightarrow D^0\pi^+$ decays.

$\Gamma(c \rightarrow \ell^+ \text{anything})/\Gamma(c \rightarrow \text{anything})$

This is an average (not a sum) of e^+ and μ^+ measurements.

VALUE	EVTS	DOCUMENT ID	TECN	COMMENT
0.096 ± 0.004 OUR AVERAGE				
0.0958 ± 0.0042 ± 0.0028	1828	⁶ ABREU	000 DLPH	$Z^0 \rightarrow c\bar{c}$
0.095 ± 0.006 ± 0.007	854	⁷ ABBIENDI	99K OPAL	$Z^0 \rightarrow c\bar{c}$

⁶ ABREU 000 uses leptons opposite fully reconstructed $D^*(2010)^+$, D^+ , or D^0 mesons.

⁷ ABBIENDI 99K uses the excess of right-sign over wrong-sign leptons opposite reconstructed $D^*(2010)^+ \rightarrow D^0\pi^+$ decays in $Z^0 \rightarrow c\bar{c}$.

$\Gamma(c \rightarrow D^*(2010)^+ \text{anything})/\Gamma(c \rightarrow \text{anything})$

VALUE	EVTS	DOCUMENT ID	TECN	COMMENT
0.255 ± 0.015 ± 0.008	2371	⁸ ABREU	000 DLPH	$Z^0 \rightarrow c\bar{c}$

⁸ ABREU 000 uses slow pions opposite fully reconstructed $D^*(2010)^+$, D^+ , or D^0 mesons as a signal of $D^*(2010)^-$ production.

Inclusive modes

$\Gamma(e^+ \text{anything})/\Gamma_{\text{total}}$

Γ_1/Γ

VALUE	EVTS	DOCUMENT ID	TECN	COMMENT
0.172 ± 0.019 OUR AVERAGE				
0.20 ± 0.09		AGUILAR-...	87E HYBR	$\pi p, pp$ 360, 400 GeV
-0.07				
0.170 ± 0.019 ± 0.007	158	BALTRUSAIT..85B	MRK3	$e^+ e^-$ 3.77 GeV
0.168 ± 0.064	23	SCHINDLER	81	MRK2 $e^+ e^-$ 3.771 GeV
• • • We do not use the following data for averages, fits, limits, etc. • • •				
0.220 ± 0.044		BACINO	80	DLCO $e^+ e^-$ 3.77 GeV
-0.022				

$D^+ \text{and} D^0 \rightarrow (e^+ \text{anything}) / (\text{total } D^+ \text{ and } D^0)$

If measured at the $\psi(3770)$, this quantity is a weighted average of D^+ (44%) and D^0 (56%) branching fractions. Only experiments at $E_{\text{cm}} = 3.77$ GeV are included in the average here. We don't put this result in the Summary Table.

VALUE	EVTS	DOCUMENT ID	TECN	COMMENT
0.110 ± 0.011 OUR AVERAGE		Error includes scale factor of 1.1.		
0.117 ± 0.011	295	BALTRUSAIT..85B	MRK3	$e^+ e^-$ 3.77 GeV
0.10 ± 0.032		⁹ SCHINDLER	81	MRK2 $e^+ e^-$ 3.771 GeV
0.072 ± 0.028		FELLER	78	MRK1 $e^+ e^-$ 3.772 GeV

• • • We do not use the following data for averages, fits, limits, etc. • • •

$0.096 \pm 0.004 \pm 0.011$	2207	¹⁰ ALBRECHT	96C ARG	$e^+ e^- \approx 10$ GeV
$0.134 \pm 0.015 \pm 0.010$		¹¹ ABE	93E VNS	$e^+ e^- 58$ GeV
$0.098 \pm 0.009^{+0.006}_{-0.005}$	240	¹² ALBRECHT	92F ARG	$e^+ e^- \approx 10$ GeV
$0.096 \pm 0.007 \pm 0.015$		¹³ ONG	88 MRK2	$e^+ e^- 29$ GeV
$0.116^{+0.011}_{-0.009}$		¹³ PAL	86 DLCO	$e^+ e^- 29$ GeV
$0.091 \pm 0.009 \pm 0.013$		¹³ AIHARA	85 TPC	$e^+ e^- 29$ GeV
$0.092 \pm 0.022 \pm 0.040$		¹³ ALTHOFF	84J TASS	$e^+ e^- 34.6$ GeV
0.091 ± 0.013		¹³ KOOP	84 DLCO	See PAL 86
0.08 ± 0.015		¹⁴ BACINO	79 DLCO	$e^+ e^- 3.772$ GeV

⁹ Isolates D^+ and $D^0 \rightarrow e^+ X$ and weights for relative production (44%–56%).

¹⁰ ALBRECHT 96C uses e^- in the hemisphere opposite to $D^{*+} \rightarrow D^0 \pi^+$ events.

¹¹ ABE 93E also measures forward-backward asymmetries and fragmentation functions for c and b quarks.

¹² ALBRECHT 92F uses the excess of right-sign over wrong-sign leptons in a sample of events tagged by fully reconstructed $D^*(2010)^+ \rightarrow D^0 \pi^+$ decays.

¹³ Average BR for charm $\rightarrow e^+ X$. Unlike at $E_{cm} = 3.77$ GeV, the admixture of charmed mesons is unknown.

¹⁴ Not independent of BACINO 80 measurements of $\Gamma(e^+ \text{anything})/\Gamma_{\text{total}}$ for the D^+ and D^0 separately.

$\Gamma(K^- \text{anything})/\Gamma_{\text{total}}$ Γ_2/Γ

VALUE	EVTS	DOCUMENT ID	TECN	COMMENT
0.275 ± 0.024 OUR AVERAGE				
$0.278^{+0.036}_{-0.031}$		¹⁵ BARLAG	92C ACCM	π^- Cu 230 GeV
$0.271 \pm 0.023 \pm 0.024$		COFFMAN	91 MRK3	$e^+ e^- 3.77$ GeV
• • • We do not use the following data for averages, fits, limits, etc. • • •				
0.17 ± 0.07		AGUILAR-...	87E HYBR	$\pi p, pp$ 360, 400 GeV
$0.16^{+0.08}_{-0.07}$		AGUILAR-...	86B HYBR	See AGUILAR-BENITEZ 87E
0.19 ± 0.05	26	SCHINDLER	81 MRK2	$e^+ e^- 3.771$ GeV
0.10 ± 0.07	3	VUILLEMIN	78 MRK1	$e^+ e^- 3.772$ GeV

¹⁵ BARLAG 92C computes the branching fraction using topological normalization.

$[\Gamma(\bar{K}^0 \text{anything}) + \Gamma(K^0 \text{anything})]/\Gamma_{\text{total}}$ Γ_3/Γ

VALUE	EVTS	DOCUMENT ID	TECN	COMMENT
$0.612 \pm 0.065 \pm 0.043$				
• • • We do not use the following data for averages, fits, limits, etc. • • •		COFFMAN	91 MRK3	$e^+ e^- 3.77$ GeV
0.52 ± 0.18	15	SCHINDLER	81 MRK2	$e^+ e^- 3.771$ GeV
0.39 ± 0.29	3	VUILLEMIN	78 MRK1	$e^+ e^- 3.772$ GeV

$\Gamma(K^+ \text{anything})/\Gamma_{\text{total}}$ Γ_4/Γ

VALUE	EVTS	DOCUMENT ID	TECN	COMMENT
$0.055 \pm 0.013 \pm 0.009$				
• • • We do not use the following data for averages, fits, limits, etc. • • •		COFFMAN	91 MRK3	$e^+ e^- 3.77$ GeV
$0.08^{+0.06}_{-0.05}$		AGUILAR-...	87E HYBR	$\pi p, pp$ 360, 400 GeV
0.06 ± 0.04	12	SCHINDLER	81 MRK2	$e^+ e^- 3.771$ GeV
0.06 ± 0.06	2	VUILLEMIN	78 MRK1	$e^+ e^- 3.772$ GeV

$\Gamma(K^*(892)^0 \text{anything})/\Gamma_{\text{total}}$

VALUE	EVTS
0.232 ± 0.045 ± 0.030	189 ± 36

DOCUMENT ID	TECN	COMMENT
ABLIKIM	05P BES	$e^+ e^- \approx 3773 \text{ MeV}$

 Γ_5/Γ $\Gamma(K^*(892)^0 \text{anything})/\Gamma_{\text{total}}$

VALUE	CL%
<0.066	90

DOCUMENT ID	TECN	COMMENT
ABLIKIM	05P BES	$e^+ e^- \approx 3773 \text{ MeV}$

 Γ_6/Γ $D^+ \text{ and } D^0 \rightarrow (\eta \text{ anything}) / (\text{total } D^+ \text{ and } D^0)$

If measured at the $\psi(3770)$, this quantity is a weighted average of D^+ (44%) and D^0 (56%) branching fractions. Only the experiment at $E_{\text{cm}} = 3.77 \text{ GeV}$ is used.

VALUE	DOCUMENT ID	TECN	COMMENT
<0.13	PARTTRIDGE	81 CBAL	$e^+ e^- 3.77 \text{ GeV}$

• • • We do not use the following data for averages, fits, limits, etc. • • •

<0.02	16 BRANDELIK	79 DASP	$e^+ e^- 4.03 \text{ GeV}$
-------	--------------	---------	----------------------------

¹⁶ The BRANDELIK 79 result is based on the absence of an η signal at $E_{\text{cm}} = 4.03 \text{ GeV}$. PARTRIDGE 81 observes a substantially higher η cross section at 4.03 GeV.

 $\Gamma(\phi \text{ anything})/\Gamma_{\text{total}}$ Γ_8/Γ

VALUE	CL%	DOCUMENT ID	TECN	COMMENT
<0.018	90	17 BAI	00C BES	$e^+ e^- \rightarrow D\bar{D}^*, D^*\bar{D}^*$

¹⁷ BAI 00C finds the average (ϕ anything) branching fraction for the 4.03-GeV mix of D^+ and D^0 mesons to be $(1.34 \pm 0.52 \pm 0.12)\%$.

 $\Gamma(\phi e^+ \text{ anything})/\Gamma_{\text{total}}$ Γ_9/Γ

VALUE	CL%	DOCUMENT ID	TECN	COMMENT
<0.016	90	BAI	00C BES	$e^+ e^- \rightarrow D\bar{D}^*, D^*\bar{D}^*$

Leptonic and semileptonic modes $\Gamma(e^+ \nu_e)/\Gamma_{\text{total}}$ Γ_{11}/Γ

VALUE	CL%	DOCUMENT ID	TECN	COMMENT
<2.4 × 10⁻⁵	90	ARTUSO	05A CLEO	$e^+ e^- \text{ at } \psi(3770)$

 $\Gamma(\mu^+ \nu_\mu)/\Gamma_{\text{total}}$ Γ_{12}/Γ

See the "Note on Pseudoscalar-Meson Decay Constants" in the Listings for the π^\pm .

VALUE (units 10 ⁻⁴)	EVTS	DOCUMENT ID	TECN	COMMENT
4.40 ± 0.66 ± 0.09	47 ± 7	18 ARTUSO	05A CLEO	$e^+ e^- \text{ at } \psi(3770)$

• • • We do not use the following data for averages, fits, limits, etc. • • •

12.2	^{+11.1} - 5.3	± 1.0	3	19 ABLIKIM	05D BES	$e^+ e^- \approx 3.773 \text{ GeV}$
------	---------------------------	-------	---	------------	---------	-------------------------------------

3.5	± 1.4	± 0.6	7	20 BONVICINI	04A CLEO	Incl. in ARTUSO 05A
-----	-------	-------	---	--------------	----------	---------------------

8	⁺¹⁶ - 5	⁺⁵ - 2	1	21 BAI	98B BES	$e^+ e^- \rightarrow D^*+ D^-$
---	-----------------------	----------------------	---	--------	---------	--------------------------------

- 18 ARTUSO 05A obtains $f_{D^+} = 222.6 \pm 16.7^{+2.8}_{-3.4}$ MeV from this measurement.
 19 ABLIKIM 05D finds a background-subtracted 2.67 ± 1.74 $D^+ \rightarrow e^+ \nu_e$ events, and from this obtains $f_{D^+} = 371^{+129}_{-119} \pm 25$ MeV.
 20 BONVICINI 04A finds eight events with an estimated background of one, and from the branching fraction obtains $f_{D^+} = 202 \pm 41 \pm 17$ MeV.
 21 BAI 98B obtains $f_{D^+} = (300^{+180+80}_{-150-40})$ MeV from this measurement.

 $\Gamma(\bar{K}^0 e^+ \nu_e)/\Gamma_{\text{total}}$ Γ_{14}/Γ

<u>VALUE</u>	<u>EVTS</u>	<u>DOCUMENT ID</u>	<u>TECN</u>	<u>COMMENT</u>
--------------	-------------	--------------------	-------------	----------------

0.086 ± 0.005 OUR FIT**0.087 ± 0.005 OUR AVERAGE**

$0.0895 \pm 0.0159 \pm 0.0067$	34 ± 6	22 ABLIKIM	05A BES	$e^+ e^-$ at $\psi(3770)$
$0.0871 \pm 0.0038 \pm 0.0037$	545 ± 24	23 HUANG	05B CLEO	$e^+ e^-$ at $\psi(3770)$

• • • We do not use the following data for averages, fits, limits, etc. • • •

$0.06^{+0.022}_{-0.013} \pm 0.007$	13	BAI	91 MRK3	$e^+ e^- \approx 3.77$ GeV
------------------------------------	----	-----	---------	----------------------------

- 22 The ABLIKIM 05A result together with the $D^0 \rightarrow K^- e^+ \nu_e$ branching fraction of ABLIKIM 04C and Particle Data Group lifetimes gives $\Gamma(D^0 \rightarrow K^- e^+ \nu_e) / \Gamma(D^+ \rightarrow \bar{K}^0 e^+ \nu_e) = 1.08 \pm 0.22 \pm 0.07$; isospin invariance predicts the ratio is 1.0.
 23 HUANG 05B finds $\Gamma(D^0 \rightarrow K^- e^+ \nu_e) / \Gamma(D^+ \rightarrow \bar{K}^0 e^+ \nu_e) = 1.00 \pm 0.05 \pm 0.04$; isospin invariance predicts the ratio is 1.0.

 $\Gamma(\bar{K}^0 e^+ \nu_e)/\Gamma(K_S^0 \pi^+)$ Γ_{14}/Γ_{41}

<u>VALUE</u>	<u>EVTS</u>	<u>DOCUMENT ID</u>	<u>TECN</u>	<u>COMMENT</u>
--------------	-------------	--------------------	-------------	----------------

5.8 ± 0.4 OUR FIT**5.20 ± 0.70 ± 0.52**

- 24 BEAN 93C uses $\bar{K}^0 \mu^+ \nu_\mu$ as well as $\bar{K}^0 e^+ \nu_e$ events and makes a small phase-space adjustment to the number of the μ^+ events to use them as e^+ events. The value given is twice that in BEAN 93C because we are using $K_S^0 \pi^+$ and not $\bar{K}^0 \pi^+$, in the denominator.

 $\Gamma(\bar{K}^0 e^+ \nu_e)/\Gamma(K^- \pi^+ \pi^+)$ Γ_{14}/Γ_{42}

<u>VALUE</u>	<u>EVTS</u>	<u>DOCUMENT ID</u>	<u>TECN</u>	<u>COMMENT</u>
--------------	-------------	--------------------	-------------	----------------

• • • We do not use the following data for averages, fits, limits, etc. • • •

$0.66 \pm 0.09 \pm 0.14$		ANJOS	91C E691	γ Be 80–240 GeV
--------------------------	--	-------	----------	------------------------

 $\Gamma(\bar{K}^0 \mu^+ \nu_\mu)/\Gamma_{\text{total}}$ Γ_{15}/Γ

<u>VALUE</u>	<u>EVTS</u>	<u>DOCUMENT ID</u>	<u>TECN</u>	<u>COMMENT</u>
--------------	-------------	--------------------	-------------	----------------

• • • We do not use the following data for averages, fits, limits, etc. • • •

$0.07^{+0.028}_{-0.016} \pm 0.012$	14	BAI	91 MRK3	$e^+ e^- \approx 3.77$ GeV
------------------------------------	----	-----	---------	----------------------------

 $\Gamma(\bar{K}^0 \mu^+ \nu_\mu)/\Gamma(K^- \pi^+ \pi^+)$ Γ_{15}/Γ_{42}

<u>VALUE</u>	<u>EVTS</u>	<u>DOCUMENT ID</u>	<u>TECN</u>	<u>COMMENT</u>
--------------	-------------	--------------------	-------------	----------------

1.00 ± 0.08 OUR FIT**1.019 ± 0.076 ± 0.065**

$1.019 \pm 0.076 \pm 0.065$	555 ± 39	LINK	04E FOCS	γ nucleus, $\bar{E}_\gamma \approx 180$ GeV
-----------------------------	--------------	------	----------	--

$\Gamma(\bar{K}^0 \mu^+ \nu_\mu)/\Gamma(\mu^+ \text{anything})$ Γ_{15}/Γ_{10}

VALUE	EVTS	DOCUMENT ID	COMMENT
• • • We do not use the following data for averages, fits, limits, etc. • • •			
0.76 \pm 0.06	84	25 AOKI	88 π^- emulsion
25 From topological branching ratios in emulsion with an identified muon.			

 $\Gamma(K^- \pi^+ e^+ \nu_e)/\Gamma_{\text{total}}$ Γ_{16}/Γ

VALUE	CL%	EVTS	DOCUMENT ID	TECN	COMMENT
0.045 \pm 0.010 OUR FIT Error includes scale factor of 1.1.					
0.035 \pm 0.012 \pm 0.004		14	26 BAI	91 MRK3	$e^+ e^- \approx 3.77$ GeV
• • • We do not use the following data for averages, fits, limits, etc. • • •					
<0.057		90	27 AGUILAR-...	87F HYBR	$\pi p, pp$ 360, 400 GeV
26 BAI 91 finds that a fraction $0.79 \pm 0.15 \pm 0.09$ of combined D^+ and D^0 decays to $\bar{K} \pi e^+ \nu_e$ (24 events) are $\bar{K}^*(892) e^+ \nu_e$.					
27 AGUILAR-BENITEZ 87F computes the branching fraction using topological normalization.					

 $\Gamma(\bar{K}^*(892)^0 e^+ \nu_e)/\Gamma_{\text{total}}$ Γ_{27}/Γ Unseen decay modes of $\bar{K}^*(892)^0$ are included.

VALUE	EVTS	DOCUMENT ID	TECN	COMMENT
0.0561 \pm 0.0031 OUR FIT Error includes scale factor of 1.1.				
0.0556 \pm 0.0027 \pm 0.0023	422 ± 21	28 HUANG	05B CLEO	$e^+ e^-$ at $\psi(3770)$
28 HUANG 05B finds $\Gamma(D^0 \rightarrow K^{*-} e^+ \nu_e) / \Gamma(D^+ \rightarrow \bar{K}^{*0} e^+ \nu_e) = 0.98 \pm 0.08 \pm 0.04$; isospin invariance predicts the ratio is 1.0.				

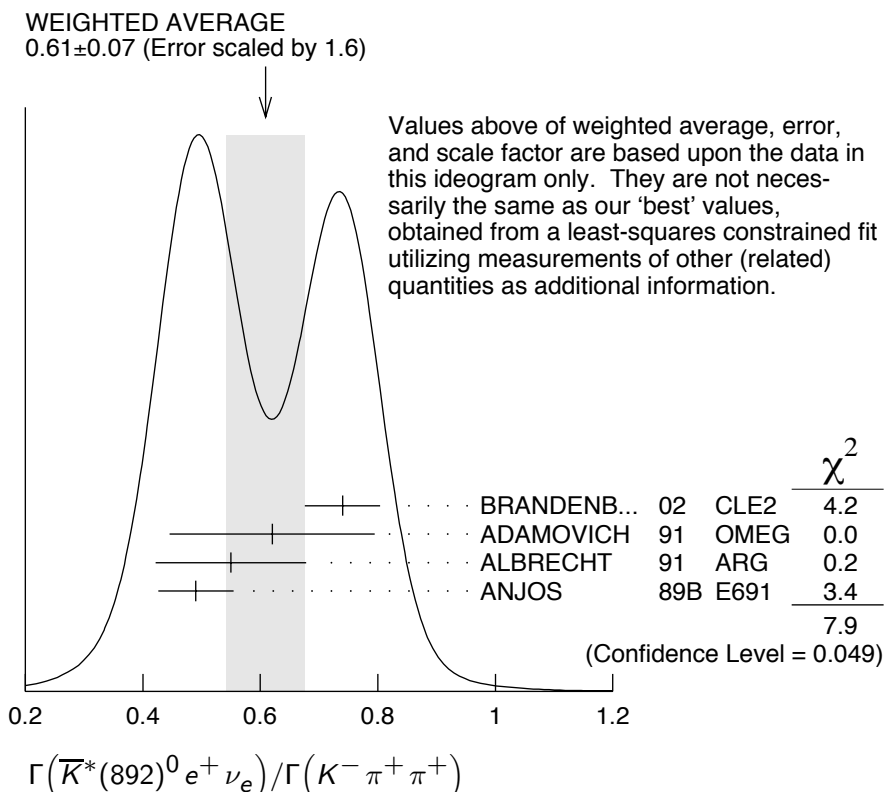
 $\Gamma(\bar{K}^*(892)^0 e^+ \nu_e)/\Gamma(K^- \pi^+ e^+ \nu_e)$ Γ_{27}/Γ_{16} Unseen decay modes of the $\bar{K}^*(892)^0$ are included. See the end of the D^+ Listings for measurements of $D^+ \rightarrow \bar{K}^*(892)^0 \ell^+ \nu_\ell$ form-factor ratios.

VALUE	EVTS	DOCUMENT ID	TECN	COMMENT
1.23 \pm 0.23 OUR FIT Error includes scale factor of 1.2.				
1.0 \pm 0.3	35	ADAMOVICH	91 OMEG	π^- 340 GeV

 $\Gamma(\bar{K}^*(892)^0 e^+ \nu_e)/\Gamma(K^- \pi^+ \pi^+)$ Γ_{27}/Γ_{42} Unseen decay modes of the $\bar{K}^*(892)^0$ are included. See the end of the D^+ Listings for measurements of $D^+ \rightarrow \bar{K}^*(892)^0 \ell^+ \nu_\ell$ form-factor ratios.

VALUE	EVTS	DOCUMENT ID	TECN	COMMENT
0.590 \pm 0.035 OUR FIT Error includes scale factor of 1.2.				
0.61 \pm 0.07 OUR AVERAGE				Error includes scale factor of 1.6. See the ideogram below.
0.74 \pm 0.04 \pm 0.05		BRANDENB...	02 CLE2	$e^+ e^- \approx \gamma(4S)$
0.62 \pm 0.15 \pm 0.09	35	ADAMOVICH	91 OMEG	π^- 340 GeV
0.55 \pm 0.08 \pm 0.10	880	ALBRECHT	91 ARG	$e^+ e^- \approx 10.4$ GeV
0.49 \pm 0.04 \pm 0.05		ANJOS	89B E691	Photoproduction
• • • We do not use the following data for averages, fits, limits, etc. • • •				
0.67 \pm 0.09 \pm 0.07	710	29 BEAN	93C CLE2	See BRANDENBURG 02

²⁹ BEAN 93C uses $\bar{K}^*(892)^0 \mu^+ \nu_\mu$ as well as $\bar{K}^*(892)^0 e^+ \nu_e$ events and makes a small phase-space adjustment to the number of the μ^+ events to use them as e^+ events.



$\Gamma(K^- \pi^+ e^+ \nu_e \text{ nonresonant}) / \Gamma_{\text{total}}$

Γ_{18}/Γ

VALUE	CL%	DOCUMENT ID	TECN	COMMENT
<0.007	90	30 ANJOS	89B E691	Photoproduction

³⁰ ANJOS 89B assumes a $\Gamma(D^+ \rightarrow K^- \pi^+ \pi^+)/\Gamma_{\text{total}} = 9.1 \pm 1.3 \pm 0.4\%$.

$\Gamma(K^- \pi^+ \mu^+ \nu_\mu) / \Gamma(\bar{K}^0 \mu^+ \nu_\mu)$

Γ_{19}/Γ_{15}

VALUE	EVTS	DOCUMENT ID	TECN	COMMENT
0.417±0.030±0.023	555 ± 39	LINK	04E FOCS	γ nucleus, $\bar{E}_\gamma \approx 180$ GeV

$\Gamma(\bar{K}^*(892)^0 \mu^+ \nu_\mu) / \Gamma_{\text{total}}$

Γ_{28}/Γ

Unseen decay modes of the $\bar{K}^*(892)^0$ are included. See the end of the D^+ Listings for measurements of $D^+ \rightarrow \bar{K}^*(892)^0 \ell^+ \nu_\ell$ form-factor ratios.

VALUE	EVTS	DOCUMENT ID	TECN	COMMENT
• • • We do not use the following data for averages, fits, limits, etc. • • •				

$0.0325 \pm 0.0071 \pm 0.0075$ 224 ³¹ KODAMA 92C E653 π^- emulsion 600 GeV

³¹ KODAMA 92C measures $\Gamma(D^+ \rightarrow \bar{K}^*(892)^0 \mu^+ \nu_\mu) / \Gamma(D^0 \rightarrow K^- \mu^+ \nu_\mu) = 0.43 \pm 0.09 \pm 0.09$ and then uses $\Gamma(D^0 \rightarrow K^- \mu^+ \nu_\mu) = (7.0 \pm 0.7) \times 10^{10} \text{ s}^{-1}$ to get the quoted branching fraction. See also the footnote to KODAMA 92C in the second data block below.

$\Gamma(\bar{K}^*(892)^0 \mu^+ \nu_\mu) / \Gamma(\bar{K}^0 \mu^+ \nu_\mu)$ Γ_{28}/Γ_{15}

Unseen decay modes of the $\bar{K}^*(892)^0$ are included.

<u>VALUE</u>	<u>EVTS</u>	<u>DOCUMENT ID</u>	<u>TECN</u>	<u>COMMENT</u>
0.58 ± 0.05 OUR FIT				
0.594 ± 0.043 ± 0.033	555 ± 39	LINK	04E FOCS	γ nucleus, $\bar{E}_\gamma \approx 180$ GeV

 $\Gamma(\bar{K}^*(892)^0 \mu^+ \nu_\mu) / \Gamma(K^- \pi^+ \pi^+)$ Γ_{28}/Γ_{42}

Unseen decay modes of the $\bar{K}^*(892)^0$ are included. See the end of the D^+ Listings for measurements of $D^+ \rightarrow \bar{K}^*(892)^0 \ell^+ \nu_\ell$ form-factor ratios.

<u>VALUE</u>	<u>EVTS</u>	<u>DOCUMENT ID</u>	<u>TECN</u>	<u>COMMENT</u>
0.58 ± 0.05 OUR FIT				Error includes scale factor of 1.1.
0.57 ± 0.06 OUR AVERAGE				Error includes scale factor of 1.2.
0.72 ± 0.10 ± 0.05		BRANDENB...	02 CLE2	$e^+ e^- \approx \gamma(4S)$
0.56 ± 0.04 ± 0.06	875	FRABETTI	93E E687	γ Be $\bar{E}_\gamma \approx 200$ GeV
0.46 ± 0.07 ± 0.08	224	32 KODAMA	92C E653	π^- emulsion 600 GeV
• • • We do not use the following data for averages, fits, limits, etc. • • •				
0.602 ± 0.010 ± 0.021	12k	33 LINK	02J FOCS	γ nucleus, ≈ 180 GeV
32 KODAMA 92C also uses the same $\bar{K}^*0 \mu^+ \nu_\mu$ events normalizing instead with $D^0 \rightarrow K^- \mu^+ \nu_\mu$ events, as reported in the second data block above.				

33 This LINK 02J result includes the effects of an interference of a small S -wave $K^- \pi^+$ amplitude with the dominant \bar{K}^*0 amplitude. (The interference effect is reported in LINK 02E.) This result is redundant with results of LINK 04E elsewhere in these Listings.

 $\Gamma(K^- \pi^+ \mu^+ \nu_\mu \text{ nonresonant}) / \Gamma(K^- \pi^+ \mu^+ \nu_\mu)$ Γ_{21}/Γ_{19}

<u>VALUE</u>	<u>EVTS</u>	<u>DOCUMENT ID</u>	<u>TECN</u>	<u>COMMENT</u>
0.0530 ± 0.0074 ± 0.0099	14k	LINK	05I FOCS	γ nucleus, $\bar{E}_\gamma \approx 180$ GeV
• • • We do not use the following data for averages, fits, limits, etc. • • •				
0.083 ± 0.029		FRABETTI	93E E687	< 0.12 (90% CL)

 $\Gamma((\bar{K}^*(892)\pi)^0 e^+ \nu_e) / \Gamma_{\text{total}}$ Γ_{22}/Γ

Unseen decay modes of the $\bar{K}^*(892)$ are included.

<u>VALUE</u>	<u>CL%</u>	<u>DOCUMENT ID</u>	<u>TECN</u>	<u>COMMENT</u>
<0.012	90	ANJOS	92 E691	Photoproduction

 $\Gamma((\bar{K}\pi\pi)^0 e^+ \nu_e \text{ non-} \bar{K}^*(892)) / \Gamma_{\text{total}}$ Γ_{23}/Γ

<u>VALUE</u>	<u>CL%</u>	<u>DOCUMENT ID</u>	<u>TECN</u>	<u>COMMENT</u>
<0.009	90	ANJOS	92 E691	Photoproduction

 $\Gamma(K^- \pi^+ \pi^0 \mu^+ \nu_\mu) / \Gamma(K^- \pi^+ \mu^+ \nu_\mu)$ Γ_{24}/Γ_{19}

<u>VALUE</u>	<u>CL%</u>	<u>DOCUMENT ID</u>	<u>TECN</u>	<u>COMMENT</u>
<0.042	90	FRABETTI	93E E687	γ Be $\bar{E}_\gamma \approx 200$ GeV

 $\Gamma(\bar{K}_1(1270)^0 \mu^+ \nu_\mu) / \Gamma(\bar{K}^*(892)^0 \mu^+ \nu_\mu)$ Γ_{29}/Γ_{28}

<u>VALUE</u>	<u>CL%</u>	<u>DOCUMENT ID</u>	<u>TECN</u>	<u>COMMENT</u>
<0.78	95	ABE	99P CDF	$\bar{p} p$ 1.8 TeV

$\Gamma(\bar{K}^*(1410)^0 \mu^+ \nu_\mu) / \Gamma(\bar{K}^*(892)^0 \mu^+ \nu_\mu)$ Γ_{30}/Γ_{28}

VALUE	CL%	DOCUMENT ID	TECN	COMMENT
$\bullet \bullet \bullet$ We do not use the following data for averages, fits, limits, etc. $\bullet \bullet \bullet$				
<0.60	95	ABE	99P CDF	$\bar{p}p$ 1.8 TeV

 $\Gamma(\bar{K}_0^*(1430)^0 \mu^+ \nu_\mu) / \Gamma(K^- \pi^+ \mu^+ \nu_\mu)$ Γ_{31}/Γ_{19}

Unseen decay modes of the $\bar{K}_0^*(1430)^0$ are included.

VALUE	EVTS	DOCUMENT ID	TECN	COMMENT
<0.0064	90	LINK	05I FOCS	γ nucleus, $\bar{E}_\gamma \approx 180$ GeV

 $\Gamma(\bar{K}_2^*(1430)^0 \mu^+ \nu_\mu) / \Gamma(\bar{K}^*(892)^0 \mu^+ \nu_\mu)$ Γ_{32}/Γ_{28}

VALUE	CL%	DOCUMENT ID	TECN	COMMENT
<0.19	95	ABE	99P CDF	$\bar{p}p$ 1.8 TeV

 $\Gamma(\bar{K}^*(1680)^0 \mu^+ \nu_\mu) / \Gamma(K^- \pi^+ \mu^+ \nu_\mu)$ Γ_{33}/Γ_{19}

Unseen decay modes of the $\bar{K}^*(1680)^0$ are included.

VALUE	EVTS	DOCUMENT ID	TECN	COMMENT
<0.04	90	LINK	05I FOCS	γ nucleus, $\bar{E}_\gamma \approx 180$ GeV

 $\Gamma(\pi^0 e^+ \nu_e) / \Gamma_{\text{total}}$ Γ_{25}/Γ

VALUE	EVTS	DOCUMENT ID	TECN	COMMENT
0.0044 ± 0.0006 ± 0.0003	63 ± 9	³⁴ HUANG	05B CLEO	$e^+ e^-$ at $\psi(3770)$

³⁴ HUANG 05B finds $\Gamma(D^0 \rightarrow \pi^- e^+ \nu_e) / 2 \Gamma(D^+ \rightarrow \pi^0 e^+ \nu_e) = 0.75^{+0.14}_{-0.11} \pm 0.04$; isospin invariance predicts the ratio is 1.0.

 $\Gamma(\pi^0 \ell^+ \nu_\ell) / \Gamma(\bar{K}^0 \ell^+ \nu_\ell)$ Γ_{26}/Γ_{13}

VALUE	EVTS	DOCUMENT ID	TECN	COMMENT
0.046 ± 0.014 ± 0.017	100	³⁵ BARTEL	97 CLE2	$e^+ e^- \approx \gamma(4S)$

$\bullet \bullet \bullet$ We do not use the following data for averages, fits, limits, etc. $\bullet \bullet \bullet$

$0.085 \pm 0.027 \pm 0.014$ 53 ³⁶ ALAM 93 CLE2 See BARTEL 97

³⁵ BARTEL 97 thus directly measures the product of ratios squared of CKM matrix elements and form factors at $q^2=0$: $|V_{cd}/V_{cs}|^2 \cdot |f_+^\pi(0)/f_+^K(0)|^2 = 0.046 \pm 0.014 \pm 0.017$.

³⁶ ALAM 93 thus directly measures the product of ratios squared of CKM matrix elements and form factors at $q^2=0$: $|V_{cd}/V_{cs}|^2 \cdot |f_+^\pi(0)/f_+^K(0)|^2 = 0.085 \pm 0.027 \pm 0.014$.

 $\Gamma(\rho^0 e^+ \nu_e) / \Gamma_{\text{total}}$ Γ_{34}/Γ

VALUE	EVTS	DOCUMENT ID	TECN	COMMENT
0.0022 ± 0.0004 OUR FIT				

0.0021 ± 0.0004 ± 0.0001 27 ± 6 ³⁷ HUANG 05B CLEO $e^+ e^-$ at $\psi(3770)$

³⁷ HUANG 05B finds $\Gamma(D^0 \rightarrow \rho^- e^+ \nu_e) / 2 \Gamma(D^+ \rightarrow \rho^0 e^+ \nu_e) = 1.2^{+0.4}_{-0.3} \pm 0.1$; isospin invariance predicts the ratio is 1.0.

 $\Gamma(\rho^0 e^+ \nu_e) / \Gamma(\bar{K}^*(892)^0 e^+ \nu_e)$ Γ_{34}/Γ_{27}

VALUE	EVTS	DOCUMENT ID	TECN	COMMENT
0.039 ± 0.007 OUR FIT				

0.045 ± 0.014 ± 0.009 49 ³⁸ AITALA 97 E791 π^- nucleus, 500 GeV

³⁸ AITALA 97 explicitly subtracts $D^+ \rightarrow \eta' e^+ \nu_e$ and other backgrounds to get this result.

$\Gamma(\rho^0 \mu^+ \nu_\mu)/\Gamma(\bar{K}^*(892)^0 \mu^+ \nu_\mu)$

Γ_{35}/Γ_{28}

VALUE	EVTS	DOCUMENT ID	TECN	COMMENT
0.061 ± 0.014 OUR AVERAGE				
0.051 ± 0.015 ± 0.009	54	39 AITALA	97 E791	π^- nucleus, 500 GeV
0.079 ± 0.019 ± 0.013	39	40 FRABETTI	97 E687	γ Be, $\bar{E}_\gamma \approx 220$ GeV
• • • We do not use the following data for averages, fits, limits, etc. • • •				
0.044 $^{+0.031}_{-0.025}$ ± 0.014	4	41 KODAMA	93C E653	π^- emulsion 600 GeV

39 AITALA 97 explicitly subtracts $D^+ \rightarrow \eta' \mu^+ \nu_\mu$ and other backgrounds to get this result.

40 Because the reconstruction efficiency for photons is low, this FRABETTI 97 result also includes any $D^+ \rightarrow \eta' \mu^+ \nu_\mu \rightarrow \gamma \rho^0 \mu^+ \nu_\mu$ events in the numerator.

41 This KODAMA 93C result is based on a final signal of $4.0^{+2.8}_{-2.3} \pm 1.3$ events; the estimates of backgrounds that affect this number are somewhat model dependent.

$\Gamma(\omega e^+ \nu_e)/\Gamma_{\text{total}}$

Γ_{36}/Γ

VALUE	EVTS	DOCUMENT ID	TECN	COMMENT
$0.0016^{+0.0007}_{-0.0006} \pm 0.0001$	$7.6^{+3.3}_{-2.7}$	HUANG	05B CLEO	$e^+ e^-$ at $\psi(3770)$

$\Gamma(\phi e^+ \nu_e)/\Gamma_{\text{total}}$

Γ_{37}/Γ

Decay modes of the ϕ not included in the search are corrected for.

VALUE	CL%	DOCUMENT ID	TECN	COMMENT
<0.0209	90	BAI	91 MRK3	$e^+ e^- \approx 3.77$ GeV

$\Gamma(\phi \mu^+ \nu_\mu)/\Gamma_{\text{total}}$

Γ_{38}/Γ

Decay modes of the ϕ not included in the search are corrected for.

VALUE	CL%	DOCUMENT ID	TECN	COMMENT
<0.0372	90	BAI	91 MRK3	$e^+ e^- \approx 3.77$ GeV

$\Gamma(\eta \ell^+ \nu_\ell)/\Gamma(\pi^0 \ell^+ \nu_\ell)$

Γ_{39}/Γ_{26}

VALUE	CL%	DOCUMENT ID	TECN	COMMENT
<1.5	90	BARTEL	97 CLE2	$e^+ e^- \approx \gamma(4S)$

$\Gamma(\eta'(958) \mu^+ \nu_\mu)/\Gamma(\bar{K}^*(892)^0 \mu^+ \nu_\mu)$

Γ_{40}/Γ_{28}

Decay modes of the $\eta'(958)$ not included in the search are corrected for.

VALUE	CL%	DOCUMENT ID	TECN	COMMENT
<0.20	90	KODAMA	93B E653	π^- emulsion 600 GeV

Hadronic modes with a \bar{K} or $\bar{K} \bar{K} \bar{K}$

$\Gamma(K_S^0 \pi^+)/\Gamma_{\text{total}}$

Γ_{41}/Γ

VALUE	EVTS	DOCUMENT ID	TECN	COMMENT
0.0147 ± 0.0006 OUR FIT Error includes scale factor of 1.1.				
0.0155 ± 0.0005 ± 0.0006	2230 ± 60	42 HE	05 CLEO	$e^+ e^-$ at $\psi(3770)$

• • • We do not use the following data for averages, fits, limits, etc. • • •

0.016 ± 0.003 ± 0.001	161	ADLER	88C MRK3	$e^+ e^-$ 3.77 GeV
0.017 ± 0.004	36	43 SCHINDLER	81 MRK2	$e^+ e^-$ 3.771 GeV
0.017 ± 0.006	17	44 PERUZZI	77 MRK1	$e^+ e^-$ 3.77 GeV

⁴² HE 05 uses single- and double-tagged events in an overall fit. The fraction here includes (unobserved) final-state photons.

⁴³ SCHINDLER 81 (MARK-2) measures $\sigma(e^+ e^- \rightarrow \psi(3770)) \times$ branching fraction to be 0.14 ± 0.03 nb. We use the MARK-3 (ADLER 88C) value of $\sigma = 4.2 \pm 0.6 \pm 0.3$ nb.

⁴⁴ PERUZZI 77 (MARK-1) measures $\sigma(e^+ e^- \rightarrow \psi(3770)) \times$ branching fraction to be 0.14 ± 0.05 nb. We use the MARK-3 (ADLER 88C) value of $\sigma = 4.2 \pm 0.6 \pm 0.3$ nb.

$\Gamma(K_S^0 \pi^+)/\Gamma(K^- \pi^+ \pi^+)$

Γ_{41}/Γ_{42}

VALUE	EVTS	DOCUMENT ID	TECN	COMMENT
0.1548 ± 0.0032 OUR FIT		Error includes scale factor of 1.3.		
0.1533 ± 0.0027 OUR AVERAGE				
0.1530 ± 0.0023 ± 0.0016	10.6k	LINK	02B FOCS	γ nucleus, $\bar{E}_\gamma \approx 180$ GeV
0.174 ± 0.012 ± 0.011	473	⁴⁵ BISHAI	97 CLE2	$e^+ e^- \approx \Upsilon(4S)$
0.137 ± 0.015 ± 0.016	264	ANJOS	90C E691	Photoproduction

⁴⁵ See BISHAI 97 for an isospin analysis of $D^+ \rightarrow \bar{K}\pi$ amplitudes.

$\Gamma(K^- \pi^+ \pi^+)/\Gamma_{\text{total}}$

Γ_{42}/Γ

VALUE	EVTS	DOCUMENT ID	TECN	COMMENT
0.0951 ± 0.0034 OUR FIT		Error includes scale factor of 1.1.		
0.0945 ± 0.0033 OUR AVERAGE				
0.095 ± 0.002 ± 0.003	15.1k ± 130	⁴⁶ HE	05 CLEO	$e^+ e^-$ at $\psi(3770)$
0.093 ± 0.006 ± 0.008	1502	⁴⁷ BALEST	94 CLE2	$e^+ e^- \approx \Upsilon(4S)$
0.091 ± 0.013 ± 0.004	1164	ADLER	88C MRK3	$e^+ e^-$ 3.77 GeV
• • • We do not use the following data for averages, fits, limits, etc. • • •				
0.064 $^{+0.015}_{-0.014}$		⁴⁸ BARLAG	92C ACCM	π^- Cu 230 GeV
0.063 $^{+0.028}_{-0.014}$ ± 0.011	8	⁴⁸ AGUILAR-...	87F HYBR	$\pi p, pp$ 360, 400 GeV
0.091 ± 0.019	239	⁴⁹ SCHINDLER 81	MRK2	$e^+ e^-$ 3.771 GeV
0.086 ± 0.020	85	⁵⁰ PERUZZI	77 MRK1	$e^+ e^-$ 3.77 GeV

⁴⁶ HE 05 uses single- and double-tagged events in an overall fit. The fraction here includes (unobserved) final-state photons.

⁴⁷ BALEST 94 measures the ratio of $D^+ \rightarrow K^- \pi^+ \pi^+$ and $D^0 \rightarrow K^- \pi^+$ branching fractions to be $2.35 \pm 0.16 \pm 0.16$ and uses their absolute measurement of the $D^0 \rightarrow K^- \pi^+$ fraction (AKERIB 93).

⁴⁸ AGUILAR-BENITEZ 87F and BARLAG 92C compute the branching fraction by topological normalization.

⁴⁹ SCHINDLER 81 (MARK-2) measures $\sigma(e^+ e^- \rightarrow \psi(3770)) \times$ branching fraction to be 0.38 ± 0.05 nb. We use the MARK-3 (ADLER 88C) value of $\sigma = 4.2 \pm 0.6 \pm 0.3$ nb.

⁵⁰ PERUZZI 77 (MARK-1) measures $\sigma(e^+ e^- \rightarrow \psi(3770)) \times$ branching fraction to be 0.36 ± 0.06 nb. We use the MARK-3 (ADLER 88C) value of $\sigma = 4.2 \pm 0.6 \pm 0.3$ nb.

DALITZ PLOT ANALYSIS FORMALISM

Written January 2006 by D. Asner (Carleton University)

Introduction: Weak nonleptonic decays of D and B mesons are expected to proceed dominantly through resonant two-body decays [1]; see Ref. [2] for a review of resonance phenomenology.

The amplitudes are typically calculated with the Dalitz-plot analysis technique [3], which uses the minimum number of independent observable quantities. For three-body decays of a spin-0 particle to all pseudo-scalar final states, D or $B \rightarrow abc$, the decay rate [4] is

$$\Gamma = \frac{1}{(2\pi)^3 32\sqrt{s^3}} |\mathcal{M}|^2 dm_{ab}^2 dm_{bc}^2, \quad (1)$$

where m_{ij} is the invariant mass of particles i and j . The coefficient of the amplitude includes all kinematic factors, and $|\mathcal{M}|^2$ contains the dynamics. The scatter plot in m_{ab}^2 versus m_{bc}^2 is the Dalitz plot. If $|\mathcal{M}|^2$ is constant, the kinematically allowed region of the plot will be populated uniformly with events. Any variation in the population over the Dalitz plot is due to dynamical rather than kinematical effects. It is straightforward to extend the formalism beyond three-body final states. For N -body final states with only spin-0 particles, phase space has dimension $3N - 7$. Other decays of interest include one vector particle or a fermion/anti-fermion pair (*e.g.*, $B \rightarrow D^*\pi\pi$, $B \rightarrow \bar{\Lambda}_c p\pi$, $B \rightarrow K\ell\ell$) in the final state. For the first case, phase space has dimension $3N - 5$, and for the latter two the dimension is $3N - 4$.

Formalism: The amplitude for the process, $R \rightarrow rc, r \rightarrow ab$ where R is a D or B , r is an intermediate resonance, and a, b, c are pseudo-scalars, is given by

$$\begin{aligned} \mathcal{M}_r(J, L, l, m_{ab}, m_{bc}) &= \sum_{\lambda} \langle ab|r_{\lambda}\rangle T_r(m_{ab}) \langle cr_{\lambda}|R_J\rangle \quad (2) \\ &= Z(J, L, l, \vec{p}, \vec{q}) B_L^R(|\vec{p}|) B_L^r(|\vec{q}|) T_r(m_{ab}). \end{aligned}$$

The sum is over the helicity states λ of r , J is the total angular momentum of R (for D and B decays, $J=0$), L is the orbital

angular momentum between r and c , l is the orbital angular momentum between a and b (the spin of r), \vec{p} and \vec{q} are the momenta of c and of a in the r rest frame, Z describes the angular distribution of the final-state particles, B_L^R and B_L^r are the barrier factors for the production of rc and of ab , and T_r is the dynamical function describing the resonance r . The amplitude for modeling the Dalitz plot is a phenomenological object. Differences in the parametrizations of Z , B_L , and T_r , as well as in the set of resonances r , complicate the comparison of results from different experiments.

Usually the resonances are modeled with a Breit-Wigner form, although some more recent analyses use a K -matrix formalism [5,6,7] with the P -vector approximation [8] to describe the $\pi\pi$ S-wave.

The nonresonant (NR) contribution to $D \rightarrow abc$ is parametrized as constant (S-wave) with no variation in magnitude or phase across the Dalitz plot. The available phase space is much greater for B decays, and the nonresonant contribution to $B \rightarrow abc$ requires a more sophisticated parametrization. Theoretical models of the NR amplitude [9-12] do not reproduce the distributions observed in the data. Experimentally, several parametrizations have been used [13,14].

Barrier Factor B_L : The maximum angular momentum L in a strong decay is limited by the linear momentum q . Decay particles moving slowly with an impact parameter (meson radius) d of order 1 fm have difficulty generating sufficient angular momentum to conserve the spin of the resonance. The Blatt-Weisskopf [15,16] functions B_L , given in Table 1, weight the reaction amplitudes to account for this spin-dependent effect. These functions are normalized to give $B_L = 1$ for $z = (|q|d)^2 = 1$. Another common formulation, B'_L , also in

Table 1, is normalized to give $B'_L = 1$ for $z = z_0 = (|q_0| d)^2$ where q_0 is the value of q when $m_{ab} = m_r$.

Table 1: Blatt-Weisskopf barrier factors.

L	$B_L(q)$	$B'_L(q, q_0)$
0	1	1
1	$\sqrt{\frac{2z}{1+z}}$	$\sqrt{\frac{1+z_0}{1+z}}$
2	$\sqrt{\frac{13z^2}{(z-3)^2+9z}}$	$\sqrt{\frac{(z_0-3)^2+9z_0}{(z-3)^2+9z}}$

where $z = (|q| d)^2$ and $z_0 = (|q_0| d)^2$

Angular distribution: The tensor or Zemach formalism [17,18] and the helicity formalism [19,18] yield identical descriptions of the angular distributions for the decay process $R \rightarrow rc, r \rightarrow ab$ when a, b and c all have spin-0. The angular distributions for $L = 0, 1$, and 2 are given in Table 2. For final-state particles with non-zero spin (*e.g.*, radiative decays), the helicity formalism is required.

Dynamical Function T_r : The dynamical function T_r is derived from the S -matrix formalism. In general, the amplitude that a final state f couples to an initial state i is $S_{fi} = \langle f | S | i \rangle$, where the scattering operator S is unitary and satisfies $SS^\dagger = S^\dagger S = I$. The Lorentz-invariant transition operator \hat{T} is defined by separating the probability that $f = i$, yielding

$$S = I + 2iT = I + 2i \{ \rho \}^{1/2} \hat{T} \{ \rho \}^{1/2}, \quad (3)$$

Table 2: Angular distributions for $L = 0, 1, 2$ where θ is the angle between particles a and c in the rest frame of resonance r , $\sqrt{1 + \zeta^2} = E_r/m_{ab}$ is a relativistic correction, and $E_r = (m_R^2 + m_{ab}^2 - m_c^2)/2m_R$.

$J \rightarrow L + l$	Angular distribution
$0 \rightarrow 0+0$	uniform
$0 \rightarrow 1+1$	$(1 + \zeta^2) \cos^2 \theta$
$0 \rightarrow 2+2$	$\left(\zeta^2 + \frac{3}{2}\right)^2 (\cos^2 \theta - 1/3)^2$

where I is the identity operator, ρ is the diagonal phase-space matrix, with $\rho_{ii} = 2q_i/m$, and q_i is the momentum of a in the r rest frame for decay channel i . In the single-channel S-wave case, $S = e^{2i\delta}$ satisfies unitarity and

$$\hat{T} = \frac{1}{\rho} e^{i\delta} \sin \delta. \quad (4)$$

There are three common formulations of the dynamical function. The Breit-Wigner formalism—the first term in a Taylor expansion about a T -matrix pole—is the simplest formulation. The K -matrix formalism [5] is more general (allowing more than one T -matrix pole and coupled channels while preserving unitarity). The Flatté distribution [20] is used to parametrize resonances near threshold and is equivalent to a one-pole, two-channel K -matrix.

Breit-Wigner Formulation: The common formulation of a Breit-Wigner resonance decaying to spin-0 particles a and b is

$$T_r(m_{ab}) = \frac{1}{m_r^2 - m_{ab}^2 - im_r \Gamma_{ab}(q)}. \quad (5)$$

The “mass-dependent” width Γ is

$$\Gamma = \Gamma_r \left(\frac{q}{q_r} \right)^{2L+1} \left(\frac{m_r}{m_{ab}} \right) B'_L(q, q_0)^2, \quad (6)$$

and $B'_L(q, q_0)$ is the Blatt-Weisskopf barrier factor from Table 1. A Breit-Wigner parametrization best describes isolated, non-overlapping resonances far from the threshold of additional decay channels. For the ρ and $\rho(1450)$ a more complex parametrization suggested by Gounaris-Sakurai [21] is often used [22-26]. Unitarity can be violated when the dynamical function is parametrized as the sum of two or more overlapping Breit-Wigners. The proximity of a threshold to a resonance distorts the line shape from a simple Breit-Wigner. Here the Flatté formula provides a better description and is discussed below.

K-matrix Formalism: The T matrix can be written as

$$\hat{T} = (I - i\hat{K}\rho)^{-1}\hat{K}, \quad (7)$$

where \hat{K} is the Lorentz-invariant K -matrix describing the scattering process and ρ is the phase-space factor. Resonances appear as poles in the K -matrix:

$$\hat{K}_{ij} = \sum_{\alpha} \frac{\sqrt{m_{\alpha}\Gamma_{\alpha i}(m)m_{\alpha}\Gamma_{\alpha j}(m)}}{(m_{\alpha}^2 - m^2)\sqrt{\rho_i\rho_j}}. \quad (8)$$

The K -matrix is real by construction, and so the associated T -matrix respects unitarity.

For a single pole in a single channel, K is

$$K = \frac{m_0\Gamma(m)}{m_0^2 - m^2} \quad (9)$$

and

$$T = K(1 - iK)^{-1} = \frac{m_0\Gamma(m)}{m_0^2 - m^2 - im_0\Gamma(m)}, \quad (10)$$

which is the relativistic Breit-Wigner formula. For two poles in a single channel, K is

$$K = \frac{m_\alpha \Gamma_\alpha(m)}{m_\alpha^2 - m^2} + \frac{m_\beta \Gamma_\beta(m)}{m_\beta^2 - m^2}. \quad (11)$$

If m_α and m_β are far apart relative to the widths, the T matrix is approximately the sum of two Breit-Wigners, $T(K_\alpha + K_\beta) \approx T(K_\alpha) + T(K_\beta)$, each of the form of Eq. (10). This approximation is not valid for two nearby resonances, in which case T can violate unitarity.

This formulation, which applies to S -channel production in two-body scattering, $ab \rightarrow cd$, can be generalized to describe the production of resonances in processes such as the decay of charm mesons. The key assumption here is that the two-body system described by the K -matrix does *not* interact with the rest of the final state [8]. The validity of this assumption varies with the production process and is appropriate for reactions such as $\pi^- p \rightarrow \pi^0 \pi^0 n$ and semileptonic decays such as $D \rightarrow K \pi \ell \nu$. The assumption may be of limited validity for production processes such as $p\bar{p} \rightarrow \pi\pi\pi$ or $D \rightarrow \pi\pi\pi$. In these cases, the two-body Lorentz-invariant amplitude, \hat{F} , is given by

$$\hat{F}_i = (I - i\hat{K}\rho)^{-1}_{ij} \hat{P}_j = (\hat{T}\hat{K}^{-1})_{ij} \hat{P}_j, \quad (12)$$

where P is the production vector that parametrizes the resonance production in the open channels.

For the $\pi\pi$ S-wave, a common formulation of the K -matrix [7,24,25] is

$$K_{ij}(s) = \left[\sum_\alpha \left(\frac{g_i^{(\alpha)} g_j^{(\alpha)}}{m_\alpha^2 - s} \right) + f_{ij}^{sc} \frac{1 - s_0^{sc}}{s - s_0^{sc}} \right] \left[\frac{(s - s_A m_\pi^2 / 2)(1 - s_{A0})}{(s - s_{A0})} \right]. \quad (13)$$

The factor $g_i^{(\alpha)}$ is the real coupling constant of the K -matrix pole m_α to meson channel i ; the parameters f_{ij}^{sc} and s_0^{sc} describe a smooth part of the K -matrix elements; the second factor in square brackets suppresses a false kinematical singularity near the $\pi\pi$ threshold (the Adler zero); and the number 1 has units GeV^2 .

The production vector, with $i = 1$ denoting $\pi\pi$, is

$$P_j(s) = \left[\sum_{\alpha} \left(\frac{\beta_{\alpha} g_j^{(\alpha)}}{m_{\alpha}^2 - s} \right) + f_{1j}^{pr} \frac{1 - s_0^{pr}}{s - s_0^{pr}} \right] \left[\frac{(s - s_A m_{\pi}^2/2)(1 - s_{A0})}{(s - s_{A0})} \right]. \quad (14)$$

where the free parameters of the Dalitz plot fit are the complex production couplings β_{α} and the production-vector background parameters f_{1j}^{pr} and s_0^{pr} . All other parameters are fixed by scattering experiments. Ref. [6] describes the $\pi\pi$ scattering data with a 4-pole, 2-channel ($\pi\pi$, $K\bar{K}$) model, while Ref. [7] describes the scattering data with 5-pole, 5-channel ($\pi\pi$, $K\bar{K}$, $\eta\eta$, $\eta'\eta'$ and 4π) model. The former has been implemented by CLEO [27] and the latter by FOCUS [25] and BABAR [24]. In both cases, only the $\pi\pi$ channel was analyzed. A more complete coupled-channel analysis would simultaneously fit all final states accessible by rescattering.

Flatté Formalism: The Flatté formulation is used when a second channel opens close to a resonance:

$$\hat{T}(m_{ab}) = \frac{1}{m_r^2 - m_{ab}^2 - i(\rho_1 g_1^2 + \rho_2 g_2^2)}, \quad (15)$$

where $g_1^2 + g_2^2 = m_0 \Gamma_r$. This situation occurs in the $\pi\pi$ S-wave where the $f_0(980)$ is near the $K\bar{K}$ threshold, and in the $\pi\eta$ channel where the $a_0(980)$ also lies near the $K\bar{K}$ threshold. For the $a_0(980)$ resonance, the relevant coupling constants are

$g_1 = g_{\pi\eta}$ and $g_2 = g_{KK}$, and the phase space terms are $\rho_1 = \rho_{\pi\eta}$ and $\rho_2 = \rho_{KK}$, where

$$\rho_{ab} = \sqrt{\left(1 - \left(\frac{m_a - m_b}{m_{ab}}\right)^2\right) \left(1 + \left(\frac{m_a - m_b}{m_{ab}}\right)^2\right)}. \quad (16)$$

For the $f_0(980)$ the relevant coupling constants are $g_1 = g_{\pi\pi}$ and $g_2 = g_{KK}$, and the phase space terms are $\rho_1 = \rho_{\pi\pi}$ and $\rho_2 = \rho_{KK}$. The charged and neutral K channels are usually assumed to have the same coupling constant but different phase space factors, due to $m_{K^+} \neq m_{K^0}$; the result is

$$\rho_{KK} = \frac{1}{2} \left(\sqrt{1 - \left(\frac{2m_{K^\pm}}{m_{KK}}\right)^2} + \sqrt{1 - \left(\frac{2m_{K^0}}{m_{KK}}\right)^2} \right). \quad (17)$$

Branching Ratios from Dalitz Plot Fits: A fit to the Dalitz plot distribution using either a Breit-Wigner or a K -matrix formalism factorizes into a resonant contribution to the amplitude \mathcal{M}_j and a complex coefficient, $a_j e^{i\delta_j}$, where a_j and δ_j are real. The definition of a rate of a single process, given a set of amplitudes a_j and phases δ_j , is the square of the relevant matrix element (see Eq. (1)). The “fit fraction” is usually defined as the integral over the Dalitz plot (m_{ab} vs. m_{bc}) of a single amplitude squared divided by the integral over the Dalitz plot of the square of the coherent sum of all amplitudes, or

$$\text{fit fraction}_j = \frac{\int |a_j e^{i\delta_j} \mathcal{M}_j|^2 dm_{ab}^2 dm_{bc}^2}{\int |\sum_k a_k e^{i\delta_k} \mathcal{M}_k|^2 dm_{ab}^2 dm_{bc}^2}, \quad (18)$$

where \mathcal{M}_j is defined in Eq. (2) and described in Ref. [28]. In general, the sum of the fit fractions for all components will not be unity due to interference.

When the K -matrix of Eq. (12) is used to describe a wave (*e.g.*, the $\pi\pi$ S-wave), then \mathcal{M}_j refers to the entire wave. In

this case, it may not be straightforward to separate \mathcal{M}_j into a sum of individual resonances unless these are narrow and well separated.

Reconstruction Efficiency and Resolution: The efficiency for reconstructing an event as a function of position on the Dalitz plot is in general non-uniform. Typically, a Monte Carlo sample generated with a uniform distribution in phase space is used to determine the efficiency. The variation in efficiency across the Dalitz plot varies with experiment and decay mode. Most recent analyses utilize a full GEANT [29] detector simulation.

Finite detector resolution can usually be safely neglected as most resonances are comparatively broad. Notable exceptions where detector resolution effects must be modeled are $\phi \rightarrow K^+K^-$, $\omega \rightarrow \pi^+\pi^-$, and $a_0 \rightarrow \eta\pi^0$. One approach is to convolve the resolution function in the Dalitz-plot variables m_{ab}^2 and m_{bc}^2 with the function that parametrizes the resonant amplitudes. In high-statistics data samples, resolution effects near the phase-space boundary typically contribute to a poor goodness of fit. The momenta of the final-state particles can be recalculated with a D or B mass constraint, which forces the kinematic boundaries of the Dalitz plot to be strictly respected. If the three-body mass is not constrained, then the efficiency (and the parametrization of background) may also depend on the reconstructed mass.

Backgrounds: The contribution of background to the D and B samples varies by experiment and final state. The background naturally falls into five categories: (i) purely combinatoric background containing no resonances; (ii) combinatoric background containing intermediate resonances, such as a real K^{*-} or ρ , plus additional random particles; (iii) final states

containing identical particles as in $D^0 \rightarrow K_S^0\pi^0$ background to $D^0 \rightarrow \pi^+\pi^-\pi^0$ and $B \rightarrow D\pi$ background to $B \rightarrow K\pi\pi$; (iv) mistagged decays such as a real \overline{D}^0 or \overline{B}^0 incorrectly identified as a D^0 or B^0 ; and (v) particle misidentification of the decay products such as $D^+ \rightarrow \pi^-\pi^+\pi^+$ or $D_s^+ \rightarrow K^-K^+\pi^+$ reconstructed as $D^+ \rightarrow K^-\pi^+\pi^+$.

The contribution from combinatoric background with intermediate resonances is distinct from the resonances in the signal because the former do *not* interfere with the latter since they are not from true resonances. Similarly, $D^0 \rightarrow \rho\pi$ and $D^0 \rightarrow K_S^0\pi^0$ do not interfere since strong and weak transitions proceed on different time scales. The usual identification tag of the initial particle as a D^0 or a \overline{D}^0 is the charge of the distinctive slow pion in the decay sequence $D^{*+} \rightarrow D^0\pi_s^+$ or $D^{*-} \rightarrow \overline{D}^0\pi_s^-$. Another possibility is the identification or “tagging” of one of the D mesons from $\psi(3770) \rightarrow D^0\overline{D}^0$, as is done for B mesons from $\Upsilon(4S)$. The mistagged background is subtle and may be mistakenly enumerated in the *signal* fraction determined by a D^0 mass fit. Mistagged decays contain true \overline{D}^0 's or \overline{B}^0 's and so the resonances in the mistagged sample exhibit interference on the Dalitz plot.

References

1. M Bauer, B. Stech and M. Wirbel, Z. Phys. C **34**, 103 (1987); P. Bedaque, A. Das and V.S. Mathur, Phys. Rev. D **49**, 269 (1994); L.-L. Chau and H.-Y. Cheng, Phys. Rev. D **36**, 137 (1987); K. Terasaki, Int. J. Mod. Phys. A **10**, 3207 (1995); F. Buccella, M. Lusignoli and A. Pugliese, Phys. Lett. B **379**, 249 (1996).
2. J. D. Jackson, Nuovo Cim. **34**, 1644 (1964).
3. R. H. Dalitz, Phil. Mag. **44**, 1068 (1953).
4. See the note on Kinematics in this *Review*.
5. S.U. Chung *et al.*, Ann. Physik. **4**, 404 (1995).

6. K. L. Au, D. Morgan and M. R. Pennington, Phys. Rev. D **35**, 1633 (1987).
7. V. V. Anisovich and A. V. Sarantsev, Eur. Phys. J. A **16**, 229 (2003).
8. I. J. R. Aitchison, Nucl. Phys. A **189**, 417 (1972).
9. S. Fajfer, R. J. Oakes and T. N. Pham, Phys. Rev. D **60**, 054029 (1999).
10. H. Y. Cheng and K. C. Yang, Phys. Rev. D **66**, 054015 (2002).
11. S. Fajfer, T. N. Pham and A. Prapotnik, Phys. Rev. D **70**, 034033 (2004).
12. H. Y. Cheng, C. K. Chua and A. Soni, arXiv:hep-ph/0506268.
13. A. Garmash *et al.* (Belle Collab.), Phys. Rev. D **71**, 092003 (2005).
14. B. Aubert *et al.* (BABAR Collab.), arXiv:hep-ex/0507094.
15. J. Blatt and V. Weisskopf, *Theoretical Nuclear Physics*, New York: John Wiley & Sons (1952).
16. F. von Hippel and C. Quigg, Phys. Rev. D **5**, 624, (1972).
17. C. Zemach, Phys. Rev. B **133**, 1201 (1964); C. Zemach, Phys. Rev. B **140**, 97 (1965).
18. V. Filippini, A. Fontana and A. Rotondi, Phys. Rev. D **51**, 2247 (1995).
19. M. Jacob and G. C. Wick, Annals Phys. **7**, 404 (1959) [Annals Phys. **281**, 774 (2000)]; S. U. Chung, Phys. Rev. D **48**, 1225, (1993); J. D. Richman, CALT-68-1148.
20. S. M. Flatté, Phys. Lett. B **63**, 224 (1976).
21. G. J. Gounaris and J. J. Sakurai, Phys. Rev. Lett. **21** 244, (1968).
22. B. Aubert *et al.* (BABAR Collab.), arXiv:hep-ex/0408073.
23. K. Abe *et al.* (Belle Collab.), arXiv:hep-ex/0504013.
24. B. Aubert *et al.* (BABAR Collab.), arXiv:hep-ex/0507101.
25. J. M. Link *et al.* (FOCUS Collab.), Phys. Lett. B **585**, 200 (2004).

26. B. Aubert *et al.* (BABAR Collab.), arXiv:hep-ex/0408099.
27. D. Cronin-Hennessy *et al.* (CLEO Collab.), Phys. Rev. D **72**, 031102 (2005).
28. S. Kopp *et al.* (CLEO Collab.), Phys. Rev. D **63**, 092001 (2001).
29. R. Brun *et al.*, GEANT 3.15, CERN Report No. DD/EE/84-1 (1987); R. Brun *et al.*, GEANT 3.21, CERN Program Library Long Writeup W5013 (1993), unpublished; S. Agostinelli *et al.* (GEANT4 Collab.), Nucl. Instrum. Meth. A **506**, 250 (2003).

REVIEW OF CHARM DALITZ PLOT ANALYSES

Written January 2006 by D. Asner (Carleton University)

For references given here in the form SMITH 05, see the references at the end of the D^+ , D^0 , and D_s^+ Listings.

The formalism of Dalitz-Plot analysis is reviewed in the preceeding note. Table 1 lists reported analyses of D mesons. In the following, we discuss a number of subjects of current interest: (1) $D^0 \rightarrow K_S^0 \pi^+ \pi^-$; (2) $D \rightarrow \pi\pi\pi$: a $\sigma(500)$ or $f_0(600)$; (3) $D^+ \rightarrow K^-\pi^+\pi^+$: a $\kappa(800)$? (4) the $f_0(980)$, $f_0(1370)$ and $f_0(1500)$; (5) doubly Cabibbo-suppressed decays; and (6) CP violation.

$D^0 \rightarrow K_S^0 \pi^+ \pi^-$: Several experiments have analyzed $D^0 \rightarrow K_S^0 \pi^+ \pi^-$ decay (see Table 1). The most precise results are from CLEO (BABAR and Belle, discussed below, have not yet evaluated systematic uncertainties). The CLEO analysis included ten resonances: $K_S^0 \rho^0$, $K_S^0 \omega$, $K_S^0 f_0(980)$, $K_S^0 f_2(1270)$, $K_S^0 f_0(1370)$, $K^*(892)^-\pi^+$, $K_0^*(1430)^-\pi^+$, $K_2^*(1430)^-\pi^+$, $K^*(1680)^-\pi^+$, and the doubly Cabibbo-suppressed mode $K^*(892)^+\pi^-$. CLEO found a much smaller nonresonant contribution than did the earliest experiments.

Table 1: Reported Dalitz plot analyses.

Decay	Experiment(s)
$D^0 \rightarrow K_S^0 \pi^+ \pi^-$	Mark II ^a , Mark III ^b , E691 ^c , E687 ^{d,e} , ARGUS ^f , CLEO ^g , Belle [10,11], BABAR [12,13]
$D^0 \rightarrow K^- \pi^+ \pi^0$	Mark III ^b , E687 ^e , E691 ^c , CLEO ^h
$D^0 \rightarrow \bar{K}^0 K^+ \pi^-$	BABAR [14]
$D^0 \rightarrow K^0 K^- \pi^+$	BABAR [14]
$D^0 \rightarrow K_S^0 \eta \pi^0$	CLEO ⁱ
$D^0 \rightarrow \pi^+ \pi^- \pi^0$	CLEO ^j
$D^0 \rightarrow K_S^0 K^+ K^-$	BABAR ^k
$D^0 \rightarrow K^- K^+ K^- \pi^+$	FOCUS ^l
$D^0 \rightarrow K^- K^+ \pi^- \pi^+$	FOCUS ^m
$D^+ \rightarrow K^- \pi^+ \pi^+$	Mark III ^b , E687 ^e , E691 ^c , E791 ⁿ
$D^+ \rightarrow \bar{K}^0 \pi^+ \pi^0$	Mark III ^b
$D^+ \rightarrow \pi^+ \pi^+ \pi^-$	E687 ^o , E791 ^p , FOCUS [5] ^q
$D^+ \rightarrow K^+ K^- \pi^+$	FOCUS [15], E687 ^r , BABAR ^s
$D^+ \rightarrow K^+ \pi^+ \pi^-$	E791 ^t , FOCUS ^u
$D_s^+ \rightarrow K^+ K^- \pi^+$	E687 ^r , FOCUS [15]
$D_s^+ \rightarrow \pi^+ \pi^+ \pi^-$	E687 ^o , E791 ^v , FOCUS [5]
$D_s^+ \rightarrow K^+ \pi^+ \pi^-$	FOCUS ^u

See the end of the D^+ , D^0 and D_s^+ Listings for these references:

^aSCHINDLER 81, ^bADLER 87, ^cANJOS 93, ^dFRAZETTI 92B, ^eFRAZETTI 94G, ^fALBRECHT 93D, ^gMURAMATSU 02, ^hKOPP 01, ⁱRUBIN 04, ^jCRONIN-HENNESSY 05, ^kAUBERT 05B, ^lLINK 03G, ^mLINK 05C, ⁿAITALA 02, ^oFRAZETTI 97D, ^pAITALA 01B, ^qLINK 04, ^rFRAZETTI 95B, ^sAUBERT 05A, ^tAITALA 97C, ^uLINK 04F, ^vAITALA 01A.

The source of the nonresonant component found in the early

experiments has been attributed to the broad scalar resonances, the $K_0^*(1430)^-$ and $f_0(1370)$, found in the later, larger data samples. The observation of a small but significant nonresonant component in the largest data samples suggests the presence of additional broad scalar resonances, the $\kappa(800)$ and $\sigma(500)$. The CLEO analysis could accommodate the $\sigma(500)$ in lieu of the nonresonant component, but found no evidence for the $\kappa(800)$.

The ten quasi-two-body intermediate states in the CLEO analysis include both CP -even and CP -odd eigenstates and one doubly Cabibbo-suppressed channel. A time-dependent analysis of the Dalitz plot allows simultaneous determination of the strong transition amplitudes and phases and the mixing parameters x and y without phase or sign ambiguity. Using 9 fb^{-1} , CLEO obtained $(-4.5 < x < 9.3)\%$ and $(-6.4 < y < 3.6)\%$ [1].

The decay $D^0 \rightarrow K_S^0\pi^+\pi^-$, important for the study of the CKM angle γ/ϕ_3 [6], is under study by Belle [10,11] and BABAR [12,13]. The CLEO model does not provide a good description of the higher-statistics BABAR and Belle data samples. An improved description is obtained in two ways: First, by adding more Breit-Wigner resonances, including two $\pi\pi$ resonances with arbitrary mass and width, denoted as σ_1 and σ_2 . Second, following the methodology of FOCUS [LINK 04], by applying a K -matrix model to the $\pi\pi$ S-wave [12].

Charm Dalitz-plot analyses might also prove useful for calibrating tools used to study B decays: specifically, to extract α from $B^0 \rightarrow \pi^+\pi^-\pi^0$, β from $b \rightarrow s$ penguin decays (*e.g.*, $B^0 \rightarrow \bar{K}^0 K^+ K^-$), and γ from $B^\pm \rightarrow D K^\pm$ followed by $D^0 \rightarrow \pi^+\pi^-\pi^0$ or $K_S^0 K^+ K^-$ or $K^+ K^-\pi^0$, in addition to the well-studied $D^0 \rightarrow K_S^0\pi^+\pi^-$ [2, 3].

$D \rightarrow \pi\pi\pi$: $\sigma(500)$ or $f_0(600)$: The decay $D^+ \rightarrow \pi^+\pi^+\pi^-$ has been studied by the E687, E791 and FOCUS experiments (see Table 1). The E687 analysis considered the modes $\rho(770)^0\pi^+$, $f_0(980)\pi^+$, $f_2(1270)\pi^+$, and a nonresonant component. E791 included, in addition, $f_0(1370)\pi^+$ and $\rho(1450)^0\pi^+$. Both analyses found a very large fraction ($\sim 50\%$) for the nonresonant component, perhaps indicating a broad scalar contribution. E791 found the nonresonant amplitude to be consistent with zero if a broad scalar resonance was included. FOCUS analyzed its data using both the Breit-Wigner formalism and the K -matrix formalism for the $\pi^+\pi^-$ S-wave, following a 5-pole, 5-resonance model of Anisovich and Sarantsev [16]. The Breit-Wigner analysis included $\rho(770)^0$, $f_0(980)$, $f_2(1270)^0$, $f_0(1500)$, $\sigma(500)$, and a nonresonant component. The K -matrix formalism, with Breit-Wigner forms for the $\rho(770)$ and $f_2(1270)$, also describe the FOCUS data well. None of these analyses has modeled the dynamics of the $\pi^+\pi^+$ interaction. Consideration of the $I = 2$ S- and D-wave phase shifts, also measured in $\pi^+p \rightarrow \pi^+\pi^+n$ [18], could affect the $\pi^+\pi^-$ S-wave result.

Using the E791 data, Bediaga and Miranda [19] found additional evidence that the low-mass $\pi^+\pi^-$ feature is resonant by examining the phase of the $\pi^+\pi^-$ amplitude in the vicinity of the reported $\sigma(500)$ mass. The phase variation with invariant mass is consistent with a resonant interpretation.

Table 1 gives the parameters of the $\sigma(500)$ determined in charm Dalitz-plot analyses. A consistent relative phase between the $\sigma(500)$ and $\rho(770)$ resonances is observed.

Table 2: Parameters of the $\sigma(500)$ resonance.
The amplitude and phase are relative to the
 $\rho(770)$.

Experiment	E791 ^a	CLEO ^b	FOCUS [5]
Decay mode	$D^+ \rightarrow \pi^+ \pi^+ \pi^-$	$D^0 \rightarrow K_S^0 \pi^+ \pi^-$	$D^+ \rightarrow \pi^+ \pi^+ \pi^-$
Amplitude	$1.17 \pm 0.13 \pm 0.06$	0.57 ± 0.13	—
Phase (°)	$205.7 \pm 8.0 \pm 5.2$	214 ± 11	200 ± 31
m (MeV/c ²)	$478^{+24}_{-23} \pm 17$	513 ± 32	443 ± 27
Γ (MeV/c ²)	$324^{+42}_{-40} \pm 21$	335 ± 67	443 ± 80

See the end of the D^+ and D^0 listings for these references:

^aAITALA 01B, ^bMURAMATSU 02.

CLEO has studied $D^0 \rightarrow \pi^+ \pi^- \pi^0$ (see Table 1). Only the three $\rho(770)\pi$ resonant contributions are observed. No evidence is found for any $\pi\pi$ S -wave, either with the Breit-Wigner or with a K -matrix parametrization, using the 4-pole, 2-resonance model of Au, Morgan, and Pennington [17].

$D^+ \rightarrow K^- \pi^+ \pi^+$: a $\kappa(800)$?: Evidence for a broad $K\pi$ scalar resonance has been found by E791 in $D^+ \rightarrow K^- \pi^+ \pi^+$ (see Table 1). Fitting the Dalitz plot with $\bar{K}^*(892)^0 \pi^+$, $\bar{K}_0^*(1430)^0 \pi^+$, $\bar{K}_2^*(1430)^0 \pi^+$, and $\bar{K}^*(1680)^0 \pi^+$, plus a constant nonresonant component, E791 found results consistent with earlier analyses by E691 and E687, with a nonresonant fit fraction of over 90%. With more events than the other experiments, E791 was then led to include an extra low-mass S -wave $\bar{K}\pi$ resonance to account for the poor fit already seen by earlier experiments. A $\kappa(800)$ with mass $797 \pm 19 \pm 43$ MeV and width $410 \pm 43 \pm 87$ MeV much improved the fit. The $\kappa(800)$ became the dominant resonance and the nonresonant fit fraction was reduced from $90.9 \pm 2.6\%$ to $13.0 \pm 5.8 \pm 4.4\%$.

In addition, E791 modeled the $K\pi$ S-wave phase variation as a function of $K\pi$ mass with only the $K_0^*(1430)$ resonance and a nonresonant component following a parametrization of LASS [20]. It was necessary to relax the unitarity constraint to describe the data [21]. The $K\pi$ S-wave phase behavior in this model was consistent with the model that included the κ resonance.

Finally, E791 performed a model-independent partial-wave analysis [AITALA 05] of the S -wave component of the $K\pi$ system, finding the amplitude and phase from the $K\pi$ threshold up to 1.72 GeV. No assumptions were made regarding dependence on invariant mass, but the analysis did use the relatively well-understood P - and D -waves, described by the $K^*(892)$ and $K^*(1680)$ and by the $K_2(1430)$, respectively. The results were similar to those obtained by AITALA 02, which parametrized the S -wave with κ and $K_0(1430)$ Breit-Wigner forms and a constant complex non-resonant term. As with the $\sigma(500)$, the $K^-\pi^+$ S-wave result could be affected by including dynamics of the $I = 2 \pi^+\pi^+$ interaction; however in AITALA 05, the $I = 2$ elastic amplitude was found to be negligible compared to the κ .

CLEO allowed scalar $K\pi$ resonances in fits to $D^0 \rightarrow K^-\pi^+\pi^0$ and $D^0 \rightarrow K_S^0\pi^+\pi^-$ (see Table 1), and observed a significant contribution from only the $K_0^*(1430)$ [22]. BABAR fit $D^0 \rightarrow K^0K^-\pi^+$ with both positively charged and neutral $\overline{K}^*(892)$, $\overline{K}_0^*(1430)$, $\overline{K}_2^*(1430)$, and $\overline{K}^*(1680)$ resonances, as well as the $a_0(980)^-$, $a_0(1450)^-$, and $a_2(1310)^-$ resonances, and a nonresonant component [14]. BABAR also fit $D^0 \rightarrow \overline{K}^0K^+\pi^-$ with the same resonances except for the $a_2(1310)^-$. In both cases, a good fit was obtained without including the κ .

FOCUS has conclusively observed a $K\pi$ S-wave as a distortion of the $K^*(892)$ line-shape in semileptonic charm decays [LINK 02E, LINK 05D].

The $f_0(980)$, $f_0(1370)$ and $f_0(1500)$: The meson content of the 0^{++} nonet and the quark content of the $f_0(980)$, $a_0(980)$, $f_0(1370)$, $f_0(1500)$, and $f_0(1710)$ mesons are current puzzles in light-meson spectroscopy [22]. Measuring branching fractions and couplings to different final states and comparing scalar-meson production rates among D^0 , D^+ , and D_s^+ mesons may help solve these puzzles.

For example: A large contribution of $f_0(980)$ to $D^0 \rightarrow K_S^0 K^+ K^-$ was reported by ARGUS [ALBRECHT 87E] and by BABAR [14]. This is inconsistent with the smaller contribution of $f_0(980)$ observed in $D^0 \rightarrow K_S^0 \pi^+ \pi^-$ by CLEO. The explanation is that $D^0 \rightarrow K_S^0 K^+ K^-$ has a large contribution from $a_0(980)^0 \rightarrow K^+ K^-$. Therefore CLEO studied $D^0 \rightarrow K_S^0 \eta \pi^0$ [RUBIN 04], where the dominant contribution is from $K_S^0 a_0(980)^0$, $a_0(980)^0 \rightarrow \eta \pi^0$, and there can be no $f_0(980)$. A more recent BABAR analysis of $D^0 \rightarrow K_s^0 K^+ K^-$ found a large amount of $a_0(980) \rightarrow K\bar{K}$ and little $f_0(980)$ [AUBERT 05B].

The proximity of the $K\bar{K}$ threshold requires either a coupled-channel Breit-Wigner function [23] or a Flatte parametrization [24] of the $f_0(980)$. The width of the $f_0(980)$ is poorly known. E791 and FOCUS [LINK 05C] [5] used a coupled-channel Breit-Wigner function to describe the $f_0(980)$ in $D_s^+ \rightarrow \pi^+ \pi^+ \pi^-$. BESII studied the $f_0(980)$ in $J/\psi \rightarrow \phi \pi^+ \pi^-$ and $\phi K^+ K^-$ [25]. The values found for the couplings to the $\pi\pi$ and $K\bar{K}$ channels, $g_{\pi\pi}$ and g_{KK} , were not consistent. Results such as these are desirable for input to the analysis of $D_s^+ \rightarrow K^+ K^- \pi^+$ [15], which includes both the $f_0(980)$ and $a_0(980)$.

The quark content of the $f_0(1370)$ and $f_0(1500)$ can perhaps be inferred from how they populate various Dalitz plots. Results so far are confusing. The E791 analysis of

$D^+ \rightarrow \pi^+\pi^+\pi^-$ [AITALA 01B] found some $f_0(1370)$ but no $f_0(1500)$, while the FOCUS analysis [5] of this mode found little $f_0(1370)$. In $D_s^+ \rightarrow \pi^+\pi^+\pi^-$, E687 and FOCUS [5] found no $f_0(1370)$, but did find a resonance with parameters similar to the $f_0(1500)$, whereas E791 found a $\pi^+\pi^-$ resonance with mass $1434 \pm 18 \pm 9$ MeV and width $172 \pm 32 \pm 6$ MeV, consistent with neither the $f_0(1370)$ or $f_0(1500)$. BABAR [AUBERT 05B] in $D^0 \rightarrow \bar{K}^0 K^+ K^-$ found neither the $f_0(1370)$ nor the $f_0(1500)$, but did observe a $K^+ K^-$ resonance consistent with the values from E791 given above, while CLEO has observed the $f_0(1370)$ in $D^0 \rightarrow K_S^0 \pi^+ \pi^-$. The FOCUS analysis that used the K -matrix formalism for the $\pi\pi$ S-wave observed significant couplings to five T -matrix poles— $f_0(980), f_0(1300), f_0(1200-1600), f_0(1500), f_0(1750)$ —in both $D^+ \rightarrow \pi^+\pi^-\pi^+$ and $D_s^+ \rightarrow \pi^+\pi^-\pi^+$. Again, the quark content of each pole might be inferred from the coupling to various Dalitz plots.

It is noteworthy that the S-wave observed in B Dalitz-plot analyses appears to be different than that observed in D -meson decays.

Doubly Cabibbo-Suppressed Decays: There are two classes of multibody doubly Cabibbo-suppressed (DCS) decays of D mesons. The first consists of those in which the DCS and corresponding Cabibbo-favored (CF) decays populate distinct Dalitz plots: the pairs $D^0 \rightarrow K^+\pi^-\pi^0$ and $D^0 \rightarrow K^-\pi^+\pi^0$, or $D^+ \rightarrow K^+\pi^+\pi^-$ and $D^+ \rightarrow K^-\pi^+\pi^+$, are examples. CLEO [BRANDENBURG 01] and Belle [TIAN 05] have reported $\Gamma(D^0 \rightarrow K^+\pi^-\pi^0)/\Gamma(D^0 \rightarrow K^-\pi^+\pi^0) = (0.43^{+0.11}_{-0.10} \pm 0.07)\%$ and $(0.229 \pm 0.015^{+0.013}_{-0.009})\%$, respectively. E791 and FOCUS have reported $\Gamma(D^+ \rightarrow K^+\pi^-\pi^+)/\Gamma(D^+ \rightarrow K^-\pi^+\pi^+) = (0.77 \pm 0.17 \pm 0.08)\%$ and $(0.65 \pm 0.08 \pm 0.04)\%$, respectively.

The second class consists of decays in which the DCS and CF modes populate the same Dalitz plot; for example, $D^0 \rightarrow K^{*-}\pi^+$ and $D^0 \rightarrow K^{*+}\pi^-$ both contribute to $D^0 \rightarrow K_S^0\pi^+\pi^-$. In this case, the potential for interference of DCS and CF amplitudes increases the sensitivity to the DCS amplitude. CLEO found the relative amplitude and phase to be $(7.1 \pm 1.3_{-0.6}^{+2.6}_{-0.6})\%$ and $(189 \pm 10 \pm 3_{-5}^{+15})^\circ$, corresponding to $\Gamma(D^0 \rightarrow K^*(892)^+\pi^-)/\Gamma(D^0 \rightarrow K^*(892)^-\pi^+) = (0.5 \pm 0.2_{-0.1}^{+0.5}_{-0.1})\%$. In addition to $D^0 \rightarrow K^*(892)^+\pi^-$, Belle [10,11] and BABAR [12,13] have found evidence for $D^0 \rightarrow K_0(1430)^+\pi^-$ and $K_2(1430)^+\pi^-$, and Belle has also found evidence for $K^*(1680)^+\pi^-$.

CP Violation: In the limit of CP conservation, charge conjugate decays will have the same Dalitz-plot distribution. The $D^{*\pm}$ tag enables the discrimination between D^0 and \overline{D}^0 . The integrated CP violation across the Dalitz plot is determined in two ways. The first uses

$$\mathcal{A}_{CP} = \int \left(\frac{|\mathcal{M}|^2 - |\overline{\mathcal{M}}|^2}{|\mathcal{M}|^2 + |\overline{\mathcal{M}}|^2} \right) dm_{ab}^2 dm_{bc}^2 \Big/ \int dm_{ab}^2 dm_{bc}^2, \quad (1)$$

where \mathcal{M} and $\overline{\mathcal{M}}$ are the D^0 and \overline{D}^0 Dalitz-plot amplitudes. The second uses the asymmetry in the efficiency-corrected D^0 and \overline{D}^0 yields,

$$\mathcal{A}_{CP} = \frac{N_{D^0} - N_{\overline{D}^0}}{N_{D^0} + N_{\overline{D}^0}}. \quad (2)$$

These expressions are less sensitive to CP violation than are the individual resonant submodes [ASNER 04A]. Table 3 lists the results for CP violation. No evidence of CP violation has been observed in D -meson decays.

Table 3: Dalitz-plot-integrated CP violation. Measurements computing \mathcal{A}_{CP} with Eq. (2) rather than Eq. (1) are denoted † .

Experiment	Decay mode	$\mathcal{A}_{CP}(\%)$
BABAR ^a	$D^+ \rightarrow K^+ K^- \pi^+$	$1.4 \pm 1.0 \pm 0.8$
Belle ^{b\dagger}	$D^0 \rightarrow K^+ \pi^- \pi^0$	-0.6 ± 5.3
Belle ^{b\dagger}	$D^0 \rightarrow K^+ \pi^- \pi^+ \pi^-$	-1.8 ± 4.4
CLEO ^c	$D^0 \rightarrow K^- \pi^+ \pi^0$	-3.1 ± 8.6
CLEO ^{d\dagger}	$D^0 \rightarrow K^+ \pi^- \pi^0$	$+9^{+22}_{-25}$
CLEO ^e	$D^0 \rightarrow K_S^0 \pi^+ \pi^-$	$-0.9 \pm 2.1^{+1.0+1.3}_{-4.3-3.7}$
CLEO ^f	$D^0 \rightarrow \pi^+ \pi^- \pi^0$	$+1^{+9}_{-7} \pm 9$

See the end of the D^+ and D^0 Listings for these references:

^aAUBERT 05A, ^bTIAN 05, ^cKOPP 01, ^dBRANDENBURG 01,

^eASNER 04A, ^fCRONIN-HENNESSY 05.

The possibility of interference between CP -conserving and CP -violating amplitudes provides a more sensitive probe of CP violation. The constraints on the square of the CP -violating amplitude obtained in the resonant submodes of $D^0 \rightarrow K_S^0 \pi^+ \pi^-$ range from 3.5×10^{-4} to 28.4×10^{-4} at 95% confidence level [ASNER 04A].

References

1. See the note on “ D^0 – \overline{D}^0 Mixing” in this *Review*.
2. See the note on “The CKM Quark Mixing Matrix” in this *Review*.
3. See the note on “ CP Violation in Meson Decays” in this *Review*.
4. Dalitz plot analysis of the wrong sign rate $D^0 \rightarrow K^+ \pi^- \pi^0$ [BRANDENBURG 01] and the time dependence of Dalitz

- plot analysis of $D^0 \rightarrow K_S^0 \pi^+ \pi^-$ [ASNER 05] are two candidate processes.
5. S. Malvezzi, AIP Conf. Proc. **688**, 276 (2004) [Nucl. Phys. Proc. Suppl. **126**, 220 (2004)].
 6. A. Giri *et al.*, Phys. Rev. **D68**, 054018 (2003).
 7. A. Bondar and A. Poluektov, [hep-ph/0510246](#).
 8. J. Blatt and V. Weisskopf, *Theoretical Nuclear Physics*, New York: John Wiley & Sons (1952).
 9. F. von Hippel and C. Quigg, Phys. Rev. **D5**, 624, (1972).
 10. A. Poluektov *et al.* (Belle Collab.), Phys. Rev. D **70**, 072003 (2004).
 11. K. Abe *et al.* Belle Collaboration, [hep-ex/0411049](#).
 12. B. Aubert *et al.* (BABAR Collab.), Phys. Rev. Lett. **95**, 121802 (2005).
 13. B. Aubert *et al.* (BABAR Collab.), [hep-ex/0507101](#).
 14. B. Aubert *et al.* (BABAR Collab.), [hep-ex/0207089](#); contributed to the 31st International Conference on High Energy Physics (ICHEP 2002).
 15. S. Malvezzi, AIP Conf. Proc. **549**, 569 (2002).
 16. V. V. Anisovich and A. V. Sarantsev, Eur. Phys. J. A **16**, 229 (2003).
 17. K. L. Au *et al.*, Phys. Rev. D **35**, 1633 (1987).
 18. W. Hoogland *et al.*, Nucl. Phys. **B69**, 266 (1974).
 19. I. Bediaga (E791 Collab.), AIP Conf. Proc. **688**, 252 (2004).
 20. D. Aston *et al.* (LASS Collab.), Nucl. Phys. **B296**, 493 (1988).
 21. C. Gobel (Fermilab E791 Collab.), AIP Conf. Proc. **688**, 266 (2004).
 22. See the “Note on Scalar Mesons” in this *Review*.
 23. T. A. Armstrong *et al.* (WA76 Collab.), Z. Phys. **C51**, 351 (1991).
 24. S. M. Flatte, Phys. Lett. **B63**, 224 (1976).

25. M. Ablikim *et al.* (BES Collab.), Phys. Lett. B **607**, 243 (2005).

$\Gamma(\bar{K}_0^*(800)^0 \pi^+, \bar{K}_0^*(800) \rightarrow K^- \pi^+)/\Gamma(K^- \pi^+ \pi^+)$ **Γ_{43}/Γ_{42}**

This is the “fit fraction” from the Dalitz-plot analysis. The $K_0^*(800)$ is a broad scalar resonance that may not exist and is not included in the Summary Tables. AITALA 02 finds that including such a resonance in the fit to the $D^+ \rightarrow K^- \pi^+ \pi^+$ Dalitz plot greatly improves the fit. However, the results of AITALA 02 for the $D^+ \rightarrow K^- \pi^+ \pi^+$ Dalitz plot analysis so disagree with earlier analyses that averaging the results makes no sense. For now, we exclude AITALA 02 from the average.

VALUE	DOCUMENT ID	TECN	COMMENT
$\bullet \bullet \bullet$ We do not use the following data for averages, fits, limits, etc. $\bullet \bullet \bullet$			
$0.478 \pm 0.121 \pm 0.053$	AITALA	02 E791	π^- nucleus, 500 GeV

$\Gamma(\bar{K}^*(892)^0 \pi^+, \bar{K}^*(892)^0 \rightarrow K^- \pi^+)/\Gamma(K^- \pi^+ \pi^+)$ **Γ_{44}/Γ_{42}**

This is the “fit fraction” from the Dalitz-plot analysis.

VALUE	DOCUMENT ID	TECN	COMMENT
0.140 ± 0.010 OUR AVERAGE			
$0.137 \pm 0.006 \pm 0.009$	FRABETTI	94G E687	γ Be, $\bar{E}_\gamma \approx 220$ GeV
$0.170 \pm 0.009 \pm 0.034$	ANJOS	93 E691	γ Be 90–260 GeV
$0.14 \pm 0.04 \pm 0.04$	ALVAREZ	91B NA14	Photoproduction
$0.13 \pm 0.01 \pm 0.07$	ADLER	87 MRK3	$e^+ e^-$ 3.77 GeV
$\bullet \bullet \bullet$ We do not use the following data for averages, fits, limits, etc. $\bullet \bullet \bullet$			
$0.123 \pm 0.010 \pm 0.009$	51 AITALA	02 E791	π^- nucleus, 500 GeV

⁵¹ AITALA 02 includes a broad scalar $K_0^*(800)$ in the fit to the $D^+ \rightarrow K^- \pi^+ \pi^+$ Dalitz plot. This (a) greatly improves the fit, and (b) gives results in other channels that greatly disagree with previous analyses. The disagreement is so large that it makes no sense to average the results with those of earlier experiments. For now, we exclude AITALA 02 from the average.

$\Gamma(\bar{K}_0^*(1430)^0 \pi^+, \bar{K}_0^*(1430)^0 \rightarrow K^- \pi^+)/\Gamma(K^- \pi^+ \pi^+)$ **Γ_{45}/Γ_{42}**

This is the “fit fraction” from the Dalitz-plot analysis.

VALUE	DOCUMENT ID	TECN	COMMENT
0.253 ± 0.024 OUR AVERAGE			
$0.284 \pm 0.022 \pm 0.059$	FRABETTI	94G E687	γ Be, $\bar{E}_\gamma \approx 220$ GeV
$0.248 \pm 0.019 \pm 0.017$	ANJOS	93 E691	γ Be 90–260 GeV
$\bullet \bullet \bullet$ We do not use the following data for averages, fits, limits, etc. $\bullet \bullet \bullet$			
$0.125 \pm 0.014 \pm 0.005$	52 AITALA	02 E791	π^- nucleus, 500 GeV

⁵² AITALA 02 includes a broad scalar $K_0^*(800)$ in the fit to the $D^+ \rightarrow K^- \pi^+ \pi^+$ Dalitz plot. This (a) greatly improves the fit, and (b) gives results in other channels that greatly disagree with previous analyses. The disagreement is so large that it makes no sense to average the results with those of earlier experiments. For now, we exclude AITALA 02 from the average.

$\Gamma(\bar{K}_2^*(1430)^0 \pi^+, \bar{K}_2^*(1430)^0 \rightarrow K^- \pi^+)/\Gamma(K^- \pi^+ \pi^+)$ Γ_{46}/Γ_{42}

This is the "fit fraction" from the Dalitz-plot analysis.

VALUE	DOCUMENT ID	TECN	COMMENT
• • • We do not use the following data for averages, fits, limits, etc. • • •			
$0.005 \pm 0.001 \pm 0.002$	⁵³ AITALA	02 E791	π^- nucleus, 500 GeV
53 AITALA 02 includes a broad scalar $K_0^*(800)$ in the fit to the $D^+ \rightarrow K^- \pi^+ \pi^+$ Dalitz plot. This (a) greatly improves the fit, and (b) gives results in other channels that greatly disagree with previous analyses. The disagreement is so large that it makes no sense to average the results with those of earlier experiments. For now, we exclude AITALA 02 from the average.			

 $\Gamma(\bar{K}^*(1680)^0 \pi^+, \bar{K}^*(1680)^0 \rightarrow K^- \pi^+)/\Gamma(K^- \pi^+ \pi^+)$ Γ_{47}/Γ_{42}

This is the "fit fraction" from the Dalitz-plot analysis.

VALUE	DOCUMENT ID	TECN	COMMENT
0.042 ± 0.008 OUR AVERAGE			
$0.047 \pm 0.006 \pm 0.007$	FRABETTI	94G E687	γ Be, $\bar{E}_\gamma \approx 220$ GeV
$0.030 \pm 0.004 \pm 0.013$	ANJOS	93 E691	γ Be 90–260 GeV
• • • We do not use the following data for averages, fits, limits, etc. • • •			
$0.025 \pm 0.007 \pm 0.003$	⁵⁴ AITALA	02 E791	π^- nucleus, 500 GeV
54 AITALA 02 includes a broad scalar $K_0^*(800)$ in the fit to the $D^+ \rightarrow K^- \pi^+ \pi^+$ Dalitz plot. This (a) greatly improves the fit, and (b) gives results in other channels that greatly disagree with previous analyses. The disagreement is so large that it makes no sense to average the results with those of earlier experiments. For now, we exclude AITALA 02 from the average.			

 $\Gamma(K^- \pi^+ \pi^+ \text{ nonresonant})/\Gamma(K^- \pi^+ \pi^+)$ Γ_{48}/Γ_{42}

This is the "fit fraction" from the Dalitz-plot analysis.

VALUE	DOCUMENT ID	TECN	COMMENT
0.95 ± 0.07 OUR AVERAGE			
$0.998 \pm 0.037 \pm 0.072$	FRABETTI	94G E687	γ Be, $\bar{E}_\gamma \approx 220$ GeV
$0.838 \pm 0.088 \pm 0.275$	ANJOS	93 E691	γ Be 90–260 GeV
$0.79 \pm 0.07 \pm 0.15$	ADLER	87 MRK3	$e^+ e^-$ 3.77 GeV
• • • We do not use the following data for averages, fits, limits, etc. • • •			
$0.130 \pm 0.058 \pm 0.044$	⁵⁵ AITALA	02 E791	π^- nucleus, 500 GeV
55 AITALA 02 includes a broad scalar $K_0^*(800)$ in the fit to the $D^+ \rightarrow K^- \pi^+ \pi^+$ Dalitz plot. This (a) greatly improves the fit, and (b) gives results in other channels that greatly disagree with previous analyses. The disagreement is so large that it makes no sense to average the results with those of earlier experiments. For now, we exclude AITALA 02 from the average.			

 $\Gamma(K_S^0 \pi^+ \pi^0)/\Gamma_{\text{total}}$ Γ_{49}/Γ

VALUE	EVTS	DOCUMENT ID	TECN	COMMENT
0.070 ± 0.005 OUR FIT Error includes scale factor of 1.2.				
$0.072 \pm 0.002 \pm 0.004$	5090 ± 100	⁵⁶ HE	05 CLEO	$e^+ e^-$ at $\psi(3770)$
• • • We do not use the following data for averages, fits, limits, etc. • • •				

0.051 ± 0.013 ± 0.008 159 ADLER 88C MRK3 $e^+ e^-$ 3.77 GeV
 0.09 ± 0.06 10 SCHINDLER 81 MRK2 $e^+ e^-$ 3.771 GeV

⁵⁶ HE 05 uses single- and double-tagged events in an overall fit. The fraction here includes (unobserved) final-state photons.

⁵⁷ SCHINDLER 81 (MARK-2) measures $\sigma(e^+ e^- \rightarrow \psi(3770)) \times$ branching fraction to be 0.78 ± 0.48 nb. We use the MARK-3 (ADLER 88C) value of $\sigma = 4.2 \pm 0.6 \pm 0.3$ nb.

$\Gamma(K_S^0 \rho^+)/\Gamma(K_S^0 \pi^+ \pi^0)$ Γ_{50}/Γ_{49}

This is the "fit fraction" from the Dalitz-plot analysis.

VALUE	DOCUMENT ID	TECN	COMMENT
0.68±0.08±0.12	ADLER	87	MRK3 $e^+ e^-$ 3.77 GeV

 $\Gamma(\bar{K}^*(892)^0 \pi^+, \bar{K}^*(892)^0 \rightarrow K_S^0 \pi^0)/\Gamma(K_S^0 \pi^+ \pi^0)$ Γ_{51}/Γ_{49}

This is the "fit fraction" from the Dalitz-plot analysis.

VALUE	DOCUMENT ID	TECN	COMMENT
0.19±0.06±0.06	ADLER	87	MRK3 $e^+ e^-$ 3.77 GeV

 $\Gamma(K_S^0 \pi^+ \pi^0 \text{ nonresonant})/\Gamma(K_S^0 \pi^+ \pi^0)$ Γ_{52}/Γ_{49}

This is the "fit fraction" from the Dalitz-plot analysis.

VALUE	DOCUMENT ID	TECN	COMMENT
0.13±0.07±0.08	ADLER	87	MRK3 $e^+ e^-$ 3.77 GeV

 $\Gamma(K^- \pi^+ \pi^+ \pi^0)/\Gamma_{\text{total}}$ Γ_{53}/Γ

VALUE	EVTS	DOCUMENT ID	TECN	COMMENT
0.060±0.002 ±0.002	4840 ± 100	58 HE	05 CLEO	$e^+ e^-$ at $\psi(3770)$

• • • We do not use the following data for averages, fits, limits, etc. • • •

0.058±0.012 ±0.012 142 COFFMAN 92B MRK3 $e^+ e^-$ 3.77 GeV0.063^{+0.014}_{-0.013} ±0.012 175 BALTRUSAIT...86E MRK3 See COFFMAN 92B

58 HE 05 uses single- and double-tagged events in an overall fit. The fraction here includes (unobserved) final-state photons.

 $\Gamma(K^- \pi^+ \pi^+ \pi^0)/\Gamma(K^- \pi^+ \pi^+)$ Γ_{53}/Γ_{42}

VALUE	EVTS	DOCUMENT ID	TECN	COMMENT
• • • We do not use the following data for averages, fits, limits, etc. • • •				

0.76±0.11±0.12 91 ANJOS 92C E691 γ Be 90–260 GeV

0.69±0.10±0.16 ANJOS 89E E691 See ANJOS 92C

 $\Gamma(\bar{K}^*(892)^0 \rho^+ \text{ total})/\Gamma(K^- \pi^+ \pi^+ \pi^0)$ Γ_{79}/Γ_{53} Unseen decay modes of the $\bar{K}^*(892)^0$ are included.

VALUE	DOCUMENT ID	TECN	COMMENT
0.33±0.165±0.12	59 ANJOS	92C E691	γ Be 90–260 GeV

59 See, however, the next entry, where the two experiments disagree completely.

 $\Gamma(\bar{K}^*(892)^0 \rho^+ S\text{-wave})/\Gamma(K^- \pi^+ \pi^+ \pi^0)$ Γ_{80}/Γ_{53} Unseen decay modes of the $\bar{K}^*(892)^0$ are included. The two experiments here disagree completely.

VALUE	DOCUMENT ID	TECN	COMMENT
0.26 ±0.25 OUR AVERAGE	Error includes scale factor of 3.1.		
0.15 ±0.075±0.045	ANJOS	92C E691	γ Be 90–260 GeV
0.833±0.116±0.165	COFFMAN	92B MRK3	$e^+ e^-$ 3.77 GeV

 $\Gamma(\bar{K}^*(892)^0 \rho^+ P\text{-wave})/\Gamma_{\text{total}}$ Γ_{81}/Γ Unseen decay modes of the $\bar{K}^*(892)^0$ are included.

VALUE	CL%	DOCUMENT ID	TECN	COMMENT
<0.001	90	ANJOS	92C E691	γ Be 90–260 GeV

• • • We do not use the following data for averages, fits, limits, etc. • • •

<0.005 90 COFFMAN 92B MRK3 $e^+ e^-$ 3.77 GeV

$\Gamma(\bar{K}^*(892)^0 \rho^+ D\text{-wave})/\Gamma(K^- \pi^+ \pi^+ \pi^0)$ Γ_{82}/Γ_{53} Unseen decay modes of the $\bar{K}^*(892)^0$ are included.

<u>VALUE</u>	<u>DOCUMENT ID</u>	<u>TECN</u>	<u>COMMENT</u>
0.15±0.09±0.045	ANJOS	92C E691	γ Be 90–260 GeV

 $\Gamma(\bar{K}^*(892)^0 \rho^+ D\text{-wave longitudinal})/\Gamma_{\text{total}}$ Γ_{83}/Γ Unseen decay modes of the $\bar{K}^*(892)^0$ are included.

<u>VALUE</u>	<u>CL%</u>	<u>DOCUMENT ID</u>	<u>TECN</u>	<u>COMMENT</u>
<0.007	90	COFFMAN	92B MRK3	$e^+ e^-$ 3.77 GeV

 $\Gamma(\bar{K}_1(1400)^0 \pi^+)/\Gamma(K^- \pi^+ \pi^+ \pi^0)$ Γ_{85}/Γ_{53} Unseen decay modes of the $\bar{K}_1(1400)^0$ are included.

<u>VALUE</u>	<u>DOCUMENT ID</u>	<u>TECN</u>	<u>COMMENT</u>
0.79 ±0.32 OUR FIT			Error includes scale factor of 1.2.
0.907±0.218±0.180	COFFMAN	92B MRK3	$e^+ e^-$ 3.77 GeV

 $\Gamma(K^- \rho^+ \pi^+ \text{total})/\Gamma(K^- \pi^+ \pi^+ \pi^0)$ Γ_{56}/Γ_{53} This includes $\bar{K}^*(892)^0 \rho^+$, etc. The next entry gives the specifically 3-body fraction.

<u>VALUE</u>	<u>DOCUMENT ID</u>	<u>TECN</u>	<u>COMMENT</u>
0.48±0.13±0.09	ANJOS	92C E691	γ Be 90–260 GeV

 $\Gamma(K^- \rho^+ \pi^+ \text{3-body})/\Gamma(K^- \pi^+ \pi^+ \pi^0)$ Γ_{57}/Γ_{53}

<u>VALUE</u>	<u>DOCUMENT ID</u>	<u>TECN</u>	<u>COMMENT</u>
0.17 ±0.06 OUR AVERAGE			
0.18 ±0.08 ±0.04	ANJOS	92C E691	γ Be 90–260 GeV
0.159±0.065±0.060	COFFMAN	92B MRK3	$e^+ e^-$ 3.77 GeV

 $\Gamma(\bar{K}^*(892)^0 \pi^+ \pi^0 \text{total})/\Gamma(K^- \pi^+ \pi^+ \pi^0)$ Γ_{87}/Γ_{53} This includes $\bar{K}^*(892)^0 \rho^+$, etc. The next two entries give the specifically 3-body fraction. Unseen decay modes of the $\bar{K}^*(892)^0$ are included.

<u>VALUE</u>	<u>DOCUMENT ID</u>	<u>TECN</u>	<u>COMMENT</u>
1.05±0.11±0.08	ANJOS	92C E691	γ Be 90–260 GeV

 $\Gamma(\bar{K}^*(892)^0 \pi^+ \pi^0 \text{3-body})/\Gamma_{\text{total}}$ Γ_{88}/Γ Unseen decay modes of the $\bar{K}^*(892)^0$ are included.

<u>VALUE</u>	<u>CL%</u>	<u>DOCUMENT ID</u>	<u>TECN</u>	<u>COMMENT</u>
• • • We do not use the following data for averages, fits, limits, etc. • • •				

<0.008 90 ⁶⁰ COFFMAN 92B MRK3 $e^+ e^-$ 3.77 GeV

60 See, however, the next entry: ANJOS 92C sees a large signal in this channel.

 $\Gamma(\bar{K}^*(892)^0 \pi^+ \pi^0 \text{3-body})/\Gamma(K^- \pi^+ \pi^+ \pi^0)$ Γ_{88}/Γ_{53} Unseen decay modes of the $\bar{K}^*(892)^0$ are included.

<u>VALUE</u>	<u>DOCUMENT ID</u>	<u>TECN</u>	<u>COMMENT</u>
0.66±0.09±0.17	ANJOS	92C E691	γ Be 90–260 GeV

 $\Gamma(K^*(892)^- \pi^+ \pi^+ \text{3-body})/\Gamma(K^- \pi^+ \pi^+ \pi^0)$ Γ_{90}/Γ_{53} Unseen decay modes of the $K^*(892)^-$ are included.

<u>VALUE</u>	<u>DOCUMENT ID</u>	<u>TECN</u>	<u>COMMENT</u>
0.32±0.16 OUR FIT			Error includes scale factor of 1.2.
0.24±0.12±0.09	ANJOS	92C E691	γ Be 90–260 GeV

$\Gamma(K^-\pi^+\pi^+\pi^0 \text{ nonresonant})/\Gamma_{\text{total}}$ Γ_{61}/Γ

<u>VALUE</u>	<u>CL%</u>	<u>DOCUMENT ID</u>	<u>TECN</u>	<u>COMMENT</u>
• • • We do not use the following data for averages, fits, limits, etc. • • •				
<0.002	90	61 ANJOS	92C E691	γBe 90–260 GeV
61 Whereas ANJOS 92C finds no signal here, COFFMAN 92B finds a fairly large one; see the next entry.				

 $\Gamma(K^-\pi^+\pi^+\pi^0 \text{ nonresonant})/\Gamma(K^-\pi^+\pi^+\pi^0)$ Γ_{61}/Γ_{53}

<u>VALUE</u>	<u>DOCUMENT ID</u>	<u>TECN</u>	<u>COMMENT</u>
0.184±0.070±0.050	COFFMAN	92B MRK3	e^+e^- 3.77 GeV

 $\Gamma(K_S^0\pi^+\pi^+\pi^-)/\Gamma_{\text{total}}$ Γ_{62}/Γ

<u>VALUE</u>	<u>EVTS</u>	<u>DOCUMENT ID</u>	<u>TECN</u>	<u>COMMENT</u>
0.0311±0.0021 OUR FIT Error includes scale factor of 1.1.				
0.032 ±0.001 ±0.002	3210 ± 85	62 HE	05 CLEO	e^+e^- at $\psi(3770)$
• • • We do not use the following data for averages, fits, limits, etc. • • •				
0.021 $^{+0.010}_{-0.009}$		63 BARLAG	92C ACCM	π^- Cu 230 GeV
0.033 ± 0.008	± 0.002	168 ADLER	88C MRK3	e^+e^- 3.77 GeV
0.122 $^{+0.032}_{-0.021}$	± 0.021	11 63 AGUILAR-...	87F HYBR	$\pi p, pp$ 360, 400 GeV
0.06 ± 0.03		21 64 SCHINDLER	81 MRK2	e^+e^- 3.771 GeV

62 HE 05 uses single- and double-tagged events in an overall fit. The fraction here includes (unobserved) final-state photons.

63 AGUILAR-BENITEZ 87F and BARLAG 92C compute the branching fraction by topological normalization.

64 SCHINDLER 81 (MARK-2) measures $\sigma(e^+e^- \rightarrow \psi(3770)) \times$ branching fraction to be 0.51 ± 0.08 nb. We use the MARK-3 (ADLER 88C) value of $\sigma = 4.2 \pm 0.6 \pm 0.3$ nb.

 $\Gamma(K_S^0\pi^+\pi^+\pi^-)/\Gamma(K^-\pi^+\pi^+)$ Γ_{62}/Γ_{42}

<u>VALUE</u>	<u>EVTS</u>	<u>DOCUMENT ID</u>	<u>TECN</u>	<u>COMMENT</u>
0.327±0.018 OUR FIT Error includes scale factor of 1.1.				
0.39 ±0.04 ±0.06	229 ± 17	ANJOS	92C E691	γBe 90–260 GeV

 $\Gamma(K_S^0 a_1(1260)^+)/\Gamma(K_S^0\pi^+\pi^+\pi^-)$ Γ_{77}/Γ_{62}

Unseen decay modes of the $a_1(1260)^+$ are included, assuming that the $a_1(1260)^+$ decays entirely to $\rho\pi$ [or at least to $(\pi\pi)_{I=1}\pi$].

<u>VALUE</u>	<u>DOCUMENT ID</u>	<u>TECN</u>	<u>COMMENT</u>
1.15 ±0.19 OUR AVERAGE Error includes scale factor of 1.1.			
1.66 ± 0.28	± 0.40	ANJOS	92C E691 γBe 90–260 GeV
1.078 ± 0.114	± 0.140	COFFMAN	92B MRK3 e^+e^- 3.77 GeV

 $\Gamma(K_S^0 a_2(1320)^+)/\Gamma_{\text{total}}$ Γ_{78}/Γ

Unseen decay modes of the $a_2(1320)^+$ are included.

<u>VALUE</u>	<u>CL%</u>	<u>DOCUMENT ID</u>	<u>TECN</u>	<u>COMMENT</u>
<0.0015	90	ANJOS	92C E691	γBe 90–260 GeV
• • • We do not use the following data for averages, fits, limits, etc. • • •				
<0.004	90	COFFMAN	92B MRK3	e^+e^- 3.77 GeV

$\Gamma(\bar{K}_1(1270)^0\pi^+)/\Gamma_{\text{total}}$ Γ_{84}/Γ Unseen decay modes of the $\bar{K}_1(1270)^0$ are included.

<u>VALUE</u>	<u>CL%</u>	<u>DOCUMENT ID</u>	<u>TECN</u>	<u>COMMENT</u>
<0.007	90	ANJOS	92C E691	γBe 90–260 GeV
• • • We do not use the following data for averages, fits, limits, etc. • • •				
<0.011	90	COFFMAN	92B MRK3	e^+e^- 3.77 GeV

 $\Gamma(\bar{K}_1(1400)^0\pi^+)/\Gamma_{\text{total}}$ Γ_{85}/Γ Unseen decay modes of the $\bar{K}_1(1400)^0$ are included.

<u>VALUE</u>	<u>CL%</u>	<u>DOCUMENT ID</u>	<u>TECN</u>	<u>COMMENT</u>
• • • We do not use the following data for averages, fits, limits, etc. • • •				
<0.009	90	65 ANJOS	92C E691	γBe 90–260 GeV
65 ANJOS 92C sees no evidence for $\bar{K}_1(1400)^0\pi^+$ in either the $\bar{K}^0\pi^+\pi^+\pi^-$ or $K^-\pi^+\pi^+\pi^0$ channels, whereas COFFMAN 92B finds the $\bar{K}_1(1400)^0\pi^+$ branching fraction to be large; see the next entry.				

 $\Gamma(\bar{K}_1(1400)^0\pi^+)/\Gamma(K_S^0\pi^+\pi^+\pi^-)$ Γ_{85}/Γ_{62} Unseen decay modes of the $\bar{K}_1(1400)^0$ are included.

<u>VALUE</u>	<u>DOCUMENT ID</u>	<u>TECN</u>	<u>COMMENT</u>
1.4 ± 0.5 OUR FIT	Error includes scale factor of 1.2.		
1.246 ± 0.212 ± 0.360	COFFMAN	92B MRK3	e^+e^- 3.77 GeV

 $\Gamma(\bar{K}^*(1410)^0\pi^+)/\Gamma_{\text{total}}$ Γ_{86}/Γ

<u>VALUE</u>	<u>CL%</u>	<u>DOCUMENT ID</u>	<u>TECN</u>	<u>COMMENT</u>
• • • We do not use the following data for averages, fits, limits, etc. • • •				
<0.007	90	COFFMAN	92B MRK3	e^+e^- 3.77 GeV

 $\Gamma(K^*(892)^-\pi^+\pi^+\text{total})/\Gamma(K_S^0\pi^+\pi^+\pi^-)$ Γ_{89}/Γ_{62} Unseen decay modes of the $K^*(892)^-$ are included.

<u>VALUE</u>	<u>EVTS</u>	<u>DOCUMENT ID</u>	<u>TECN</u>	<u>COMMENT</u>
• • • We do not use the following data for averages, fits, limits, etc. • • •				
0.82 ± 0.28	14	ALEEV	94 BIS2	nN 20–70 GeV

 $\Gamma(K^*(892)^-\pi^+\pi^+\text{3-body})/\Gamma_{\text{total}}$ Γ_{90}/Γ Unseen decay modes of the $\bar{K}^*(892)^0$ are included.

<u>VALUE</u>	<u>CL%</u>	<u>DOCUMENT ID</u>	<u>TECN</u>	<u>COMMENT</u>
• • • We do not use the following data for averages, fits, limits, etc. • • •				
<0.013	90	COFFMAN	92B MRK3	e^+e^- 3.77 GeV

 $\Gamma(K^*(892)^-\pi^+\pi^+\text{3-body})/\Gamma(K_S^0\pi^+\pi^+\pi^-)$ Γ_{90}/Γ_{62} Unseen decay modes of the $K^*(892)^-$ are included.

<u>VALUE</u>	<u>DOCUMENT ID</u>	<u>TECN</u>	<u>COMMENT</u>
0.57 ± 0.35 OUR FIT Error includes scale factor of 1.2.			
1.00 ± 0.18 ± 0.42	ANJOS	92C E691	γBe 90–260 GeV

$\Gamma(K_S^0 \rho^0 \pi^+ \text{total})/\Gamma(K_S^0 \pi^+ \pi^+ \pi^-)$ Γ_{66}/Γ_{62}

This includes $\bar{K}^0 a_1(1260)^+$. The next two entries give the specifically 3-body reaction.

<u>VALUE</u>	<u>CL%</u>	<u>DOCUMENT ID</u>	<u>TECN</u>	<u>COMMENT</u>
0.60±0.10±0.17	90	ANJOS	92C E691	γ Be 90–260 GeV

 $\Gamma(K_S^0 \rho^0 \pi^+ \text{3-body})/\Gamma_{\text{total}}$ Γ_{67}/Γ

<u>VALUE</u>	<u>CL%</u>	<u>DOCUMENT ID</u>	<u>TECN</u>	<u>COMMENT</u>
• • • We do not use the following data for averages, fits, limits, etc. • • •				
<0.002	90	COFFMAN	92B MRK3	$e^+ e^-$ 3.77 GeV

 $\Gamma(K_S^0 \rho^0 \pi^+ \text{3-body})/\Gamma(K_S^0 \pi^+ \pi^+ \pi^-)$ Γ_{67}/Γ_{62}

<u>VALUE</u>	<u>DOCUMENT ID</u>	<u>TECN</u>	<u>COMMENT</u>
0.07±0.04±0.06	ANJOS	92C E691	γ Be 90–260 GeV

 $\Gamma(K_S^0 f_0(980) \pi^+)/\Gamma_{\text{total}}$ Γ_{91}/Γ

<u>VALUE</u>	<u>CL%</u>	<u>DOCUMENT ID</u>	<u>TECN</u>	<u>COMMENT</u>
• • • We do not use the following data for averages, fits, limits, etc. • • •				
<0.0025	90	ANJOS	92C E691	γ Be 90–260 GeV

 $\Gamma(K_S^0 \pi^+ \pi^+ \pi^- \text{nonresonant})/\Gamma(K_S^0 \pi^+ \pi^+ \pi^-)$ Γ_{68}/Γ_{62}

<u>VALUE</u>	<u>DOCUMENT ID</u>	<u>TECN</u>	<u>COMMENT</u>
0.12±0.06 OUR AVERAGE			
0.10±0.04 ± 0.06	ANJOS	92C E691	γ Be 90–260 GeV
0.17±0.056±0.100	COFFMAN	92B MRK3	$e^+ e^-$ 3.77 GeV

 $\Gamma(K^- 3\pi^+ \pi^-)/\Gamma(K^- \pi^+ \pi^+)$ Γ_{69}/Γ_{42}

<u>VALUE</u>	<u>EVTS</u>	<u>DOCUMENT ID</u>	<u>TECN</u>	<u>COMMENT</u>
0.061±0.005 OUR FIT				Error includes scale factor of 1.1.
0.062±0.008 OUR AVERAGE				Error includes scale factor of 1.3.
• • • We do not use the following data for averages, fits, limits, etc. • • •				
0.09 ± 0.01 ± 0.01	113	ANJOS	90D E691	Photoproduction

 $\Gamma(\bar{K}^*(892)^0 \pi^+ \pi^+ \pi^-, \bar{K}^*(892)^0 \rightarrow K^- \pi^+)/\Gamma(K^- 3\pi^+ \pi^-)$ Γ_{70}/Γ_{69}

<u>VALUE</u>	<u>DOCUMENT ID</u>	<u>TECN</u>	<u>COMMENT</u>
0.21±0.04±0.06	LINK	03D FOCS	γ A, \bar{E}_γ ≈ 180 GeV

 $\Gamma(\bar{K}^*(892)^0 \rho^0 \pi^+, \bar{K}^*(892)^0 \rightarrow K^- \pi^+)/\Gamma(K^- 3\pi^+ \pi^-)$ Γ_{71}/Γ_{69}

<u>VALUE</u>	<u>DOCUMENT ID</u>	<u>TECN</u>	<u>COMMENT</u>
0.40±0.03±0.06	LINK	03D FOCS	γ A, \bar{E}_γ ≈ 180 GeV

 $\Gamma(\bar{K}^*(892)^0 \rho^0 \pi^+, \bar{K}^*(892)^0 \rightarrow K^- \pi^+)/\Gamma(K^- \pi^+ \pi^+)$ Γ_{71}/Γ_{42}

<u>VALUE</u>	<u>DOCUMENT ID</u>	<u>TECN</u>	<u>COMMENT</u>	
• • • We do not use the following data for averages, fits, limits, etc. • • •				
0.016±0.007±0.004	FRABETTI	97C E687	γ Be, \bar{E}_γ ≈ 200 GeV	

$\Gamma(\overline{K}^*(892)^0 \pi^+ \pi^+ \pi^- \text{no-}\rho, \overline{K}^*(892)^0 \rightarrow K^- \pi^+)/\Gamma(K^- \pi^+ \pi^+)$ Γ_{72}/Γ_{42}

<u>VALUE</u>	<u>DOCUMENT ID</u>	<u>TECN</u>	<u>COMMENT</u>
• • • We do not use the following data for averages, fits, limits, etc. • • •			
$0.032 \pm 0.010 \pm 0.008$	FRABETTI 97C E687	γ Be, \bar{E}_γ	≈ 200 GeV

 $\Gamma(K^- \rho^0 \pi^+ \pi^+)/\Gamma(K^- \pi^+ \pi^+)$ Γ_{73}/Γ_{42}

<u>VALUE</u>	<u>DOCUMENT ID</u>	<u>TECN</u>	<u>COMMENT</u>
• • • We do not use the following data for averages, fits, limits, etc. • • •			
$0.034 \pm 0.009 \pm 0.005$	FRABETTI 97C E687	γ Be, \bar{E}_γ	≈ 200 GeV

 $\Gamma(K^- \rho^0 \pi^+ \pi^+)/\Gamma(K^- 3\pi^+ \pi^-)$ Γ_{73}/Γ_{69}

<u>VALUE</u>	<u>DOCUMENT ID</u>	<u>TECN</u>	<u>COMMENT</u>
0.30 ± 0.04 ± 0.01	LINK	03D FOCS	γ A, \bar{E}_γ ≈ 180 GeV

 $\Gamma(\overline{K}^*(892)^0 a_1(1260)^+)/\Gamma(K^- \pi^+ \pi^+)$ Γ_{92}/Γ_{42} Unseen decay modes of the $\overline{K}^*(892)^0$ and $a_1(1260)^+$ are included.

<u>VALUE</u>	<u>DOCUMENT ID</u>	<u>TECN</u>	<u>COMMENT</u>
0.099 ± 0.008 ± 0.018	LINK	03D FOCS	γ A, \bar{E}_γ ≈ 180 GeV

 $\Gamma(K^- 3\pi^+ \pi^- \text{ nonresonant})/\Gamma(K^- 3\pi^+ \pi^-)$ Γ_{74}/Γ_{69}

<u>VALUE</u>	<u>CL%</u>	<u>DOCUMENT ID</u>	<u>TECN</u>	<u>COMMENT</u>
0.07 ± 0.05 ± 0.01		LINK	03D FOCS	γ A, \bar{E}_γ ≈ 180 GeV

• • • We do not use the following data for averages, fits, limits, etc. **• • •**

<0.026	90	FRABETTI 97C E687	γ Be, \bar{E}_γ	≈ 200 GeV
--------	----	-------------------	-------------------------------	-------------------

 $\Gamma(K^+ 2K_S^0)/\Gamma(K^- \pi^+ \pi^+)$ Γ_{75}/Γ_{42}

<u>VALUE</u>	<u>EVTS</u>	<u>DOCUMENT ID</u>	<u>TECN</u>	<u>COMMENT</u>
0.049 ± 0.022 OUR AVERAGE				Error includes scale factor of 2.4.
0.035 ± 0.010 ± 0.005	39 ± 9	ALBRECHT 94I ARG	$e^+ e^-$	≈ 10 GeV
0.085 ± 0.018	70 ± 12	AMMAR 91 CLEO	$e^+ e^-$	≈ 10.5 GeV

 $\Gamma(K^+ K^- K_S^0 \pi^+)/\Gamma(K_S^0 \pi^+ \pi^+ \pi^-)$ Γ_{76}/Γ_{62}

<u>VALUE (units 10^{-3})</u>	<u>EVTS</u>	<u>DOCUMENT ID</u>	<u>TECN</u>	<u>COMMENT</u>
7.7 ± 1.5 ± 0.9	35 ± 7	LINK	01C FOCS	γ nucleus, \bar{E}_γ ≈ 180 GeV

Pionic modes $\Gamma(\pi^+ \pi^0)/\Gamma(K^- \pi^+ \pi^+)$ Γ_{93}/Γ_{42}

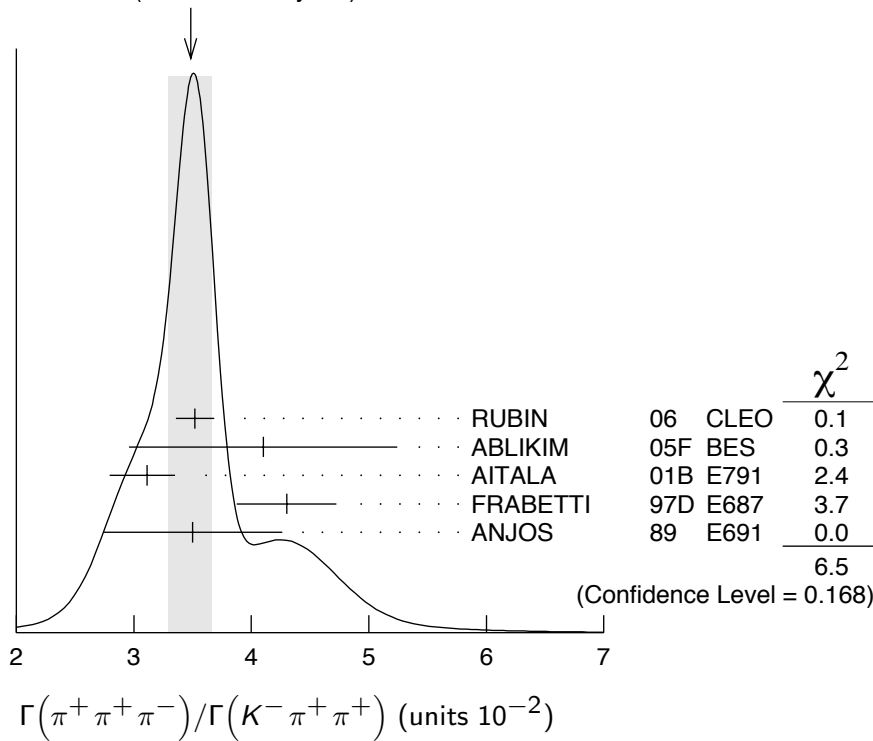
<u>VALUE (units 10^{-2})</u>	<u>EVTS</u>	<u>DOCUMENT ID</u>	<u>TECN</u>	<u>COMMENT</u>
1.35 ± 0.08 OUR AVERAGE				
1.33 ± 0.07 ± 0.06	914 ± 46	RUBIN 06	CLEO	$e^+ e^-$ at $\psi(3770)$
1.44 ± 0.19 ± 0.10	171 ± 22	ARMS 04	CLEO	$e^+ e^-$ ≈ 10 GeV
• • • We do not use the following data for averages, fits, limits, etc. • • •				
2.8 ± 0.6 ± 0.5	34	SELEN 93	CLE2	See ARMS 04

$\Gamma(\pi^+\pi^+\pi^-)/\Gamma(K^-\pi^+\pi^+)$

Γ_{94}/Γ_{42}

VALUE (units 10^{-2})	EVTS	DOCUMENT ID	TECN	COMMENT
3.48 ± 0.19 OUR AVERAGE	Error includes scale factor of 1.4. See the ideogram below.			
$3.52 \pm 0.11 \pm 0.12$	3303 ± 95	RUBIN	06 CLEO	e^+e^- at $\psi(3770)$
$4.1 \pm 1.1 \pm 0.3$	85 ± 22	ABLIKIM	05F BES	$e^+e^- \approx \psi(3770)$
$3.11 \pm 0.18^{+0.16}_{-0.26}$	1172	AITALA	01B E791	π^- nucleus, 500 GeV
$4.3 \pm 0.3 \pm 0.3$	236	FRABETTI	97D E687	γ Be \approx 200 GeV
$3.5 \pm 0.7 \pm 0.3$	83	ANJOS	89 E691	Photoproduction
$\bullet \bullet \bullet$ We do not use the following data for averages, fits, limits, etc. $\bullet \bullet \bullet$				
$3.2 \pm 1.1 \pm 0.3$	20	ADAMOVICH	93 WA82	π^- 340 GeV
$4.2 \pm 1.6 \pm 1.0$	57	BALTRUSAIT..85E	MRK3	e^+e^- 3.77 GeV

WEIGHTED AVERAGE
 3.48 ± 0.19 (Error scaled by 1.4)



$\Gamma(\rho^0\pi^+)/\Gamma(\pi^+\pi^+\pi^-)$

Γ_{95}/Γ_{94}

This is the "fit fraction" from the Dalitz-plot analysis.

VALUE	DOCUMENT ID	TECN	COMMENT
0.322 ± 0.027 OUR AVERAGE			
$0.3082 \pm 0.0314 \pm 0.0230$	LINK	04 FOCS	Dalitz fit, 1527 ± 51 evts
$0.336 \pm 0.032 \pm 0.022$	AITALA	01B E791	Dalitz fit, 1172 evts
$\bullet \bullet \bullet$ We do not use the following data for averages, fits, limits, etc. $\bullet \bullet \bullet$			
$0.289 \pm 0.055 \pm 0.058$	66 FRABETTI	97D E687	γ Be \approx 200 GeV

⁶⁶ FRABETTI 97D also includes $f_2(1270)\pi^+$ and $f_0(980)\pi^+$ modes in the fit, but the resulting decay fractions are not statistically significant.

$\Gamma(\pi^+(\pi^+\pi^-)_{S\text{-wave}})/\Gamma(\pi^+\pi^+\pi^-)$

Γ_{96}/Γ_{94}

This is the “fit fraction” from the Dalitz-plot analysis. See also the next three data blocks.

VALUE	DOCUMENT ID	TECN	COMMENT
0.5600±0.0324±0.0214	67 LINK	04 FOCS	Dalitz fit, 1527 ± 51 evts

67 LINK 04 borrows a K-matrix parametrization from ANISOVICH 03 of the full $\pi\pi$ S-wave isoscalar scattering amplitude to describe the $\pi^+\pi^-$ S-wave component of the $\pi^+\pi^+\pi^-$ state. The fit fraction given above is a sum over five f_0 mesons, the $f_0(980)$, $f_0(1300)$, $f_0(1200\text{--}1600)$, $f_0(1500)$, and $f_0(1750)$. See LINK 04 for details and discussion.

$\Gamma(\sigma\pi^+, \sigma \rightarrow \pi^+\pi^-)/\Gamma(\pi^+\pi^+\pi^-)$

Γ_{97}/Γ_{94}

This is the “fit fraction” from the Dalitz-plot analysis.

VALUE	DOCUMENT ID	TECN	COMMENT
0.463±0.090±0.021	AITALA	01B E791	Dalitz fit, 1172 evts

$\Gamma(f_0(980)\pi^+, f_0(980) \rightarrow \pi^+\pi^-)/\Gamma(\pi^+\pi^+\pi^-)$

Γ_{98}/Γ_{94}

This is the “fit fraction” from the Dalitz-plot analysis.

VALUE	DOCUMENT ID	TECN	COMMENT
0.062±0.013±0.004	AITALA	01B E791	Dalitz fit, 1172 evts

$\Gamma(f_0(1370)\pi^+, f_0(1370) \rightarrow \pi^+\pi^-)/\Gamma(\pi^+\pi^+\pi^-)$

Γ_{99}/Γ_{94}

This is the “fit fraction” from the Dalitz-plot analysis.

VALUE	DOCUMENT ID	TECN	COMMENT
0.023±0.015±0.008	AITALA	01B E791	Dalitz fit, 1172 evts

$\Gamma(f_2(1270)\pi^+, f_2(1270) \rightarrow \pi^+\pi^-)/\Gamma(\pi^+\pi^+\pi^-)$

Γ_{100}/Γ_{94}

This is the “fit fraction” from the Dalitz-plot analysis.

VALUE	DOCUMENT ID	TECN	COMMENT
0.15 ± 0.04 OUR AVERAGE	Error includes scale factor of 2.4.		
0.1174±0.0190±0.0029	LINK	04 FOCS	Dalitz fit, 1527 ± 51 evts

0.194 ± 0.025 ± 0.004 AITALA 01B E791 Dalitz fit, 1172 evts

$\Gamma(\rho(1450)^0\pi^+, \rho(1450)^0 \rightarrow \pi^+\pi^-)/\Gamma(\pi^+\pi^+\pi^-)$

Γ_{101}/Γ_{94}

This is the “fit fraction” from the Dalitz-plot analysis.

VALUE	DOCUMENT ID	TECN	COMMENT
• • • We do not use the following data for averages, fits, limits, etc. • • •			

0.007±0.007±0.003 AITALA 01B E791 Dalitz fit, 1172 evts

$\Gamma(\pi^+\pi^+\pi^- \text{ nonresonant})/\Gamma(\pi^+\pi^+\pi^-)$

Γ_{102}/Γ_{94}

This is the “fit fraction” from the Dalitz-plot analysis. The big difference between the results here of AITALA 01B and FRABETTI 97D is the addition of the $\sigma\pi^+$ channel to the AITALA 01B fit. LINK 04 (see earlier data blocks), in agreement with AITALA 01B, finds no evidence for a large nonresonant fraction.

VALUE	DOCUMENT ID	TECN	COMMENT
• • • We do not use the following data for averages, fits, limits, etc. • • •			
0.078±0.060±0.027 AITALA 01B E791 Dalitz fit, 1172 evts			

0.589±0.105±0.081 68 FRABETTI 97D E687 γ Be ≈ 200 GeV

68 FRABETTI 97D also includes $f_2(1270)\pi^+$ and $f_0(980)\pi^+$ modes in the fit, but the resulting decay fractions are not statistically significant.

$\Gamma(\pi^+ 2\pi^0)/\Gamma(K^- \pi^+ \pi^+)$ Γ_{103}/Γ_{42}

<u>VALUE</u> (units 10^{-2})	<u>EVTS</u>
5.0 ± 0.3 ± 0.3	1535 ± 89

<u>DOCUMENT ID</u>	<u>TECN</u>	<u>COMMENT</u>
RUBIN	06	CLEO $e^+ e^-$ at $\psi(3770)$

 $\Gamma(\pi^+ \pi^+ \pi^- \pi^0)/\Gamma(K^- \pi^+ \pi^+)$ Γ_{104}/Γ_{42}

<u>VALUE</u> (units 10^{-2})	<u>EVTS</u>
12.4 ± 0.5 ± 0.6	5701 ± 205

<u>DOCUMENT ID</u>	<u>TECN</u>	<u>COMMENT</u>
RUBIN	06	CLEO $e^+ e^-$ at $\psi(3770)$

 $\Gamma(\eta \pi^+)/\Gamma(\phi \pi^+)$ $\Gamma_{109}/\Gamma_{131}$ Unseen decay modes of the η are included.

<u>VALUE</u>	<u>EVTS</u>	<u>DOCUMENT ID</u>	<u>TECN</u>	<u>COMMENT</u>
0.54 ± 0.06 OUR FIT				
0.49 ± 0.08	275	JESSOP	98	CLE2 $e^+ e^- \approx \gamma(4S)$

 $\Gamma(\eta \pi^+)/\Gamma(K^- \pi^+ \pi^+)$ Γ_{109}/Γ_{42} Unseen decay modes of the η are included.

<u>VALUE</u> (units 10^{-2})	<u>EVTS</u>	<u>DOCUMENT ID</u>	<u>TECN</u>	<u>COMMENT</u>
3.68 ± 0.31 OUR FIT				
3.81 ± 0.26 ± 0.21	377 ± 26	RUBIN	06	CLEO $e^+ e^-$ at $\psi(3770)$

• • • We do not use the following data for averages, fits, limits, etc. • • •

8.3 ± 2.3 ± 1.4	99	DAOUDI	92	CLE2 See JESSOP 98
-------------------------	----	--------	----	--------------------

 $\Gamma(\omega \pi^+)/\Gamma_{\text{total}}$ Γ_{110}/Γ Unseen decay modes of the ω are included.

<u>VALUE</u>	<u>CL%</u>	<u>DOCUMENT ID</u>	<u>TECN</u>	<u>COMMENT</u>
<3.4 × 10⁻⁴	90	RUBIN	06	CLEO $e^+ e^-$ at $\psi(3770)$

 $\Gamma(3\pi^+ 2\pi^-)/\Gamma(K^- \pi^+ \pi^+)$ Γ_{107}/Γ_{42}

<u>VALUE</u> (units 10^{-2})	<u>EVTS</u>	<u>DOCUMENT ID</u>	<u>TECN</u>	<u>COMMENT</u>
1.77 ± 0.17 OUR FIT				
1.73 ± 0.20 ± 0.17	732 ± 77	RUBIN	06	CLEO $e^+ e^-$ at $\psi(3770)$

• • • We do not use the following data for averages, fits, limits, etc. • • •

2.3 ± 0.4 ± 0.2	58	FRABETTI	97C E687	γ Be, $\bar{E}_\gamma \approx 200$ GeV
-------------------------	----	----------	----------	---

 $\Gamma(3\pi^+ 2\pi^-)/\Gamma(K^- 3\pi^+ \pi^-)$ Γ_{107}/Γ_{69}

<u>VALUE</u>	<u>EVTS</u>	<u>DOCUMENT ID</u>	<u>TECN</u>	<u>COMMENT</u>
0.289 ± 0.019 OUR FIT				
0.290 ± 0.017 ± 0.011	835	LINK	03D FOCS	γ A, $\bar{E}_\gamma \approx 180$ GeV

 $\Gamma(\eta \rho^+)/\Gamma(\phi \pi^+)$ $\Gamma_{111}/\Gamma_{131}$ Unseen decay modes of the η are included.

<u>VALUE</u>	<u>CL%</u>	<u>DOCUMENT ID</u>	<u>TECN</u>	<u>COMMENT</u>
<1.11	90	JESSOP	98	CLE2 $e^+ e^- \approx \gamma(4S)$

 $\Gamma(\eta'(958)\pi^+)/\Gamma(\phi \pi^+)$ $\Gamma_{112}/\Gamma_{131}$ Unseen decay modes of the $\eta'(958)$ are included.

<u>VALUE</u>	<u>EVTS</u>	<u>DOCUMENT ID</u>	<u>TECN</u>	<u>COMMENT</u>
0.82 ± 0.14	126	JESSOP	98	CLE2 $e^+ e^- \approx \gamma(4S)$

$\Gamma(\eta'(958)\rho^+)/\Gamma(\phi\pi^+)$ $\Gamma_{113}/\Gamma_{131}$ Unseen decay modes of the $\eta'(958)$ are included.

VALUE	CL%	DOCUMENT ID	TECN	COMMENT
<0.86	90	JESSOP	98	CLE2 $e^+ e^- \approx \gamma(4S)$

Hadronic modes with a $K\bar{K}$ pair $\Gamma(K^+ K_S^0)/\Gamma(K_S^0 \pi^+)$ Γ_{114}/Γ_{41}

VALUE	EVTS	DOCUMENT ID	TECN	COMMENT
0.201 ± 0.011 OUR FIT				
0.206 ± 0.014 OUR AVERAGE				

0.222 ± 0.037 ± 0.013	63 ± 10	ABLIKIM	05F BES	$e^+ e^- \approx \psi(3770)$
0.1892 ± 0.0155 ± 0.0073	278 ± 21	ARMS	04 CLEO	$e^+ e^- \approx 10 \text{ GeV}$
0.25 ± 0.04 ± 0.02	129	FRABETTI	95 E687	$\gamma \text{Be } \bar{E}_\gamma \approx 200 \text{ GeV}$
0.271 ± 0.065 ± 0.039	69	ANJOS	90C E691	γBe
0.317 ± 0.086 ± 0.048	31	BALTRUSAIT..85E	MRK3	$e^+ e^- 3.77 \text{ GeV}$
0.25 ± 0.15	6	SCHINDLER	81 MRK2	$e^+ e^- 3.771 \text{ GeV}$

• • • We do not use the following data for averages, fits, limits, etc. • • •

0.1996 ± 0.0119 ± 0.0096	949	LINK	02B FOCS	$\gamma \text{A}, \bar{E}_\gamma \approx 180 \text{ GeV}$
0.222 ± 0.041 ± 0.019	70	BISHAI	97 CLE2	See ARMS 04

⁶⁹ This LINK 02B result is redundant with a result in the next datablock.

⁷⁰ This BISHAI 97 result is redundant with results elsewhere in the Listings.

 $\Gamma(K^+ K_S^0)/\Gamma(K^- \pi^+ \pi^+)$ Γ_{114}/Γ_{42}

VALUE (units 10^{-2})	EVTS	DOCUMENT ID	TECN	COMMENT
3.11 ± 0.17 OUR FIT				
3.02 ± 0.18 ± 0.15	949	LINK	02B FOCS	$\gamma \text{nucleus}, \bar{E}_\gamma \approx 180 \text{ GeV}$

• • • We do not use the following data for averages, fits, limits, etc. • • •

3.86 ± 0.69 ± 0.37	70	71 BISHAI	97 CLE2	See ARMS 04
--------------------	----	-----------	---------	-------------

⁷¹ See BISHAI 97 for an isospin analysis of $D^+ \rightarrow K\bar{K}$ amplitudes.

 $\Gamma(K^+ K^- \pi^+)/\Gamma_{\text{total}}$ Γ_{115}/Γ

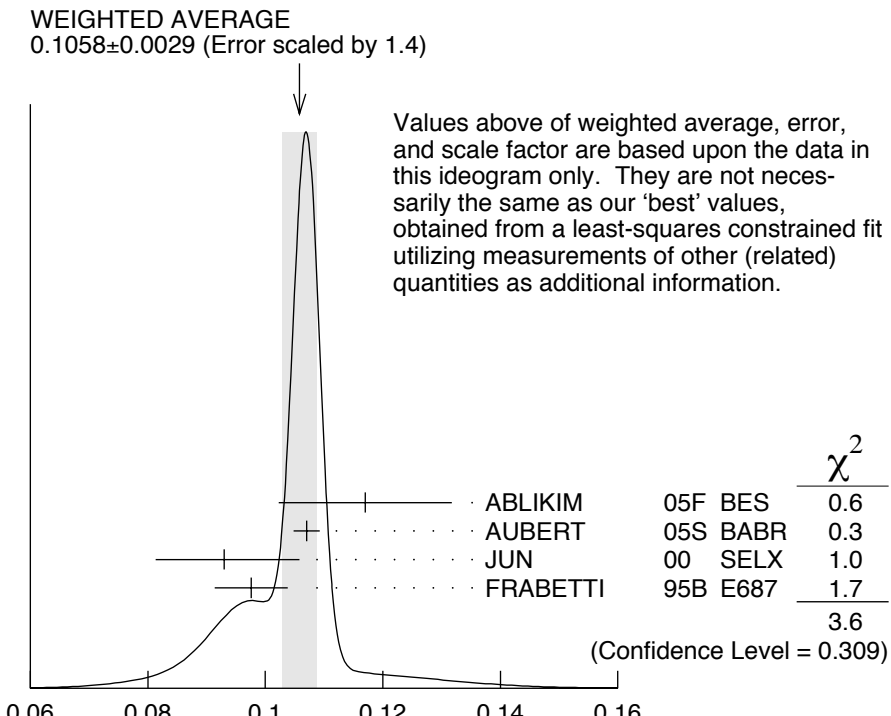
VALUE	EVTS	DOCUMENT ID	TECN	COMMENT
0.0100 ± 0.0004 OUR FIT				Error includes scale factor of 1.2.
0.0097 ± 0.0004 ± 0.0004	1250 ± 40	72 HE	05 CLEO	$e^+ e^- \text{ at } \psi(3770)$

⁷² HE 05 uses single- and double-tagged events in an overall fit. The fraction here includes (unobserved) final-state photons.

 $\Gamma(K^+ K^- \pi^+)/\Gamma(K^- \pi^+ \pi^+)$ Γ_{115}/Γ_{42}

VALUE	EVTS	DOCUMENT ID	TECN	COMMENT
0.1054 ± 0.0025 OUR FIT				Error includes scale factor of 1.3.
0.1058 ± 0.0029 OUR AVERAGE				Error includes scale factor of 1.4. See the ideogram below.

0.117 ± 0.013 ± 0.007	181 ± 20	ABLIKIM	05F BES	$e^+ e^- \approx \psi(3770)$
0.107 ± 0.001 ± 0.002	43k	AUBERT	05S BABR	$e^+ e^- \approx \gamma(4S)$
0.093 ± 0.010	+0.008 -0.006	JUN	00 SELX	$\Sigma^- \text{nucleus}, 600 \text{ GeV}$
0.0976 ± 0.0042 ± 0.0046		FRABETTI	95B E687	$\gamma \text{Be}, \bar{E}_\gamma \approx 200 \text{ GeV}$



$$\Gamma(K^+ K^- \pi^+)/\Gamma(K^- \pi^+ \pi^+)$$

$$\Gamma_{115}/\Gamma_{42}$$

$$\Gamma(\phi\pi^+, \phi \rightarrow K^+ K^-)/\Gamma(K^+ K^- \pi^+)$$

$$\Gamma_{116}/\Gamma_{115}$$

This is the "fit fraction" from the Dalitz-plot analysis.

VALUE	DOCUMENT ID	TECN	COMMENT
0.317±0.034 OUR FIT			
0.292±0.031±0.030	FRABETTI	95B E687	Dalitz fit, 915 evts

$$\Gamma(\phi\pi^+, \phi \rightarrow K^+ K^-)/\Gamma(\phi\pi^+)$$

$$\Gamma_{116}/\Gamma_{131}$$

VALUE	DOCUMENT ID
0.491±0.006 OUR FIT	
0.491±0.006	73 PDG 06

⁷³ This is, of course, just the $\phi \rightarrow K^+ K^-$ branching fraction, but we need it to connect other modes in the fit.

$$\Gamma(\phi\pi^+)/\Gamma(K^- \pi^+ \pi^+)$$

$$\Gamma_{131}/\Gamma_{42}$$

Unseen decay modes of the ϕ are included. However, we now get branching fractions for resonant submodes of $K^+ K^- \pi^+$ decays from Dalitz-plot analyses.

VALUE	EVTS	DOCUMENT ID	TECN	COMMENT
• • • We do not use the following data for averages, fits, limits, etc. • • •				
0.062±0.017±0.006	19	ADAMOVICH 93 WA82	π^- 340 GeV	
0.077±0.011±0.005	128	DAOUDI 92 CLE2	$e^+ e^- \approx 10.5$ GeV	
0.098±0.032±0.014	12	ALVAREZ 90c NA14	Photoproduction	
0.071±0.008±0.007	84	ANJOS 88 E691	Photoproduction	
0.084±0.021±0.011	21	BALTRUSAIT..85E MRK3	$e^+ e^-$ 3.77 GeV	

$$\Gamma(K^+ \bar{K}^*(892)^0, \bar{K}^*(892)^0 \rightarrow K^- \pi^+)/\Gamma(K^+ K^- \pi^+) \quad \Gamma_{117}/\Gamma_{115}$$

This is the “fit fraction” from the Dalitz-plot analysis.

<u>VALUE</u>	<u>DOCUMENT ID</u>	<u>TECN</u>	<u>COMMENT</u>
0.301±0.020±0.025	FRABETTI	95B E687	Dalitz fit, 915 evts

$$\Gamma(K^+ \bar{K}_0^*(1430)^0, \bar{K}_0^*(1430)^0 \rightarrow K^- \pi^+)/\Gamma(K^+ K^- \pi^+) \quad \Gamma_{118}/\Gamma_{115}$$

This is the “fit fraction” from the Dalitz-plot analysis.

<u>VALUE</u>	<u>DOCUMENT ID</u>	<u>TECN</u>	<u>COMMENT</u>
0.370±0.035±0.018	FRABETTI	95B E687	Dalitz fit, 915 evts

$$\Gamma(K^+ \bar{K}^*(892)^0)/\Gamma(K^- \pi^+ \pi^+) \quad \Gamma_{134}/\Gamma_{42}$$

Unseen decay modes of the $\bar{K}^*(892)^0$ are included. However, we now get branching fractions for resonant submodes of $K^+ K^- \pi^+$ decays from Dalitz-plot analyses.

<u>VALUE</u>	<u>EVTS</u>	<u>DOCUMENT ID</u>	<u>TECN</u>	<u>COMMENT</u>
• • • We do not use the following data for averages, fits, limits, etc. • • •				
0.058±0.009±0.006	73	ANJOS	88 E691	Photoproduction
0.048±0.021±0.011	14	BALTRUSAIT..85E	MRK3	$e^+ e^-$ 3.77 GeV

$$\Gamma(K^+ K^- \pi^+ \text{ nonresonant})/\Gamma(K^- \pi^+ \pi^+) \quad \Gamma_{119}/\Gamma_{42}$$

<u>VALUE</u>	<u>EVTS</u>	<u>DOCUMENT ID</u>	<u>TECN</u>	<u>COMMENT</u>
• • • We do not use the following data for averages, fits, limits, etc. • • •				
0.049±0.008±0.006	95	ANJOS	88 E691	Photoproduction
0.059±0.026±0.009	37	BALTRUSAIT..85E	MRK3	$e^+ e^-$ 3.77 GeV

$$\Gamma(K^*(892)^+ K_S^0)/\Gamma(K_S^0 \pi^+) \quad \Gamma_{135}/\Gamma_{41}$$

Unseen decay modes of the $K^*(892)^+$ are included.

<u>VALUE</u>	<u>EVTS</u>	<u>DOCUMENT ID</u>	<u>TECN</u>	<u>COMMENT</u>
1.1±0.3±0.4	67	FRABETTI	95 E687	γ Be $\bar{E}_\gamma \approx 200$ GeV

$$\Gamma(\phi \pi^+ \pi^0)/\Gamma_{\text{total}} \quad \Gamma_{132}/\Gamma$$

Unseen decay modes of the ϕ are included.

<u>VALUE</u>	<u>DOCUMENT ID</u>	<u>TECN</u>	<u>COMMENT</u>
0.023±0.010	74 BARLAG	92C ACCM	π^- Cu 230 GeV

⁷⁴ BARLAG 92C computes the branching fraction using topological normalization.

$$\Gamma(\phi \pi^+ \pi^0)/\Gamma(K^- \pi^+ \pi^+) \quad \Gamma_{132}/\Gamma_{42}$$

Unseen decay modes of the ϕ are included.

<u>VALUE</u>	<u>CL%</u>	<u>DOCUMENT ID</u>	<u>TECN</u>	<u>COMMENT</u>
• • • We do not use the following data for averages, fits, limits, etc. • • •				
<0.58	90	ALVAREZ	90C NA14	Photoproduction
<0.28	90	ANJOS	89E E691	Photoproduction

$$\Gamma(\phi \rho^+)/\Gamma(K^- \pi^+ \pi^+) \quad \Gamma_{133}/\Gamma_{42}$$

Unseen decay modes of the ϕ are included.

<u>VALUE</u>	<u>CL%</u>	<u>DOCUMENT ID</u>	<u>TECN</u>	<u>COMMENT</u>
<0.16	90	DAOUDI	92 CLE2	$e^+ e^- \approx 10.5$ GeV

$\Gamma(K^+ K^- \pi^+ \pi^0 \text{non-}\phi)/\Gamma_{\text{total}}$ Γ_{125}/Γ

VALUE	DOCUMENT ID	TECN	COMMENT
0.015\pm0.007 -0.006	75 BARLAG	92C ACCM	π^- Cu 230 GeV

75 BARLAG 92C computes the branching fraction using topological normalization.

$\Gamma(K^+ K^- \pi^+ \pi^0 \text{non-}\phi)/\Gamma(K^- \pi^+ \pi^+)$ Γ_{125}/Γ_{42}

VALUE	CL%	DOCUMENT ID	TECN	COMMENT
• • • We do not use the following data for averages, fits, limits, etc. • • •				
<0.25	90	ANJOS	89E E691	Photoproduction

$\Gamma(K^+ K_S^0 \pi^+ \pi^-)/\Gamma(K_S^0 \pi^+ \pi^+ \pi^-)$ Γ_{126}/Γ_{62}

VALUE (units 10^{-2})	EVTS	DOCUMENT ID	TECN	COMMENT
5.62\pm0.39\pm0.40	469 ± 32	LINK	01C FOCS	γ nucleus, $\bar{E}_\gamma \approx 180$ GeV

$\Gamma(K_S^0 K^- \pi^+ \pi^+)/\Gamma(K_S^0 \pi^+ \pi^+ \pi^-)$ Γ_{127}/Γ_{62}

VALUE (units 10^{-2})	EVTS	DOCUMENT ID	TECN	COMMENT
7.68\pm0.41\pm0.32	670 ± 35	LINK	01C FOCS	γ nucleus, $\bar{E}_\gamma \approx 180$ GeV

$\Gamma(K^*(892)^+ \bar{K}^*(892)^0)/\Gamma_{\text{total}}$ Γ_{136}/Γ

Unseen decay modes of the $K^*(892)$'s are included.

VALUE	DOCUMENT ID	TECN	COMMENT
0.026\pm0.008\pm0.007	ALBRECHT	92B ARG	$e^+ e^- \simeq 10.4$ GeV

$\Gamma(K_S^0 K^- \pi^+ \pi^+ (\text{non-}K^*+\bar{K}^{*0}))/\Gamma_{\text{total}}$ Γ_{129}/Γ

VALUE	CL%	DOCUMENT ID	TECN	COMMENT
<0.004	90	ALBRECHT	92B ARG	$e^+ e^- \simeq 10.4$ GeV

$\Gamma(K^+ K^- \pi^+ \pi^+ \pi^-)/\Gamma(K^- 3\pi^+ \pi^-)$ Γ_{130}/Γ_{69}

VALUE	EVTS	DOCUMENT ID	TECN	COMMENT
0.040\pm0.009\pm0.019	38	LINK	03D FOCS	γ A, $\bar{E}_\gamma \approx 180$ GeV

———— Doubly Cabibbo-suppressed modes ——

$\Gamma(K^+ \pi^0)/\Gamma_{\text{total}}$ Γ_{137}/Γ

VALUE	CL%	DOCUMENT ID	TECN	COMMENT
<4.2 \times 10⁻⁴	90	ARMS	04 CLEO	$e^+ e^- \approx 10$ GeV

$\Gamma(K^+ \pi^+ \pi^-)/\Gamma(K^- \pi^+ \pi^+)$ Γ_{138}/Γ_{42}

VALUE	EVTS	DOCUMENT ID	TECN	COMMENT
0.0068\pm0.0008 OUR AVERAGE				
0.0065 \pm 0.0008 \pm 0.0004	189 ± 24	LINK	04F FOCS	γ A, $\bar{E}_\gamma \approx 180$ GeV
0.0077 \pm 0.0017 \pm 0.0008	59 ± 13	AITALA	97C E791	π^- A, 500 GeV
0.0072 \pm 0.0023 \pm 0.0017	21	FRABETTI	95E E687	γ Be, $\bar{E}_\gamma = 220$ GeV

$\Gamma(K^+\rho^0)/\Gamma(K^+\pi^+\pi^-)$

$\Gamma_{139}/\Gamma_{138}$

This is the "fit fraction" from the Dalitz-plot analysis.

VALUE	DOCUMENT ID	TECN	COMMENT
0.39 ± 0.09 OUR AVERAGE			
0.3943 ± 0.0787 ± 0.0815	LINK	04F FOCS	Dalitz fit, 189 evts
0.37 ± 0.14 ± 0.07	AITALA	97C E791	Dalitz fit, 59 evts

$\Gamma(K^+f_0(980), f_0(980) \rightarrow \pi^+\pi^-)/\Gamma(K^+\pi^+\pi^-)$

$\Gamma_{141}/\Gamma_{138}$

This is the "fit fraction" from the Dalitz-plot analysis.

VALUE	DOCUMENT ID	TECN	COMMENT
0.0892 ± 0.0333 ± 0.0412	LINK	04F FOCS	Dalitz fit, 189 evts

$\Gamma(K^*(892)^0\pi^+, K^*(892)^0 \rightarrow K^+\pi^-)/\Gamma(K^+\pi^+\pi^-)$

$\Gamma_{140}/\Gamma_{138}$

This is the "fit fraction" from the Dalitz-plot analysis.

VALUE	DOCUMENT ID	TECN	COMMENT
0.47 ± 0.08 OUR AVERAGE			
0.5220 ± 0.0684 ± 0.0638	LINK	04F FOCS	Dalitz fit, 189 evts
0.35 ± 0.14 ± 0.01	AITALA	97C E791	Dalitz fit, 59 evts

$\Gamma(K_2^*(1430)^0\pi^+, K_2^*(1430)^0 \rightarrow K^+\pi^-)/\Gamma(K^+\pi^+\pi^-)$

$\Gamma_{142}/\Gamma_{138}$

This is the "fit fraction" from the Dalitz-plot analysis.

VALUE	DOCUMENT ID	TECN	COMMENT
0.0803 ± 0.0372 ± 0.0391	LINK	04F FOCS	Dalitz fit, 189 evts

$\Gamma(K^+\pi^+\pi^- \text{ nonresonant})/\Gamma(K^+\pi^+\pi^-)$

$\Gamma_{143}/\Gamma_{138}$

This is the "fit fraction" from the Dalitz-plot analysis.

VALUE	DOCUMENT ID	TECN	COMMENT
• • • We do not use the following data for averages, fits, limits, etc. • • •			
0.36 ± 0.14 ± 0.07	76 AITALA	97C E791	Dalitz fit, 59 evts

76 LINK 04F, with three times as many events, finds no need for a nonresonant amplitude.

$\Gamma(K^+K^+K^-)/\Gamma(K^-\pi^+\pi^+)$

Γ_{144}/Γ_{42}

VALUE (units 10^{-4})	CL%	EVTS	DOCUMENT ID	TECN	COMMENT
9.49 ± 2.17 ± 0.22	65	77	LINK	02I FOCS	γ nucleus, ≈ 180 GeV

• • • We do not use the following data for averages, fits, limits, etc. • • •

<16	90	78	FRABETTI	95F E687	γ Be, $\bar{E}_\gamma \approx 220$ GeV
570 ± 200 ± 70	13	ADAMOVICH	93 WA82	π^-	340 GeV

77 LINK 02I finds little evidence for ϕK^+ or $f_0(980)K^+$ submodes.

78 Using the $\phi\pi^+$ mode to normalize, FRABETTI 95F gets $\Gamma(K^+K^+K^-)/\Gamma(\phi\pi^+) < 0.025$.

$\Gamma(\phi K^+)/\Gamma(\phi\pi^+)$

$\Gamma_{145}/\Gamma_{131}$

VALUE	CL%	EVTS	DOCUMENT ID	TECN	COMMENT
• • • We do not use the following data for averages, fits, limits, etc. • • •					
<0.021	90	FRABETTI	95F E687	γ Be, $\bar{E}_\gamma \approx 220$ GeV	
0.058 ^{+0.032} _{-0.026} ± 0.007	4	79 ANJOS	92D E691	γ Be, $\bar{E}_\gamma = 145$ GeV	

79 The evidence of ANJOS 92D is a small excess of events ($4.5^{+2.4}_{-2.0}$).

Rare or forbidden modes **$\Gamma(\pi^+ e^+ e^-)/\Gamma_{\text{total}}$** **$\Gamma_{146}/\Gamma$**

A test for the $\Delta C = 1$ weak neutral current. Allowed by higher-order electroweak interactions.

VALUE	CL%	EVTS	DOCUMENT ID	TECN	COMMENT
$<7.4 \times 10^{-6}$	90		HE	05A CLEO	$e^+ e^-$ at $\psi(3770)$
• • • We do not use the following data for averages, fits, limits, etc. • • •					
$<5.2 \times 10^{-5}$	90		AITALA	99G E791	$\pi^- N$ 500 GeV
$<1.1 \times 10^{-4}$	90		FRABETTI	97B E687	γ Be, $\bar{E}_\gamma \approx 220$ GeV
$<6.6 \times 10^{-5}$	90		AITALA	96 E791	$\pi^- N$ 500 GeV
$<2.5 \times 10^{-3}$	90		WEIR	90B MRK2	$e^+ e^-$ 29 GeV
$<2.6 \times 10^{-3}$	90	39	HAAS	88 CLEO	$e^+ e^-$ 10 GeV

 $\Gamma(\pi^+ \phi, \phi \rightarrow e^+ e^-)/\Gamma_{\text{total}}$ **Γ_{147}/Γ**

This is *not* a test for the $\Delta C = 1$ weak neutral current, but leads to the $\pi^+ e^+ e^-$ final state.

VALUE	EVTS	DOCUMENT ID	TECN	COMMENT
$(2.7^{+3.6}_{-1.8} \pm 0.2) \times 10^{-6}$	2	80 HE	05A CLEO	$e^+ e^-$ at $\psi(3770)$

⁸⁰ This HE 05A result is consistent with the branching fraction for $D^+ \rightarrow \phi \pi^+$, $\phi \rightarrow K^+ K^-$.

 $\Gamma(\pi^+ \mu^+ \mu^-)/\Gamma_{\text{total}}$ **Γ_{148}/Γ**

A test for the $\Delta C = 1$ weak neutral current. Allowed by higher-order electroweak interactions.

VALUE	CL%	EVTS	DOCUMENT ID	TECN	COMMENT
$<8.8 \times 10^{-6}$	90		LINK	03F FOCS	γ nucleus, $\bar{E}_\gamma \approx 180$ GeV
• • • We do not use the following data for averages, fits, limits, etc. • • •					
$<1.5 \times 10^{-5}$	90		AITALA	99G E791	$\pi^- N$ 500 GeV
$<8.9 \times 10^{-5}$	90		FRABETTI	97B E687	γ Be, $\bar{E}_\gamma \approx 220$ GeV
$<1.8 \times 10^{-5}$	90		AITALA	96 E791	$\pi^- N$ 500 GeV
$<2.2 \times 10^{-4}$	90	0	KODAMA	95 E653	π^- emulsion 600 GeV
$<5.9 \times 10^{-3}$	90		WEIR	90B MRK2	$e^+ e^-$ 29 GeV
$<2.9 \times 10^{-3}$	90	36	HAAS	88 CLEO	$e^+ e^-$ 10 GeV

 $\Gamma(\rho^+ \mu^+ \mu^-)/\Gamma_{\text{total}}$ **Γ_{149}/Γ**

A test for the $\Delta C = 1$ weak neutral current. Allowed by higher-order electroweak interactions.

VALUE	CL%	EVTS	DOCUMENT ID	TECN	COMMENT
$<5.6 \times 10^{-4}$	90	0	KODAMA	95 E653	π^- emulsion 600 GeV

 $\Gamma(K^+ e^+ e^-)/\Gamma_{\text{total}}$ **Γ_{150}/Γ**

VALUE	CL%	DOCUMENT ID	TECN	COMMENT
$<6.2 \times 10^{-6}$	90	HE	05A CLEO	$e^+ e^-$ at $\psi(3770)$
• • • We do not use the following data for averages, fits, limits, etc. • • •				
$<2.0 \times 10^{-4}$	90	AITALA	99G E791	$\pi^- N$ 500 GeV
$<2.0 \times 10^{-4}$	90	FRABETTI	97B E687	γ Be, $\bar{E}_\gamma \approx 220$ GeV
$<4.8 \times 10^{-3}$	90	WEIR	90B MRK2	$e^+ e^-$ 29 GeV

$\Gamma(K^+ \mu^+ \mu^-)/\Gamma_{\text{total}}$ Γ_{151}/Γ

<u>VALUE</u>	<u>CL%</u>	<u>EVTS</u>	<u>DOCUMENT ID</u>	<u>TECN</u>	<u>COMMENT</u>
$<9.2 \times 10^{-6}$	90		LINK	03F FOCS	γ nucleus, $\bar{E}_\gamma \approx 180$ GeV
$\bullet \bullet \bullet$ We do not use the following data for averages, fits, limits, etc. $\bullet \bullet \bullet$					
$<4.4 \times 10^{-5}$	90		AITALA	99G E791	$\pi^- N$ 500 GeV
$<9.7 \times 10^{-5}$	90		FRABETTI	97B E687	γ Be, $\bar{E}_\gamma \approx 220$ GeV
$<3.2 \times 10^{-4}$	90	0	KODAMA	95 E653	π^- emulsion 600 GeV
$<9.2 \times 10^{-3}$	90		WEIR	90B MRK2	$e^+ e^-$ 29 GeV

 $\Gamma(\pi^+ e^\pm \mu^\mp)/\Gamma_{\text{total}}$ Γ_{152}/Γ

A test of lepton-family-number conservation.

<u>VALUE</u>	<u>CL%</u>	<u>DOCUMENT ID</u>	<u>TECN</u>	<u>COMMENT</u>
$<3.4 \times 10^{-5}$	90	AITALA	99G E791	$\pi^- N$ 500 GeV

 $\Gamma(\pi^+ e^+ \mu^-)/\Gamma_{\text{total}}$ Γ_{153}/Γ

A test of lepton-family-number conservation.

<u>VALUE</u>	<u>CL%</u>	<u>DOCUMENT ID</u>	<u>TECN</u>	<u>COMMENT</u>
$\bullet \bullet \bullet$ We do not use the following data for averages, fits, limits, etc. $\bullet \bullet \bullet$				
$<1.1 \times 10^{-4}$	90	FRABETTI	97B E687	γ Be, $\bar{E}_\gamma \approx 220$ GeV
$<3.3 \times 10^{-3}$	90	WEIR	90B MRK2	$e^+ e^-$ 29 GeV

 $\Gamma(\pi^+ e^- \mu^+)/\Gamma_{\text{total}}$ Γ_{154}/Γ

A test of lepton-family-number conservation.

<u>VALUE</u>	<u>CL%</u>	<u>DOCUMENT ID</u>	<u>TECN</u>	<u>COMMENT</u>
$\bullet \bullet \bullet$ We do not use the following data for averages, fits, limits, etc. $\bullet \bullet \bullet$				
$<1.3 \times 10^{-4}$	90	FRABETTI	97B E687	γ Be, $\bar{E}_\gamma \approx 220$ GeV
$<3.3 \times 10^{-3}$	90	WEIR	90B MRK2	$e^+ e^-$ 29 GeV

 $\Gamma(K^+ e^\pm \mu^\mp)/\Gamma_{\text{total}}$ Γ_{155}/Γ

A test of lepton-family-number conservation.

<u>VALUE</u>	<u>CL%</u>	<u>DOCUMENT ID</u>	<u>TECN</u>	<u>COMMENT</u>
$<6.8 \times 10^{-5}$	90	AITALA	99G E791	$\pi^- N$ 500 GeV

 $\Gamma(K^+ e^+ \mu^-)/\Gamma_{\text{total}}$ Γ_{156}/Γ

A test of lepton-family-number conservation.

<u>VALUE</u>	<u>CL%</u>	<u>DOCUMENT ID</u>	<u>TECN</u>	<u>COMMENT</u>
$\bullet \bullet \bullet$ We do not use the following data for averages, fits, limits, etc. $\bullet \bullet \bullet$				
$<1.3 \times 10^{-4}$	90	FRABETTI	97B E687	γ Be, $\bar{E}_\gamma \approx 220$ GeV
$<3.4 \times 10^{-3}$	90	WEIR	90B MRK2	$e^+ e^-$ 29 GeV

 $\Gamma(K^+ e^- \mu^+)/\Gamma_{\text{total}}$ Γ_{157}/Γ

A test of lepton-family-number conservation.

<u>VALUE</u>	<u>CL%</u>	<u>DOCUMENT ID</u>	<u>TECN</u>	<u>COMMENT</u>
$\bullet \bullet \bullet$ We do not use the following data for averages, fits, limits, etc. $\bullet \bullet \bullet$				
$<1.2 \times 10^{-4}$	90	FRABETTI	97B E687	γ Be, $\bar{E}_\gamma \approx 220$ GeV
$<3.4 \times 10^{-3}$	90	WEIR	90B MRK2	$e^+ e^-$ 29 GeV

$\Gamma(\pi^- e^+ e^+)/\Gamma_{\text{total}}$ Γ_{158}/Γ

A test of lepton-number conservation.

VALUE	CL%	DOCUMENT ID	TECN	COMMENT	
$<3.6 \times 10^{-6}$	90	HE	05A CLEO	$e^+ e^-$ at $\psi(3770)$	
$\bullet \bullet \bullet$ We do not use the following data for averages, fits, limits, etc. $\bullet \bullet \bullet$					
$<9.6 \times 10^{-5}$	90	AITALA	99G E791	$\pi^- N$ 500 GeV	
$<1.1 \times 10^{-4}$	90	FRABETTI	97B E687	γ Be, $\bar{E}_\gamma \approx 220$ GeV	
$<4.8 \times 10^{-3}$	90	WEIR	90B MRK2	$e^+ e^-$ 29 GeV	

 $\Gamma(\pi^- \mu^+ \mu^+)/\Gamma_{\text{total}}$ Γ_{159}/Γ

A test of lepton-number conservation.

VALUE	CL%	EVTS	DOCUMENT ID	TECN	COMMENT	
$<4.8 \times 10^{-6}$	90		LINK	03F FOCS	γ nucleus, $\bar{E}_\gamma \approx 180$ GeV	
$\bullet \bullet \bullet$ We do not use the following data for averages, fits, limits, etc. $\bullet \bullet \bullet$						
$<1.7 \times 10^{-5}$	90		AITALA	99G E791	$\pi^- N$ 500 GeV	
$<8.7 \times 10^{-5}$	90		FRABETTI	97B E687	γ Be, $\bar{E}_\gamma \approx 220$ GeV	
$<2.2 \times 10^{-4}$	90	0	KODAMA	95 E653	π^- emulsion 600 GeV	
$<6.8 \times 10^{-3}$	90		WEIR	90B MRK2	$e^+ e^-$ 29 GeV	

 $\Gamma(\pi^- e^+ \mu^+)/\Gamma_{\text{total}}$ Γ_{160}/Γ

A test of lepton-number conservation.

VALUE	CL%	DOCUMENT ID	TECN	COMMENT	
$<5.0 \times 10^{-5}$	90	AITALA	99G E791	$\pi^- N$ 500 GeV	
$\bullet \bullet \bullet$ We do not use the following data for averages, fits, limits, etc. $\bullet \bullet \bullet$					
$<1.1 \times 10^{-4}$	90	FRABETTI	97B E687	γ Be, $\bar{E}_\gamma \approx 220$ GeV	
$<3.7 \times 10^{-3}$	90	WEIR	90B MRK2	$e^+ e^-$ 29 GeV	

 $\Gamma(\rho^- \mu^+ \mu^+)/\Gamma_{\text{total}}$ Γ_{161}/Γ

A test of lepton-number conservation.

VALUE	CL%	EVTS	DOCUMENT ID	TECN	COMMENT	
$<5.6 \times 10^{-4}$	90	0	KODAMA	95 E653	π^- emulsion 600 GeV	

 $\Gamma(K^- e^+ e^+)/\Gamma_{\text{total}}$ Γ_{162}/Γ

A test of lepton-number conservation.

VALUE	CL%	DOCUMENT ID	TECN	COMMENT	
$<4.5 \times 10^{-6}$	90	HE	05A CLEO	$e^+ e^-$ at $\psi(3770)$	
$\bullet \bullet \bullet$ We do not use the following data for averages, fits, limits, etc. $\bullet \bullet \bullet$					
$<1.2 \times 10^{-4}$	90	FRABETTI	97B E687	γ Be, $\bar{E}_\gamma \approx 220$ GeV	
$<9.1 \times 10^{-3}$	90	WEIR	90B MRK2	$e^+ e^-$ 29 GeV	

 $\Gamma(K^- \mu^+ \mu^+)/\Gamma_{\text{total}}$ Γ_{163}/Γ

A test of lepton-number conservation.

VALUE	CL%	EVTS	DOCUMENT ID	TECN	COMMENT	
$<1.3 \times 10^{-5}$	90		LINK	03F FOCS	γ nucleus, $\bar{E}_\gamma \approx 180$ GeV	
$\bullet \bullet \bullet$ We do not use the following data for averages, fits, limits, etc. $\bullet \bullet \bullet$						
$<1.2 \times 10^{-4}$	90		FRABETTI	97B E687	γ Be, $\bar{E}_\gamma \approx 220$ GeV	
$<3.2 \times 10^{-4}$	90	0	KODAMA	95 E653	π^- emulsion 600 GeV	
$<4.3 \times 10^{-3}$	90		WEIR	90B MRK2	$e^+ e^-$ 29 GeV	

$\Gamma(K^- e^+ \mu^+)/\Gamma_{\text{total}}$

A test of lepton-number conservation.

VALUE	CL%	DOCUMENT ID	TECN	COMMENT
$<1.3 \times 10^{-4}$	90	FRABETTI	97B E687	γ Be, $\bar{E}_\gamma \approx 220$ GeV
$\bullet \bullet \bullet$ We do not use the following data for averages, fits, limits, etc. $\bullet \bullet \bullet$				
$<4.0 \times 10^{-3}$	90	WEIR	90B MRK2	$e^+ e^-$ 29 GeV

Γ_{164}/Γ

$\Gamma(K^*(892)^-\mu^+\mu^+)/\Gamma_{\text{total}}$

A test of lepton-number conservation.

VALUE	CL%	EVTS	DOCUMENT ID	TECN	COMMENT
$<8.5 \times 10^{-4}$	90	0	KODAMA	95 E653	π^- emulsion 600 GeV

Γ_{165}/Γ

$D^\pm CP$ -VIOLATING DECAY-RATE ASYMMETRIES

$A_{CP}(K_S^0 \pi^\pm)$ in $D^\pm \rightarrow K_S^0 \pi^\pm$

This is the difference between D^+ and D^- partial widths for these modes divided by the sum of the widths.

VALUE	EVTS	DOCUMENT ID	TECN	COMMENT
$-0.016 \pm 0.015 \pm 0.009$	10.6k	81 LINK	02B FOCS	γ nucleus, $\bar{E}_\gamma \approx 180$ GeV

81 LINK 02B measures $N(D^+ \rightarrow K_S^0 \pi^+)/N(D^+ \rightarrow K^- \pi^+ \pi^+)$, the ratio of numbers of events observed, and similarly for the D^- .

$A_{CP}(K_S^0 K^\pm)$ in $D^\pm \rightarrow K_S^0 K^\pm$

This is the difference between D^+ and D^- partial widths for these modes divided by the sum of the widths.

VALUE	EVTS	DOCUMENT ID	TECN	COMMENT
$+0.071 \pm 0.061 \pm 0.012$	949	82 LINK	02B FOCS	γ nucleus, $\bar{E}_\gamma \approx 180$ GeV

$\bullet \bullet \bullet$ We do not use the following data for averages, fits, limits, etc. $\bullet \bullet \bullet$

$+0.069 \pm 0.060 \pm 0.015$	949	83 LINK	02B FOCS	γ nucleus, $\bar{E}_\gamma \approx 180$ GeV
------------------------------	-----	---------	----------	--

82 LINK 02B measures $N(D^+ \rightarrow K_S^0 K^+)/N(D^+ \rightarrow K_S^0 \pi^+)$, the ratio of numbers of events observed, and similarly for the D^- .

83 LINK 02B measures $N(D^+ \rightarrow K_S^0 K^+)/N(D^+ \rightarrow K^- \pi^+ \pi^+)$, the ratio of numbers of events observed, and similarly for the D^- .

$A_{CP}(K^+ K^- \pi^\pm)$ in $D^\pm \rightarrow K^+ K^- \pi^\pm$

This is the difference between D^+ and D^- partial widths for these modes divided by the sum of the widths.

VALUE	EVTS	DOCUMENT ID	TECN	COMMENT
0.007 \pm 0.008 OUR AVERAGE				
$+0.014 \pm 0.010 \pm 0.008$	43k \pm 321	84 AUBERT	05S BABR	$e^+ e^- \approx \gamma(4S)$
$+0.006 \pm 0.011 \pm 0.005$	14k	85 LINK	00B FOCS	
-0.014 ± 0.029		85 AITALA	97B E791	$-0.062 < A_{CP} < +0.034$ (90% CL)
-0.031 ± 0.068		85 FRABETTI	94I E687	$-0.14 < A_{CP} < +0.081$ (90% CL)

- ⁸⁴ AUBERT 05S measures $N(D^+ \rightarrow K^+ K^- \pi^+)/N(D_s^+ \rightarrow K^+ K^- \pi^+)$, the ratio of the numbers of events observed, and similarly for the D^- .
⁸⁵ FRABETTI 94I, AITALA 98C, and LINK 00B measure $N(D^+ \rightarrow K^- K^+ \pi^+)/N(D^+ \rightarrow K^- \pi^+ \pi^+)$, the ratio of numbers of events observed, and similarly for the D^- .

$A_{CP}(K^\pm K^{*0})$ in $D^+ \rightarrow K^+ \bar{K}^{*0}$, $D^- \rightarrow K^- K^{*0}$

This is the difference between D^+ and D^- partial widths for these modes divided by the sum of the widths.

VALUE	EVTS	DOCUMENT ID	TECN	COMMENT
0.005±0.017 OUR AVERAGE				
+0.009±0.017±0.007	11k±122	86 AUBERT	05S BABR	$e^+ e^- \approx \gamma(4S)$
-0.010±0.050		87 AITALA	97B E791	$-0.092 < A_{CP} < +0.072$ (90% CL)
-0.12 ± 0.13		87 FRABETTI	94I E687	$-0.33 < A_{CP} < +0.094$ (90% CL)

- ⁸⁶ AUBERT 05S measures $N(D^+ \rightarrow K^+ \bar{K}^{*0})/N(D_s^+ \rightarrow K^+ K^- \pi^+)$, the ratio of the numbers of events observed, and similarly for the D^- .
⁸⁷ FRABETTI 94I and AITALA 97B measure $N(D^+ \rightarrow K^+ \bar{K}^*(892)^0)/N(D^+ \rightarrow K^- \pi^+ \pi^+)$, the ratio of numbers of events observed, and similarly for the D^- .

$A_{CP}(\phi\pi^\pm)$ in $D^\pm \rightarrow \phi\pi^\pm$

This is the difference between D^+ and D^- partial widths for these modes divided by the sum of the widths.

VALUE	EVTS	DOCUMENT ID	TECN	COMMENT
-0.001±0.015 OUR AVERAGE				
+0.002±0.015±0.006	10k±136	88 AUBERT	05S BABR	$e^+ e^- \approx \gamma(4S)$
-0.028±0.036		89 AITALA	97B E791	$-0.087 < A_{CP} < +0.031$ (90% CL)
+0.066±0.086		89 FRABETTI	94I E687	$-0.075 < A_{CP} < +0.21$ (90% CL)

- ⁸⁸ AUBERT 05S measures $N(D^+ \rightarrow \phi\pi^+)/N(D_s^+ \rightarrow K^+ K^- \pi^+)$, the ratio of the numbers of events observed, and similarly for the D^- .
⁸⁹ FRABETTI 94I and AITALA 97B measure $N(D^+ \rightarrow \phi\pi^+)/N(D^+ \rightarrow K^- \pi^+ \pi^+)$, the ratio of numbers of events observed, and similarly for the D^- .

$A_{CP}(\pi^+\pi^-\pi^\pm)$ in $D^\pm \rightarrow \pi^+\pi^-\pi^\pm$

This is the difference between D^+ and D^- partial widths for these modes divided by the sum of the widths.

VALUE	DOCUMENT ID	TECN	COMMENT
-0.017±0.042	90 AITALA	97B E791	$-0.086 < A_{CP} < +0.052$ (90% CL)
⁹⁰ AITALA 97B measure $N(D^+ \rightarrow \pi^+\pi^-\pi^+)/N(D^+ \rightarrow K^-\pi^+\pi^+)$, the ratio of numbers of events observed, and similarly for the D^- .			

$A_{CP}(K_S^0 K^\pm \pi^+ \pi^-)$ in $D^\pm \rightarrow K_S^0 K^\pm \pi^+ \pi^-$

This is the difference between D^+ and D^- partial widths for these modes divided by the sum of the widths.

VALUE	EVTS	DOCUMENT ID	TECN	COMMENT
-0.042±0.064±0.022	523 ± 32	LINK	05E FOCS	γA , $\bar{E}_\gamma \approx 180$ GeV

$D^+ - D^-$ T -VIOLATING DECAY-RATE ASYMMETRIES **$A_{T\text{viol}}(K_S^0 K^\pm \pi^\mp \pi^\pm)$ in $D^\pm \rightarrow K_S^0 K^\pm \pi^\pm \pi^\mp$**

$C_T \equiv \vec{p}_{K^+} \cdot (\vec{p}_{\pi^+} \times \vec{p}_{\pi^-})$ is a T -odd correlation of the K^+ , π^+ , and π^- momenta for the D^+ . $\bar{C}_T \equiv \vec{p}_{K^-} \cdot (\vec{p}_{\pi^-} \times \vec{p}_{\pi^+})$ is the corresponding quantity for the D^- . $A_T \equiv [\Gamma(C_T > 0) - \Gamma(C_T < 0)] / [\Gamma(C_T > 0) + \Gamma(C_T < 0)]$ would, in the absence of strong phases, test for T violation in D^+ decays (the Γ 's are partial widths). With $\bar{A}_T \equiv [\Gamma(-\bar{C}_T > 0) - \Gamma(-\bar{C}_T < 0)] / [\Gamma(-\bar{C}_T > 0) + \Gamma(-\bar{C}_T < 0)]$, the asymmetry $A_{T\text{viol}} \equiv \frac{1}{2}(A_T - \bar{A}_T)$ tests for T violation even with nonzero strong phases.

VALUE	EVTS	DOCUMENT ID	TECN	COMMENT
+0.023 ± 0.062 ± 0.022	523 ± 32	LINK	05E FOCS	γA , $\bar{E}_\gamma \approx 180$ GeV

 $D^+ \rightarrow \bar{K}^*(892)^0 \ell^+ \nu_\ell$ FORM FACTORS **$r_v \equiv V(0)/A_1(0)$ in $D^+ \rightarrow \bar{K}^*(892)^0 \ell^+ \nu_\ell$**

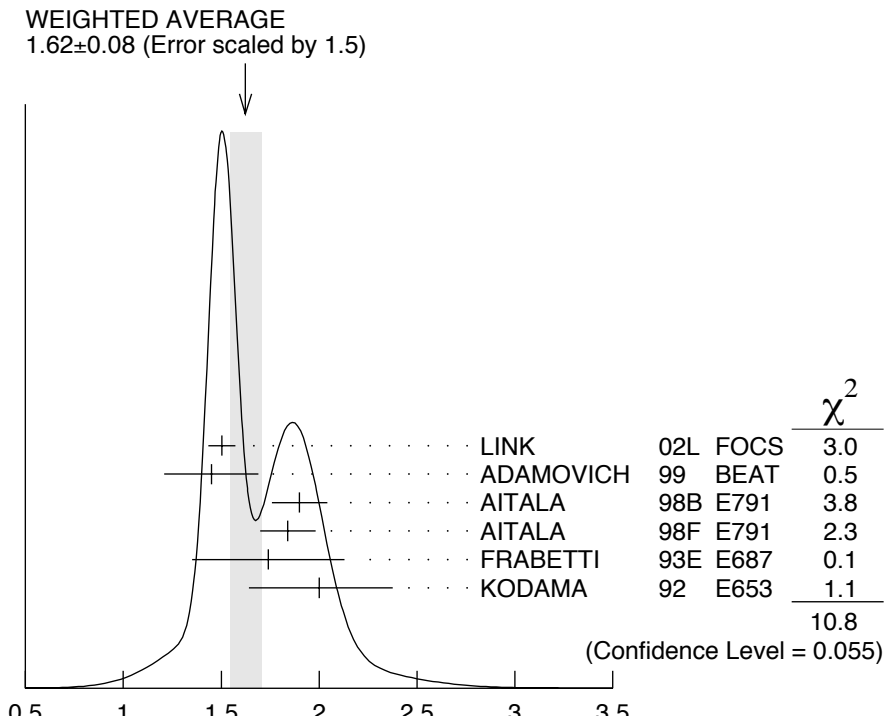
VALUE	EVTS	DOCUMENT ID	TECN	COMMENT
1.62 ± 0.08 OUR AVERAGE				Error includes scale factor of 1.5. See the ideogram below.
1.504 ± 0.057 ± 0.039	15k	91 LINK	02L FOCS	$\bar{K}^*(892)^0 \mu^+ \nu_\mu$
1.45 ± 0.23 ± 0.07	763	ADAMOVICH	99 BEAT	$\bar{K}^*(892)^0 \mu^+ \nu_\mu$
1.90 ± 0.11 ± 0.09	3000	92 AITALA	98B E791	$\bar{K}^*(892)^0 e^+ \nu_e$
1.84 ± 0.11 ± 0.09	3034	AITALA	98F E791	$\bar{K}^*(892)^0 \mu^+ \nu_\mu$
1.74 ± 0.27 ± 0.28	874	FRABETTI	93E E687	$\bar{K}^*(892)^0 \mu^+ \nu_\mu$
2.00 $^{+0.34}_{-0.32}$ ± 0.16	305	KODAMA	92 E653	$\bar{K}^*(892)^0 \mu^+ \nu_\mu$

• • • We do not use the following data for averages, fits, limits, etc. • • •

2.0 ± 0.6 ± 0.3 183 ANJOS 90E E691 $\bar{K}^*(892)^0 e^+ \nu_e$

91 LINK 02L includes the effects of interference with an S -wave background. This much improves the goodness of fit, but does not much shift the values of the form factors.

92 This is slightly different from the AITALA 98B value: see ref. [5] in AITALA 98F.



$$r_v \equiv V(0)/A_1(0) \text{ in } D^+ \rightarrow \bar{K}^*(892)^0 \ell^+ \nu_\ell$$

$$r_2 \equiv A_2(0)/A_1(0) \text{ in } D^+ \rightarrow \bar{K}^*(892)^0 \ell^+ \nu_\ell$$

VALUE	EVTS	DOCUMENT ID	TECN	COMMENT
0.83 ±0.05 OUR AVERAGE				
0.875±0.049±0.064	15k	93 LINK	02L FOCS	$\bar{K}^*(892)^0 \mu^+ \nu_\mu$
1.00 ±0.15 ±0.03	763	ADAMOVICH	99 BEAT	$\bar{K}^*(892)^0 \mu^+ \nu_\mu$
0.71 ±0.08 ±0.09	3000	AITALA	98B E791	$\bar{K}^*(892)^0 e^+ \nu_e$
0.75 ±0.08 ±0.09	3034	AITALA	98F E791	$\bar{K}^*(892)^0 \mu^+ \nu_\mu$
0.78 ±0.18 ±0.10	874	FRABETTI	93E E687	$\bar{K}^*(892)^0 \mu^+ \nu_\mu$
0.82 +0.22 -0.23 ±0.11	305	KODAMA	92 E653	$\bar{K}^*(892)^0 \mu^+ \nu_\mu$
• • • We do not use the following data for averages, fits, limits, etc. • • •				
0.0 ±0.5 ±0.2	183	ANJOS	90E E691	$\bar{K}^*(892)^0 e^+ \nu_e$

93 LINK 02L includes the effects of interference with an S-wave background. This much improves the goodness of fit, but does not much shift the values of the form factors.

$$r_3 \equiv A_3(0)/A_1(0) \text{ in } D^+ \rightarrow \bar{K}^*(892)^0 \ell^+ \nu_\ell$$

VALUE	EVTS	DOCUMENT ID	TECN	COMMENT
0.04±0.33±0.29				
3034	AITALA	98F E791		$\bar{K}^*(892)^0 \mu^+ \nu_\mu$

$$\Gamma_L/\Gamma_T \text{ in } D^+ \rightarrow \bar{K}^*(892)^0 \ell^+ \nu_\ell$$

VALUE	EVTS	DOCUMENT ID	TECN	COMMENT
1.13±0.08 OUR AVERAGE				
1.09±0.10±0.02	763	ADAMOVICH	99 BEAT	$\bar{K}^*(892)^0 \mu^+ \nu_\mu$
1.20±0.13±0.13	874	FRABETTI	93E E687	$\bar{K}^*(892)^0 \mu^+ \nu_\mu$
1.18±0.18±0.08	305	KODAMA	92 E653	$\bar{K}^*(892)^0 \mu^+ \nu_\mu$

• • • We do not use the following data for averages, fits, limits, etc. • • •

1.8 $\pm^{+0.6}_{-0.4}$ ± 0.3 183 ANJOS 90E E691 $\bar{K}^*(892)^0 e^+ \nu_e$

Γ_+/Γ_- in $D^+ \rightarrow \bar{K}^*(892)^0 \ell^+ \nu_\ell$

VALUE	EVTS	DOCUMENT ID	TECN	COMMENT
0.22\pm0.06 OUR AVERAGE Error includes scale factor of 1.6.				
0.28 \pm 0.05 \pm 0.02	763	ADAMOVICH 99	BEAT	$\bar{K}^*(892)^0 \mu^+ \nu_\mu$
0.16 \pm 0.05 \pm 0.02	305	KODAMA 92	E653	$\bar{K}^*(892)^0 \mu^+ \nu_\mu$
• • • We do not use the following data for averages, fits, limits, etc. • • •				
0.15 $\pm^{+0.07}_{-0.05}$ ± 0.03	183	ANJOS	90E E691	$\bar{K}^*(892)^0 e^+ \nu_e$

D \pm REFERENCES

PDG	06	JPG 33 1	W.-M. Yao <i>et al.</i>	(PDG Collab.)
RUBIN	06	PRL 96 081802	P. Rubin <i>et al.</i>	(CLEO Collab.)
ABLIKIM	05A	PL B608 24	M. Ablikim <i>et al.</i>	(BEPC BES Collab.)
ABLIKIM	05D	PL B610 183	M. Ablikim <i>et al.</i>	(BEPC BES Collab.)
ABLIKIM	05F	PL B622 6	M. Ablikim <i>et al.</i>	(BEPC BES Collab.)
ABLIKIM	05P	PL B625 196	M. Ablikim <i>et al.</i>	(BEPC BES Collab.)
ARTUSO	05A	PRL 95 251801	M. Artuso <i>et al.</i>	(CLEO Collab.)
AUBERT	05S	PR D71 091101R	B. Aubert <i>et al.</i>	(BABAR Collab.)
HE	05	PRL 95 121801	Q. He <i>et al.</i>	(CLEO Collab.)
HE	05A	PRL 95 221802	Q. He <i>et al.</i>	(CLEO Collab.)
HUANG	05B	PRL 95 181801	G.S. Huang <i>et al.</i>	(CLEO Collab.)
KAYIS-TOPAK..05	PL B626 24	A. Kayis-Topaksu <i>et al.</i>	(CERN CHORUS Collab.)	
LINK	05E	PL B622 239	J.M. Link <i>et al.</i>	(FNAL FOCUS Collab.)
LINK	05I	PL B621 72	J.M. Link <i>et al.</i>	(FNAL FOCUS Collab.)
ABLIKIM	04C	PL B597 39	M. Ablikim <i>et al.</i>	(BEPC BES Collab.)
ARMS	04	PR D69 071102R	K. Arms <i>et al.</i>	(CLEO Collab.)
BONVICINI	04A	PR D70 112004	G. Bonvicini <i>et al.</i>	(CLEO Collab.)
LINK	04	PL B585 200	J.M. Link <i>et al.</i>	(FNAL FOCUS Collab.)
LINK	04E	PL B598 33	J.M. Link <i>et al.</i>	(FNAL FOCUS Collab.)
LINK	04F	PL B601 10	J.M. Link <i>et al.</i>	(FNAL FOCUS Collab.)
ANISOVICH	03	EPJ A16 229	V.V. Anisovich <i>et al.</i>	
LINK	03D	PL B561 225	J.M. Link <i>et al.</i>	(FNAL FOCUS Collab.)
LINK	03F	PL B572 21	J.M. Link <i>et al.</i>	(FNAL FOCUS Collab.)
AITALA	02	PRL 89 121801	E.M. Aitala <i>et al.</i>	(FNAL E791 Collab.)
BRANDENB...	02	PRL 89 222001	G. Brandenburg <i>et al.</i>	(CLEO Collab.)
KAYIS-TOPAK..02	PL B549 48	A. Kayis-Topaksu <i>et al.</i>	(CERN CHORUS Collab.)	
LINK	02B	PRL 88 041602	J.M. Link <i>et al.</i>	(FNAL FOCUS Collab.)
Also		PRL 88 159903 (erratum)	J.M. Link <i>et al.</i>	(FNAL FOCUS Collab.)
LINK	02E	PL B535 43	J.M. Link <i>et al.</i>	(FNAL FOCUS Collab.)
LINK	02F	PL B537 192	J.M. Link <i>et al.</i>	(FNAL FOCUS Collab.)
LINK	02I	PL B541 227	J.M. Link <i>et al.</i>	(FNAL FOCUS Collab.)
LINK	02J	PL B541 243	J.M. Link <i>et al.</i>	(FNAL FOCUS Collab.)
LINK	02L	PL B544 89	J.M. Link <i>et al.</i>	(FNAL FOCUS Collab.)
AITALA	01B	PRL 86 770	E.M. Aitala <i>et al.</i>	(FNAL E791 Collab.)
LINK	01C	PRL 87 162001	J.M. Link <i>et al.</i>	(FNAL FOCUS Collab.)
ABREU	00O	EPJ C12 209	P. Abreu <i>et al.</i>	(DELPHI Collab.)
ASTIER	00D	PL B486 35	P. Astier <i>et al.</i>	(CERN NOMAD Collab.)
BAI	00C	PR D62 052001	J.Z. Bai <i>et al.</i>	(BEPC BES Collab.)
JUN	00	PRL 84 1857	S.Y. Jun <i>et al.</i>	(FNAL SELEX Collab.)
LINK	00B	PL B491 232	J.M. Link <i>et al.</i>	(FNAL FOCUS Collab.)
Also		PL B495 443 (erratum)	J.M. Link <i>et al.</i>	(FNAL FOCUS Collab.)
ABBIENDI	99K	EPJ C8 573	G. Abbiendi <i>et al.</i>	(OPAL Collab.)
ABE	99P	PR D60 092005	F. Abe <i>et al.</i>	(CDF Collab.)
ADAMOVICH	99	EPJ C6 35	M. Adamovich <i>et al.</i>	(CERN BEATRICE Collab.)
AITALA	99G	PL B462 401	E.M. Aitala <i>et al.</i>	(FNAL E791 Collab.)
BONVICINI	99	PRL 82 4586	G. Bonvicini <i>et al.</i>	(CLEO Collab.)
AITALA	98B	PRL 80 1393	E.M. Aitala <i>et al.</i>	(FNAL E791 Collab.)
AITALA	98C	PL B421 405	E.M. Aitala <i>et al.</i>	(FNAL E791 Collab.)
AITALA	98F	PL B440 435	E.M. Aitala <i>et al.</i>	(FNAL E791 Collab.)
BAI	98B	PL B429 188	J.Z. Bai <i>et al.</i>	(BEPC BES Collab.)
JESSOP	98	PR D58 052002	C.P. Jessop <i>et al.</i>	(CLEO Collab.)
AITALA	97	PL B397 325	E.M. Aitala <i>et al.</i>	(FNAL E791 Collab.)

AITALA	97B	PL B403 377	E.M. Aitala <i>et al.</i>	(FNAL E791 Collab.)
AITALA	97C	PL B404 187	E.M. Aitala <i>et al.</i>	(FNAL E791 Collab.)
BARTELT	97	PL B405 373	J. Bartelt <i>et al.</i>	(CLEO Collab.)
BISHAI	97	PRL 78 3261	M. Bishai <i>et al.</i>	(CLEO Collab.)
FRAEBETTI	97	PL B391 235	P.L. Frabetti <i>et al.</i>	(FNAL E687 Collab.)
FRAEBETTI	97B	PL B398 239	P.L. Frabetti <i>et al.</i>	(FNAL E687 Collab.)
FRAEBETTI	97C	PL B401 131	P.L. Frabetti <i>et al.</i>	(FNAL E687 Collab.)
FRAEBETTI	97D	PL B407 79	P.L. Frabetti <i>et al.</i>	(FNAL E687 Collab.)
AITALA	96	PRL 76 364	E.M. Aitala <i>et al.</i>	(FNAL E791 Collab.)
ALBRECHT	96C	PL B374 249	H. Albrecht <i>et al.</i>	(ARGUS Collab.)
FRAEBETTI	95	PL B346 199	P.L. Frabetti <i>et al.</i>	(FNAL E687 Collab.)
FRAEBETTI	95B	PL B351 591	P.L. Frabetti <i>et al.</i>	(FNAL E687 Collab.)
FRAEBETTI	95E	PL B359 403	P.L. Frabetti <i>et al.</i>	(FNAL E687 Collab.)
FRAEBETTI	95F	PL B363 259	P.L. Frabetti <i>et al.</i>	(FNAL E687 Collab.)
KODAMA	95	PL B345 85	K. Kodama <i>et al.</i>	(FNAL E653 Collab.)
ALBRECHT	94I	ZPHY C64 375	H. Albrecht <i>et al.</i>	(ARGUS Collab.)
ALEEV	94	PAN 57 1370	A.N. Aleev <i>et al.</i>	(Serpukhov BIS-2 Collab.)
		Translated from YF 57 1443.		
BALEST	94	PRL 72 2328	R. Balest <i>et al.</i>	(CLEO Collab.)
FRAEBETTI	94D	PL B323 459	P.L. Frabetti <i>et al.</i>	(FNAL E687 Collab.)
FRAEBETTI	94G	PL B331 217	P.L. Frabetti <i>et al.</i>	(FNAL E687 Collab.)
FRAEBETTI	94I	PR D50 R2953	P.L. Frabetti <i>et al.</i>	(FNAL E687 Collab.)
ABE	93E	PL B313 288	K. Abe <i>et al.</i>	(VENUS Collab.)
ADAMOVICH	93	PL B305 177	M.I. Adamovich <i>et al.</i>	(CERN WA82 Collab.)
AKERIB	93	PRL 71 3070	D.S. Akerib <i>et al.</i>	(CLEO Collab.)
ALAM	93	PRL 71 1311	M.S. Alam <i>et al.</i>	(CLEO Collab.)
ANJOS	93	PR D48 56	J.C. Anjos <i>et al.</i>	(FNAL E691 Collab.)
BEAN	93C	PL B317 647	A. Bean <i>et al.</i>	(CLEO Collab.)
FRAEBETTI	93E	PL B307 262	P.L. Frabetti <i>et al.</i>	(FNAL E687 Collab.)
KODAMA	93B	PL B313 260	K. Kodama <i>et al.</i>	(FNAL E653 Collab.)
KODAMA	93C	PL B316 455	K. Kodama <i>et al.</i>	(FNAL E653 Collab.)
SELEN	93	PRL 71 1973	M.A. Selen <i>et al.</i>	(CLEO Collab.)
ALBRECHT	92B	ZPHY C53 361	H. Albrecht <i>et al.</i>	(ARGUS Collab.)
ALBRECHT	92F	PL B278 202	H. Albrecht <i>et al.</i>	(ARGUS Collab.)
ANJOS	92	PR D45 R2177	J.C. Anjos <i>et al.</i>	(FNAL E691 Collab.)
ANJOS	92C	PR D46 1941	J.C. Anjos <i>et al.</i>	(FNAL E691 Collab.)
ANJOS	92D	PRL 69 2892	J.C. Anjos <i>et al.</i>	(FNAL E691 Collab.)
BARLAG	92C	ZPHY C55 383	S. Barlag <i>et al.</i>	(ACCMOR Collab.)
Also		ZPHY C48 29	S. Barlag <i>et al.</i>	(ACCMOR Collab.)
COFFMAN	92B	PR D45 2196	D.M. Coffman <i>et al.</i>	(Mark III Collab.)
DAOUDI	92	PR D45 3965	M. Daoudi <i>et al.</i>	(CLEO Collab.)
KODAMA	92	PL B274 246	K. Kodama <i>et al.</i>	(FNAL E653 Collab.)
KODAMA	92C	PL B286 187	K. Kodama <i>et al.</i>	(FNAL E653 Collab.)
ADAMOVICH	91	PL B268 142	M.I. Adamovich <i>et al.</i>	(WA82 Collab.)
ALBRECHT	91	PL B255 634	H. Albrecht <i>et al.</i>	(ARGUS Collab.)
ALVAREZ	91B	ZPHY C50 11	M.P. Alvarez <i>et al.</i>	(CERN NA14/2 Collab.)
AMMAR	91	PR D44 3383	R. Ammar <i>et al.</i>	(CLEO Collab.)
ANJOS	91C	PRL 67 1507	J.C. Anjos <i>et al.</i>	(FNAL-TPS Collab.)
BAI	91	PRL 66 1011	Z. Bai <i>et al.</i>	(Mark III Collab.)
COFFMAN	91	PL B263 135	D.M. Coffman <i>et al.</i>	(Mark III Collab.)
FRAEBETTI	91	PL B263 584	P.L. Frabetti <i>et al.</i>	(FNAL E687 Collab.)
ALVAREZ	90	ZPHY C47 539	M.P. Alvarez <i>et al.</i>	(CERN NA14/2 Collab.)
ALVAREZ	90C	PL B246 261	M.P. Alvarez <i>et al.</i>	(CERN NA14/2 Collab.)
ANJOS	90C	PR D41 2705	J.C. Anjos <i>et al.</i>	(FNAL E691 Collab.)
ANJOS	90D	PR D42 2414	J.C. Anjos <i>et al.</i>	(FNAL E691 Collab.)
ANJOS	90E	PRL 65 2630	J.C. Anjos <i>et al.</i>	(FNAL E691 Collab.)
BARLAG	90C	ZPHY C46 563	S. Barlag <i>et al.</i>	(ACCMOR Collab.)
WEIR	90B	PR D41 1384	A.J. Weir <i>et al.</i>	(Mark II Collab.)
ANJOS	89	PRL 62 125	J.C. Anjos <i>et al.</i>	(FNAL E691 Collab.)
ANJOS	89B	PRL 62 722	J.C. Anjos <i>et al.</i>	(FNAL E691 Collab.)
ANJOS	89E	PL B223 267	J.C. Anjos <i>et al.</i>	(FNAL E691 Collab.)
ADLER	88C	PRL 60 89	J. Adler <i>et al.</i>	(Mark III Collab.)
ALBRECHT	88I	PL B210 267	H. Albrecht <i>et al.</i>	(ARGUS Collab.)
ANJOS	88	PRL 60 897	J.C. Anjos <i>et al.</i>	(FNAL E691 Collab.)
AOKI	88	PL B209 113	S. Aoki <i>et al.</i>	(WA75 Collab.)
HAAS	88	PRL 60 1614	P. Haas <i>et al.</i>	(CLEO Collab.)
ONG	88	PRL 60 2587	R.A. Ong <i>et al.</i>	(Mark II Collab.)
RAAB	88	PR D37 2391	J.R. Raab <i>et al.</i>	(FNAL E691 Collab.)
ADAMOVICH	87	EPL 4 887	M.I. Adamovich <i>et al.</i>	(Photon Emulsion Collab.)
ADLER	87	PL B196 107	J. Adler <i>et al.</i>	(Mark III Collab.)

AGUILAR-...	87E	ZPHY C36 551	M. Aguilar-Benitez <i>et al.</i>	(LEBC-EHS Collab.)
Also		ZPHY C40 321	M. Aguilar-Benitez <i>et al.</i>	(LEBC-EHS Collab.)
AGUILAR-...	87F	ZPHY C36 559	M. Aguilar-Benitez <i>et al.</i>	(LEBC-EHS Collab.)
Also		ZPHY C38 520 (erratum)	M. Aguilar-Benitez <i>et al.</i>	(LEBC-EHS Collab.)
BARTEL	87	ZPHY C33 339	W. Bartel <i>et al.</i>	(JADE Collab.)
AGUILAR-...	86B	ZPHY C31 491	M. Aguilar-Benitez <i>et al.</i>	(LEBC-EHS Collab.)
BALTRUSAIT...	86E	PRL 56 2140	R.M. Baltrusaitis <i>et al.</i>	(Mark III Collab.)
PAL	86	PR D33 2708	T. Pal <i>et al.</i>	(DELCO Collab.)
AIHARA	85	ZPHY C27 39	H. Aihara <i>et al.</i>	(TPC Collab.)
BALTRUSAIT...	85B	PRL 54 1976	R.M. Baltrusaitis <i>et al.</i>	(Mark III Collab.)
BALTRUSAIT...	85E	PRL 55 150	R.M. Baltrusaitis <i>et al.</i>	(Mark III Collab.)
BARTEL	85J	PL 163B 277	W. Bartel <i>et al.</i>	(JADE Collab.)
ADAMOVICH	84	PL 140B 119	M.I. Adamovich <i>et al.</i>	(CERN WA58 Collab.)
ALTHOFF	84G	ZPHY C22 219	M. Althoff <i>et al.</i>	(TASSO Collab.)
ALTHOFF	84J	PL 146B 443	M. Althoff <i>et al.</i>	(TASSO Collab.)
DERRICK	84	PRL 53 1971	M. Derrick <i>et al.</i>	(HRS Collab.)
KOOP	84	PRL 52 970	D.E. Koop <i>et al.</i>	(DELCO Collab.)
PARTRIDGE	81	PRL 47 760	R. Partridge <i>et al.</i>	(Crystal Ball Collab.)
SCHINDLER	81	PR D24 78	R.H. Schindler <i>et al.</i>	(Mark II Collab.)
TRILLING	81	PRPL 75 57	G.H. Trilling	(LBL, UCB) J
BACINO	80	PRL 45 329	W.J. Bacino <i>et al.</i>	(DELCO Collab.)
ZHOLENTZ	80	PL 96B 214	A.A. Zholents <i>et al.</i>	(NOVO)
Also		SJNP 34 814	A.A. Zholents <i>et al.</i>	(NOVO)
		Translated from YAF 34	1471.	
BACINO	79	PRL 43 1073	W.J. Bacino <i>et al.</i>	(DELCO Collab.)
BRANDELIK	79	PL 80B 412	R. Brandelik <i>et al.</i>	(DASP Collab.)
FELLER	78	PRL 40 274	J.M. Feller <i>et al.</i>	(Mark I Collab.)
VUILLEMIN	78	PRL 41 1149	V. Vuillemin <i>et al.</i>	(Mark I Collab.)
GOLDHABER	77	PL 69B 503	G. Goldhaber <i>et al.</i>	(Mark I Collab.)
PERUZZI	77	PRL 39 1301	I. Peruzzi <i>et al.</i>	(Mark I Collab.)
PICCOLO	77	PL 70B 260	M. Piccolo <i>et al.</i>	(Mark I Collab.)
PERUZZI	76	PRL 37 569	I. Peruzzi <i>et al.</i>	(Mark I Collab.)

OTHER RELATED PAPERS

RICHMAN	95	RMP 67 893	J.D. Richman, P.R. Burchat	(UCSB, STAN)
ROSNER	95	CNPP 21 369	J. Rosner	(CHIC)